

CHAPTER 1

PASSIVE HF COMPONENTS

RESISTORS (1/2)

The equivalent circuit for a resistor in HF is shown in Fig. 1-1. R represents the value of the resistor, to which one must add two inductances L and a capacitance C , representing the parasitic elements needed to model its behavior in HF.

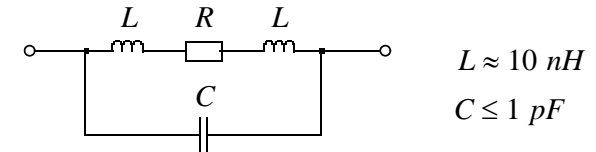


Fig 1-1: Equivalent circuit for a resistor.

The values of L and C depend on the way in which this resistor is realized. Three types of resistors are possible:

- 1) wirewound resistors;
- 2) carbon-composition resistors;
- 3) metal-film resistors.

Due to their high inductance, wirewound resistors are primarily used when the dissipated power becomes large ($> 10 \text{ W}$), but are not preferred for RF applications. Their impedance corresponds to that of a resonant parallel circuit.

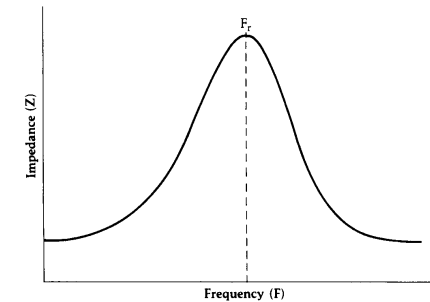


Fig 1-2: Impedance of a wirewound resistor.

RESISTORS (2/2)

Carbon-composition resistors are made of many carbon granules immersed in a binding substance. Their HF behavior is dominated by the capacitance C , due to all of the parasitic capacitances which exist between each pair of carbon granules.

Metal-film resistors are realized using a thin layer of carbon or a metallic film. As indicated in Fig. 1-3, metal-film resistors have better HF performance than carbon-composition resistors.

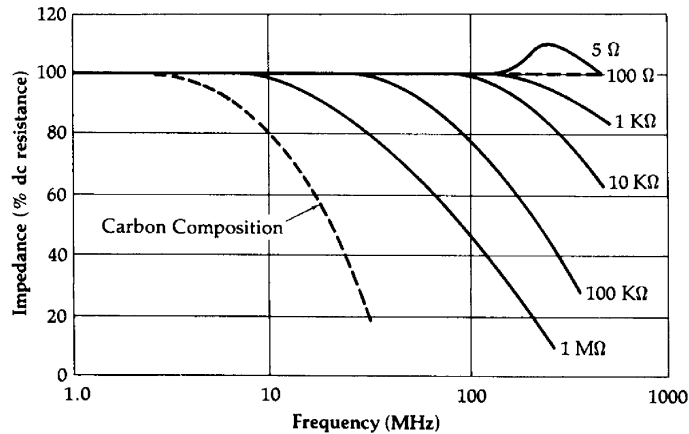


Fig 1-3: Comparison of impedances of carbon-composition and metal-film resistors.

For high-resistance resistors, the impedance decreases starting at 10 MHz due to the capacitance, while for small-resistance resistors ($< 50 \Omega$), the inductive effects of the connecting wires and the skin effect become important.

SMD (Surface Mounted Device) technology, used more and more often, has enabled the significant reduction of parasitic effects. These resistors are made of thin films of aluminum or beryllium, and have a small reactance up to frequencies of GHz.

CAPACITORS (1/2)

The capacitor is a frequently-used component for RF. It allows the realization of the following important functions:

- 1)coupling between amplifier stages;
- 2)resonant circuits;
- 3)filters.

A capacitor's characteristics essentially depend on the type of dielectric used. The equivalent circuit for a capacitor is shown in Fig. 1-4, where C is the capacitance of the capacitor, L is the inductance due to the connections (leads), R_s is the series resistance of those leads, and R_p is the equivalent resistance due to the leakage current and the losses coming from the hysteresis of the dielectric.

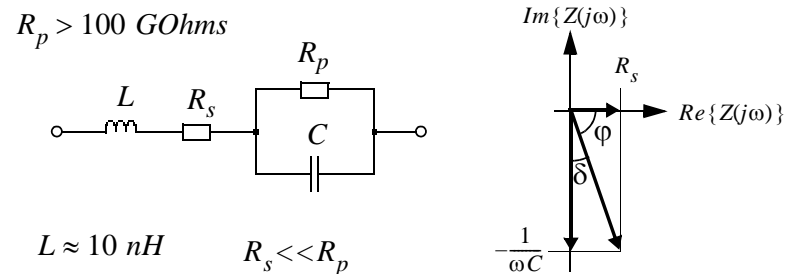


Fig 1-4: Equivalent circuit of a capacitor.

The ensemble of these losses in the dielectric and in the connective resistance is summarized by using a loss factor $\tan(\delta)$ defined as the ratio between the active dissipated power and the absolute value of the reactive power:

$$\tan(\delta) \equiv \frac{P_{active}}{|P_{reactive}|} = \frac{R}{|X|} = \omega R_s C + \frac{1}{\omega R_p C} \tag{1.1}$$

where $R \equiv Re\{Z(j\omega)\}$ and $X \equiv Im\{Z(j\omega)\}$.

CAPACITORS (2/2)

The inverse of the loss factor is the quality factor, given by:

$$Q \equiv \frac{1}{\tan(\delta)} = \frac{|P_{reactive}|}{P_{active}} = \frac{|X|}{R} = \left[\frac{1}{Q_s} + \frac{1}{Q_p} \right]^{-1} \equiv Q_s \quad (1.2)$$

where: $Q_s \equiv \frac{1}{\omega R_s C}$ et: $Q_p \equiv \omega R_p C$ (1.3)

The impedance corresponding to the diagram in Fig.1-4 for $\omega \ll 1/\sqrt{LC}$ and $R_s \ll R_p$ is therefore given by:

$$Z(j\omega) = R + jX \approx \frac{1}{j\omega C} \cdot \left[1 + j\omega R_s C - \frac{1}{j\omega R_p C} \right] \quad (1.4)$$

$$= \frac{1}{j\omega C} \cdot \left[1 + \frac{j}{Q} \right] = \frac{1}{j\omega C} \cdot [1 + j \tan(\delta)]$$

The impedance characteristic given by (1.4) is shown in Fig. 1-5. The importance of the lead inductance increases with frequency, until this inductance becomes resonant with the capacitor. Above the resonant frequency F_r , the capacitor acts as an inductor.

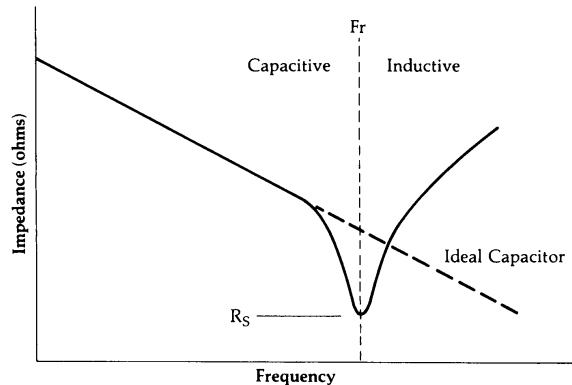


Fig 1-5: Impedance characteristic of a capacitor.

CAPACITOR TYPES (1/3)

There are several types of capacitors; in particular:

- 1)ceramic;
- 2)mica;
- 3)metallized-film;
- 4)SMD;
- 5)electrolytic.

Ceramic capacitors have relative dielectric constants between 5 and 10'000 and various temperature characteristics. As indicated in Fig. 1-6, the higher the dielectric constant, the more sensitive the capacitor to temperature.

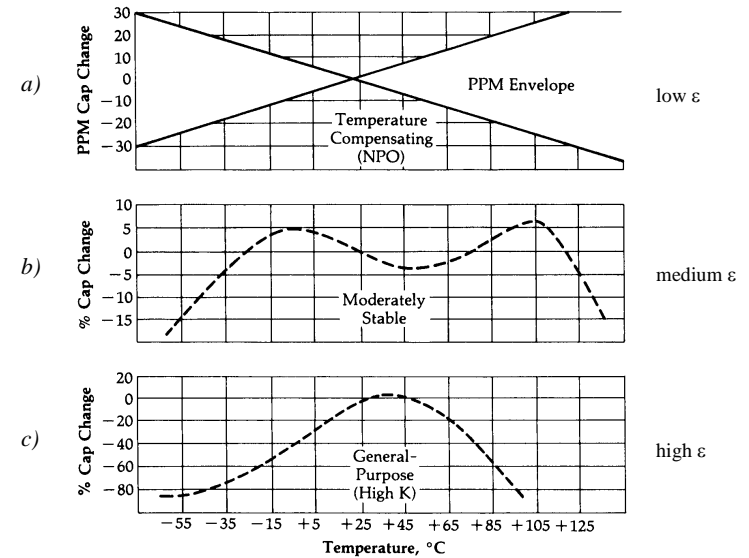


Fig 1-6: Temperature sensitivity of ceramic capacitors.

CAPACITOR TYPES (2/3)

Ceramic capacitors with a low dielectric constant (Fig. 1-6 a)) are usually fabricated from two materials with temperature coefficients of opposite signs. This type of capacitor (called NPO: Negative Positive Zero) have thermal coefficients between +150 and -4,700 ppm/°C with tolerances as low as ±15 ppm/°C. These capacitors are primarily used in oscillators.

Moderately stable ceramic capacitors (Fig. 1-6 b)) have a maximum variation of 15% of their nominal value for a temperature range from -60 to +125 °C. In addition, this relative variation is nonlinear. They are primarily used for switching applications. Their advantages over NPO capacitors are their small size and low cost.

Ceramic capacitors with a high dielectric constant (Fig. 1-6 c)) have bad thermal stability and are only used for decouplage applications which require large capacitances.

There are ceramic capacitors available, conceived for HF applications, which have high quality factors. These capacitors are, of course, more expensive.

CAPACITOR TYPES (3/3)

Mica capacitors have a low dielectric constant ($\epsilon_r \cong 6$), which explains their large size and excellent thermal stability. Silvered mica capacitors have a very low thermal coefficient (usually +20 ppm/°C for a temperature varying between -60°C and +90°C).

Metallized-film capacitors are fabricated using many different dielectrics (teflon, polystyrene, polycarbonate, paper,...). They are available with very tight tolerances (±2%) over the entire usual temperature range. With a larger size and a similar cost to that of ceramic capacitors, they don't offer any particular advantage. In addition, certain metallized-film/polystyrene capacitors have seriously degraded thermal behavior at temperatures above 85 °C.

Finally, electrolytic capacitors offer very high capacitances. Unfortunately, due to their design, their parasitic inductances are high, and make them unusable for HF.

INDUCTORS (1/3)

Inductors are made of coils which increase the magnetic flux coupling between each turn. Even though inductors are often used in HF circuits, the inductor is certainly the component that poses the most problems. In particular, the impedance changes drastically as a function of frequency. The equivalent circuit for an inductor is shown in Fig. 1-7, where L is the inductance, R_s comes from the series resistance of the coiled wire and the skin effect, and C_d represents the distributed capacitance between the turns of the coil. This capacitance is therefore inversely proportional to the distance between the turns.

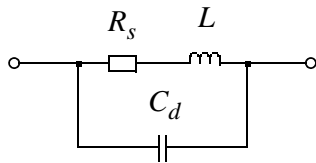


Fig 1-7: Equivalent circuit of an inductor. The corresponding impedance is given by:

$$Z(j\omega) = R + jX = \frac{R_s + j\omega L}{1 - \omega^2 LC_d + j\omega R_s C_d} \cong R_s + j\omega L \quad (1.5)$$

for $\omega \ll 1/\sqrt{LC_d}$. As indicated in Fig. 1-8, at low frequency, the inductor acts as an inductance in series with a resistance. As the frequency increases, the impedance deviates from that of an inductance and increases rapidly to reach a maximum value at the resonant frequency $\omega_0 \cong 1/\sqrt{LC_d}$. Above that point, the impedance decreases and the inductor acts as a capacitor.

INDUCTORS (2/3)

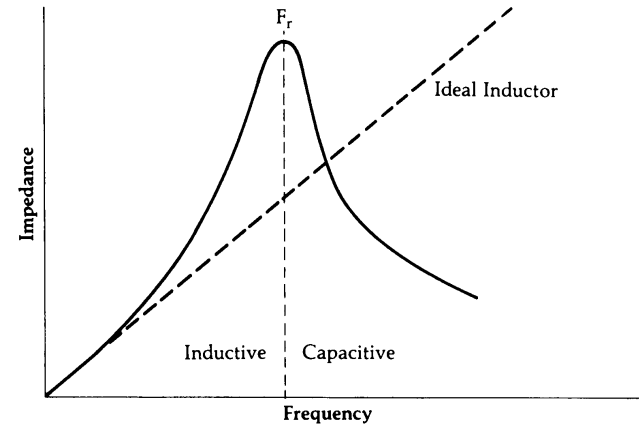


Fig 1-8: Impedance characteristic of an inductor.

All of the losses due to series resistance and skin effect are expressed by the quality factor Q , defined as the ratio between the absolute value of the reactive power absorbed and the active power dissipated by the impedance $Z(j\omega)$:

$$Q \equiv \frac{|P_{reactive}|}{P_{active}} = \frac{|X|}{R} \cong \frac{\omega L}{R_s} \quad (1.6)$$

For frequencies less than the resonant frequency, the impedance can also be written as:

$$Z(j\omega) = R + jX = jX \left(1 + \frac{R}{jX} \right) \cong j\omega L \cdot \left[1 + \frac{1}{jQ} \right] \quad (1.7)$$

The higher the quality factor, the closer the inductor to an ideal inductor, and the higher the impedance value at resonance ($Z(\omega_0) \cong Q/(\omega_0 C_d)$).

INDUCTORS (3/3)

According to Eqn. 1.6, Q increases proportionally with the frequency. But this result has been reached without considering the skin effect, which tends to increase the series resistance R_s , and therefore to reduce the rise of Q as the frequency climbs. As indicated in Fig. 1-9, the quality factor has a maximum, which corresponds to the situation in which the series resistance and the inductor reactance increase at the same rate with frequency. Beyond this maximum, the quality factor decreases rapidly due to the shunt capacitance C_d . The quality factor can be expressed as a function of the real and imaginary parts of Eqn. 1.5:

$$Q \equiv \frac{|X|}{R} \cong \frac{\omega L}{R_s(\omega)} \cdot \left[1 - \left(\frac{\omega}{\omega_0} \right)^2 \right] \quad (1.8)$$

Eqn. 1.8 shows that the quality factor is zero when the frequency equals the resonant frequency. This comes from the fact that at resonance, the reactance of the inductance is cancelled out by the reactance of the capacitance.

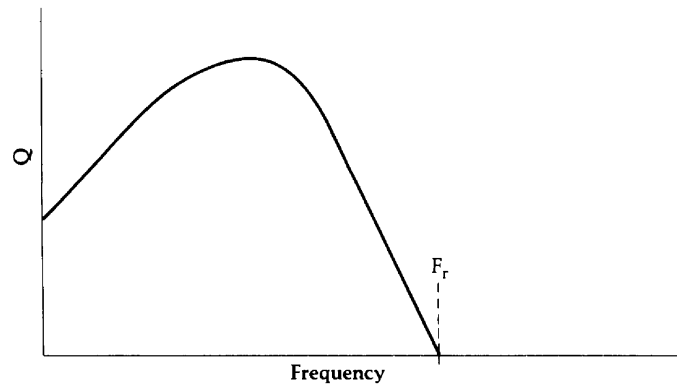


Fig 1-9: Quality factor as a function of the frequency.

INCREASING THE QUALITY FACTOR

There are various methods to increase the quality factor and the maximum frequency of use of an inductor. We can name the following possibilities:

- 1) use a larger-diameter wire, to reduce the series resistance R_s ;
- 2) spread the turns apart, which reduces the coupling capacitance C_d between turns;
- 3) increase the permeability of the core, by using a magnetic core.

AIR-CORE INDUCTORS

The inductance of a single-layer air-core inductor is approximately given by

$$L = \frac{0.394 \cdot r^2 \cdot N^2}{9r + 10l} \quad \text{in } \mu\text{H} \quad (1.9)$$

where r is the radius in cm, l the length in cm, N the number of turns, and L the inductance in μH (cf Fig. 1-10). The diameter of the wire is related to the length of the coil by:

$$d \leq \frac{l}{N} \quad (1.10)$$

Note that equation (1.9) is only true for $l > 0.67r$.

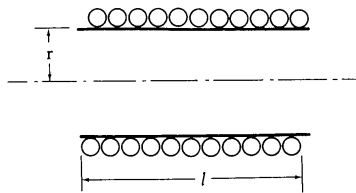


Fig 1-10: Single-layer air-core inductor.

Although the quality factor is maximum when the length l is equal to the diameter $2r$ of the inductor, in practice, the inductor is usually much longer than its diameter.

To realize an inductor with an inductance L , we choose the length and diameter of the coil, for example, and then calculate the number of turns using Eqn. 1.9. We would then choose the diameter of the wire according to Eqn. 1.10.

MAGNETIC-CORE INDUCTORS

For applications requiring large inductance values and small size, air-core inductors are not appropriate, so it is necessary to use a core with a higher permeability than air. Ferrite cores are generally used. For the same inductance, magnetic-core inductors need less turns and are therefore smaller, while having a larger quality factor (cf Fig. 1-11). They can also have a variable inductance, by inserting the core more or less deeply in the coil.

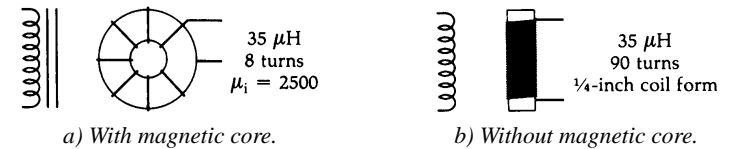


Fig 1-11: Inductor comparison.

Ferrite cores are most frequently found on the market in the form of a toroid (ring). This form is particularly suitable for the production of high quality factor inductors. The advantage of the toroid over the solenoid is that the tube of magnetic flux is closed on itself, avoiding coupling with neighboring elements (cf Fig. 1-12).

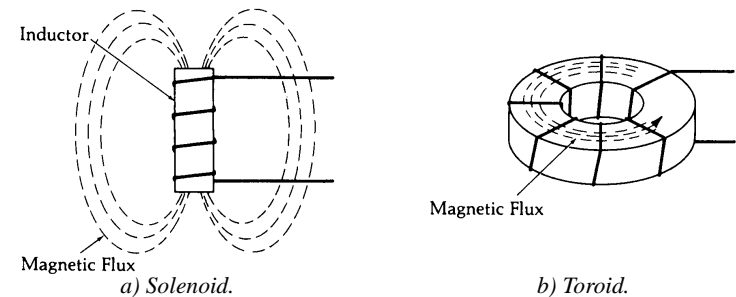


Fig 1-12: Inductor magnetic flux.

HYSTERESIS LOSSES (1/2)

Materials such as ferrite give a nonlinear magnetization curve with saturation and hysteresis as shown in Fig. 1-13 a). This hysteresis implies that a change of direction of magnetization requires the absorption of energy. To take these losses into account, we must add a resistance R_p to Fig. 1-7, connected in parallel with the inductance (cf Fig. 1-13 b)).

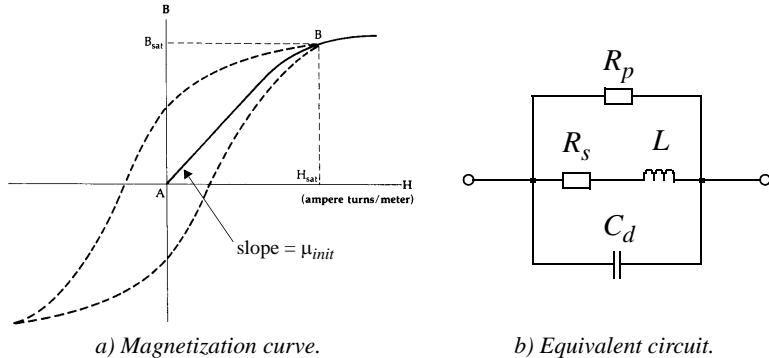


Fig 1-13: Magnetization curve and equivalent circuit for a magnetic-core inductor.

For $\omega \ll 1/\sqrt{LC}$, we can ignore the capacitance C_d , and considering that $R_s \ll R_p$, the impedance is approximately given by:

$$Z(j\omega) = R + jX \cong R_s + \frac{(\omega L)^2}{R_p} + j\omega L = j\omega L \cdot \left[1 + \frac{1}{jQ_{eq}} \right] \quad (1.11)$$

where: $Q_{eq} \equiv \frac{|X|}{R} \cong \left[\frac{1}{Q_s} + \frac{1}{Q_p} \right]^{-1}$ $Q_s \equiv \frac{\omega L}{R_s}$ $Q_p \equiv \frac{R_p}{\omega L}$ (1.12)

Q_{eq} is the global quality factor including the losses in the core represented by Q_p and the losses in the windings represented by Q_s .

HYSTERESIS LOSSES (2/2)

Eqn. 1.12 shows that the global quality factor Q_{eq} has a maximum as a function of frequency. In fact, the situation is more complicated, because the losses in the core and in the windings tend to increase with frequency. Typical quality factor curves as a function of frequency for iron-powder toroidal cores are shown in Fig. 1-14.

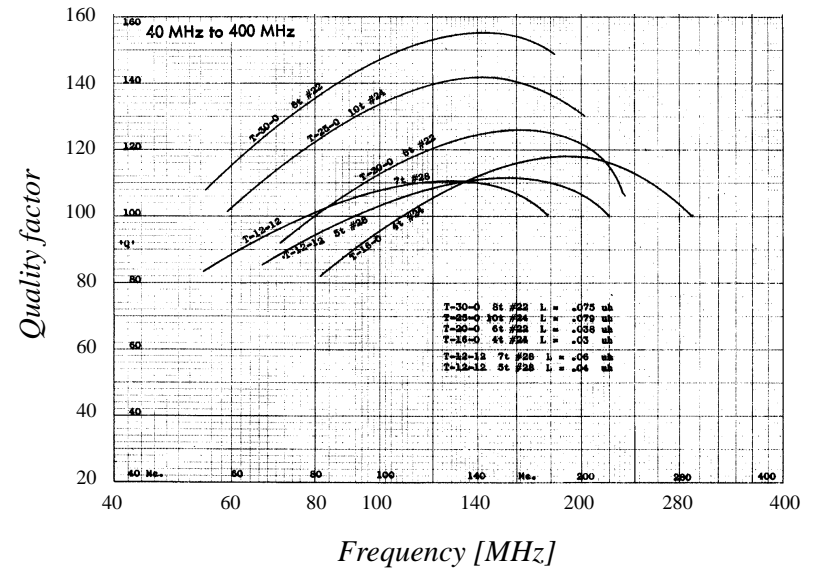


Fig 1-14: Quality factors for iron-powder toroidal cores.

TOROIDAL INDUCTOR DESIGN

The inductance of a magnetic-core toroidal inductor functioning in the linear part of its magnetization curve is approximately given by:

$$L = \frac{0.4\pi \cdot \mu_{init} \cdot A_c \times 10^{-2}}{l_e} \cdot N^2 = A_L \times 10^3 \cdot N^2 \quad [\mu H] \quad (1.13)$$

where L is the inductance in μH , μ_{init} the initial permeability, A_c the cross-section of the core in cm^2 , l_e the effective length of the core in cm and N the number of turns. A_L represents the inductance in nH for one single turn. The manufacturer usually specifies the factor A_L , which for a given inductance allows us to calculate the number of turns:

$$N = \sqrt{L/A_L} \quad (1.14)$$

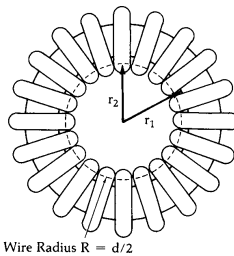


Fig 1-15: Magnetic-core toroidal inductor.

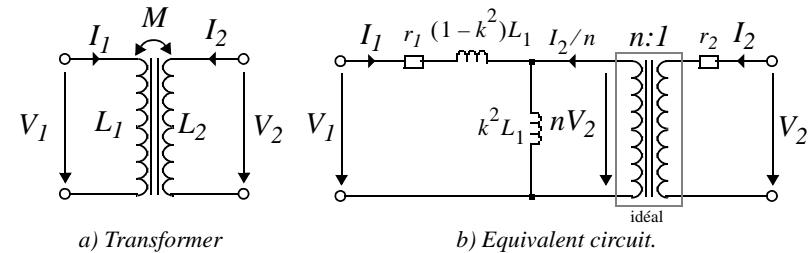
The inner radius of the toroid r_1 is also given by the manufacturer. From Fig. 1-15, we obtain the diameter of the wire:

$$d \leq \frac{2\pi r_1}{N + \pi} \quad (1.15)$$

It is best to include a margin of 10% to take the possible variation in wire diameter into consideration.

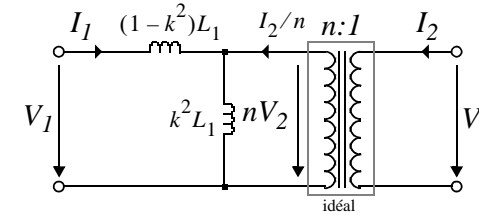
TRANSFORMERS (1/2)

Transformers are used for coupling resonant circuits, phase inversion, galvanic isolation, and impedance matching. Since the transformer already contains an inductor, we can just add a primary or (and) secondary capacitor in order to make a (two) resonant (coupled) circuits. The equivalent circuit for a transformer is shown in Fig. 1-16 b). When the series resistances r_1 and r_2 representing the losses are much smaller than the source and load impedances, they can be ignored and the equivalent circuit simplifies to that of Fig. 1-16 c).



a) Transformer

b) Equivalent circuit.



c) With negligible losses.

Fig 1-16: Equivalent circuit of transformer.

The equations corresponding to the circuit in Fig. 1-16 a) are:

$$\begin{aligned} V_1 &= sL_1 \cdot I_1 + sM \cdot I_2 \\ V_2 &= sM \cdot I_1 + sL_2 \cdot I_2 \end{aligned} \quad (1.16)$$

where M is the mutual inductance representing the coupling between the primary and the secondary.

TRANSFORMERS (2/2)

The equivalent circuit uses an ideal transformer with a transformation ratio n . The voltage at the primary of the ideal transformer is thus $n \cdot V_2$, while the current is divided by n . The equations of the equivalent circuit of Fig. 1-16 c) are given by:

$$V_1 = s(1 - k^2)L_1 \cdot I_1 + sk^2L_1 \cdot \left(I_1 + \frac{I_2}{n}\right) = sL_1 \cdot I_1 + \frac{sk^2L_1 \cdot I_2}{n} \tag{1.17}$$

$$nV_2 = sk^2L_1 \cdot \left(I_1 + \frac{I_2}{n}\right) \rightarrow V_2 = \frac{sk^2L_1 \cdot I_1}{n} + \frac{sk^2L_1 \cdot I_2}{n^2}$$

By combining equations (1.16) and (1.17), we get:

$$n = k \cdot \sqrt{\frac{L_1}{L_2}} \quad k = \frac{M}{\sqrt{L_1 \cdot L_2}} \tag{1.18}$$

In the case where the coupling coefficient k is close to one, the equivalent circuit of Fig. 1.16 c) reduces to that of Fig. 1.17.

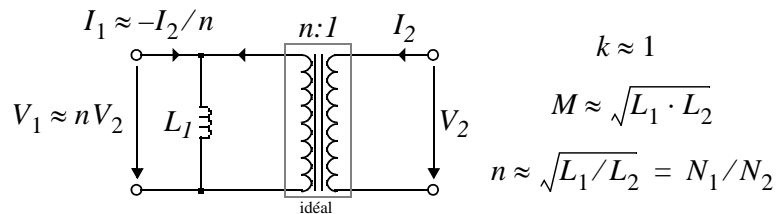


Fig 1-17: Equivalent circuit of transformer for $k \approx 1$. When a load R_L is connected to the secondary, it is seen by the primary as a load $n^2 R_L$ (cf Fig. 1.18).

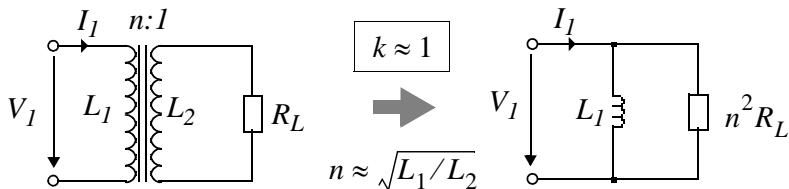


Fig 1-18: Equivalent load as seen by the primary.

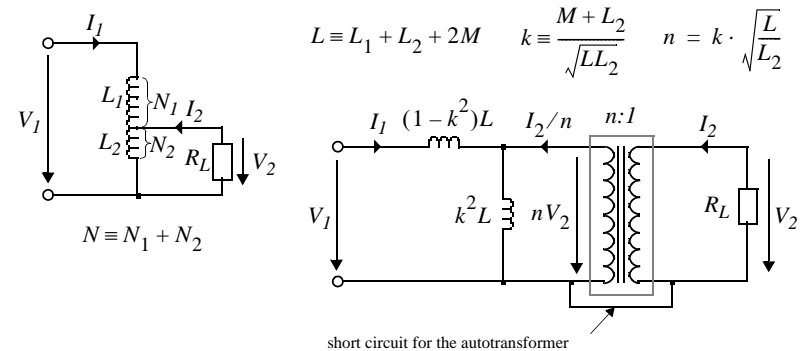
AUTOTRANSFORMERS (1/2)

A transformer can often be advantageously replaced by an autotransformer, which is a coil of N turns having an intermediary point taken between N_1 and N_2 turns from the two ends (cf Fig. 1-19 a). The loop equations corresponding to the autotransformer of Fig. 1-19 a) are:

$$V_1 = sL_1I_1 + sM(I_1 + I_2) + sL_2(I_1 + I_2) + sMI_1$$

$$= s(L_1 + L_2 + 2M)I_1 + s(L_2 + M)I_2 \tag{1.19}$$

$$V_2 = sL_2(I_1 + I_2) + sMI_1 = s(L_2 + M)I_1 + sL_2I_2$$



a) Autotransformer. b) Equivalent circuit.

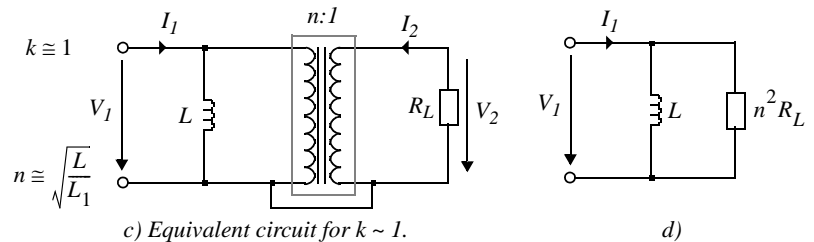


Fig 1-19: Autotransformer connected to a load.

AUTOTRANSFORMERS (2/2)

The autotransformer can be replaced by an ideal transformer with a transformation ratio n of which the negative terminals of the primary and secondary are short-circuited. The resulting diagram is shown in Fig. 1-19 b) and the corresponding equations are given by:

$$\begin{aligned} V_1 &= s(1-k^2)LI_1 + nV_2 = sLI_1 + s\frac{k^2}{n}LI_2 \\ V_2 &= \frac{1}{n} \cdot \left(sk^2L \cdot \left(I_1 + \frac{I_2}{n} \right) \right) = s\frac{k^2}{n}LI_1 + s\frac{k^2}{n^2}LI_2 \end{aligned} \quad (1.20)$$

Combining Eqn. 1.20 with Eqn. 1.19, we find:

$$L = L_1 + L_2 + 2M \quad n = k \cdot \sqrt{\frac{L}{L_2}} \quad (1.21)$$

In the case where the coupling between the two coils is perfect ($k \cong 1$), the series inductance can be ignored and the diagram of Fig. 1-19 b) reduces to that of Fig. 1-19 c). Since the load impedance as seen from the primary is simply multiplied by the transformation ratio squared, the diagram of Fig. 1-19 c) can be further simplified to that of Fig. 1-19 d).

For $k \cong 1$, the transformation ratio and therefore the multiplication factor of the load impedance is given by:

$$n = \sqrt{\frac{L}{L_2}} \quad (1.22)$$

CHAPTER 2

SERIES AND PARALLEL CIRCUITS

It is useful to remember that an impedance Z (admittance Y) can always be represented by $Z = R_s + jX_s$ ($Y = G_p + jB_p$) where R_s is the resistance and X_s the reactance (G_p is the conductance and B_p the susceptance). This representation is equivalent to a series (parallel) connection of a resistance R_s (conductance G_p) and a reactance X_s (susceptance B_p) (cf Fig. 2-1).

RESONANT CIRCUITS

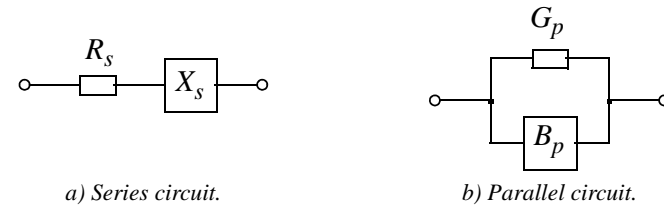


Fig 2-1: Series and parallel circuits.

The impedance and the admittance being inverses of each other, they are related by:

$$Z \equiv R_s + jX_s = \frac{1}{Y} = \frac{1}{G_p + jB_p} = \frac{G_p - jB_p}{G_p^2 + B_p^2} \quad (2.1)$$

$$Y \equiv G_p + jB_p = \frac{1}{Z} = \frac{1}{R_s + jX_s} = \frac{R_s - jX_s}{R_s^2 + X_s^2}$$

where:

$$\begin{aligned} R_s &= \frac{G_p}{G_p^2 + B_p^2} & X_s &= \frac{-B_p}{G_p^2 + B_p^2} \\ G_p &= \frac{R_s}{R_s^2 + X_s^2} & B_p &= \frac{-X_s}{R_s^2 + X_s^2} \end{aligned} \quad (2.2)$$

QUALITY FACTOR

Inductors introduce losses represented by a series resistance. The ratio between the energy stored in the inductance and the energy dissipated in the resistance is defined as the quality factor of the inductor. Likewise, the quality factor of a capacitor is the ratio between the energy stored in the capacitance and the energy dissipated in the series resistance which represents the losses in the dielectric.

In general, the quality factor of a series circuit and a parallel circuit is defined by:

$$Q \equiv \frac{|X_s|}{R_s} = \frac{|B_p|}{G_p} = \frac{R_p}{|X_p|} \quad (2.3)$$

In the cases of inductive and capacitive circuits, we have respectively:

$$Q = \frac{\omega L_s}{R_s} = \frac{R_p}{\omega L_p} \quad Q = \frac{1}{\omega R_s C_s} = \omega R_p C_p \quad (2.4)$$

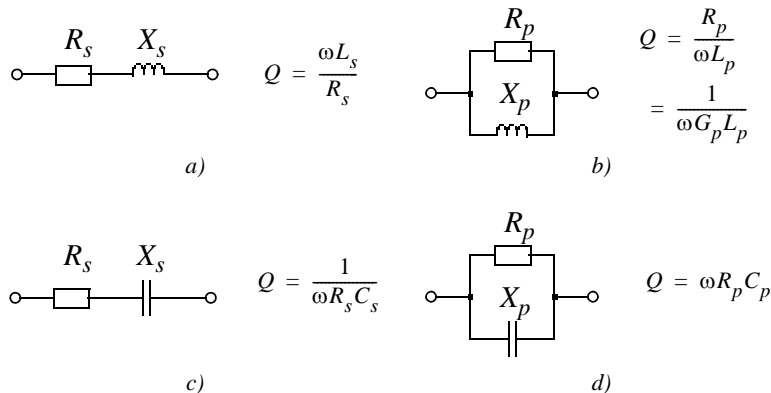
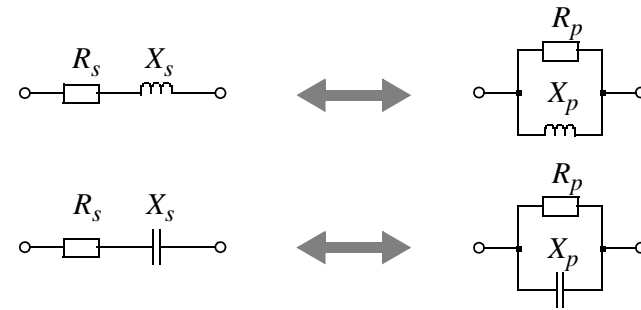


Fig 2-2: Definition of quality factor.

SERIES / PARALLEL TRANSFORMATION

It is often useful in HF to be able to convert a series circuit to its parallel equivalent or vice versa, as indicated in Fig. 2-3. This technique is used for example to synthesize an impedance matching network between two given impedances.



equivalence valid for one single frequency!

Fig 2-3: Series / parallel conversion.

When a series circuit is converted to its parallel equivalent (or vice versa), it is useful to express Eqn. 2.2 as a function of the quality factor of the circuit:

$$R_s = \frac{R_p}{1 + Q^2} \quad X_s = \frac{X_p}{1 + 1/Q^2} \quad (2.5)$$

$$R_p = R_s(1 + Q^2) \quad X_p = X_s(1 + 1/Q^2)$$

where $R_p \equiv 1/G_p$ and $X_p \equiv -1/B_p$. Note that the quality factor of the series circuit is identical to that of the parallel circuit. It is given by Eqn. 2.3 or 2.4.

In addition, it is important to notice that the reactances of series and parallel circuits depend on the frequency and therefore that this circuit conversion is only valid *for one single frequency*.

SERIES RESONANT CIRCUITS

The impedance of the series resonant circuit shown in Fig. 2-4 is given by:

$$Z \equiv \frac{V_{in}}{I} = R + j(X_L + X_C) \tag{2.6}$$

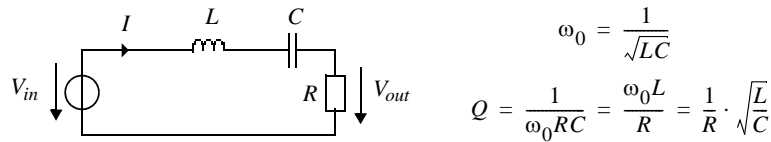


Fig 2-4: Series resonant circuit.

This impedance is minimum (and therefore the current is maximum for a constant amplitude of applied voltage), when:

$$-X_L = X_C \quad \text{or} \quad \omega_0 L = \frac{1}{\omega_0 C} \tag{2.7}$$

This equality is only true at one frequency, called the resonant frequency f_0 (or ω_0 in radians):

$$\omega_0 = 2\pi f_0 = \frac{1}{\sqrt{LC}} \tag{2.8}$$

At this frequency, the reactance of the inductor is compensated by the reactance of the capacitor, and therefore the output voltage V_{out} is equal to the input voltage V_{in} . The transfer function for the voltage is given by:

$$A_v(s) \equiv \frac{V_{out}(s)}{V_{in}(s)} = \frac{sRC}{s^2 LC + sRC + 1} = \frac{\frac{s}{\omega_0 Q}}{\left(\frac{s}{\omega_0}\right)^2 + \frac{s}{\omega_0 Q} + 1} \tag{2.9}$$

POLES

This circuit has two poles given by:

$$p_{1,2} = \begin{cases} -\frac{\omega_0}{2Q} \pm \omega_0 \cdot \sqrt{1/(2Q)^2 - 1} & \text{for: } Q < 1/2 \text{ (real poles)} \\ -\frac{\omega_0}{2Q} \pm j\omega_0 \cdot \sqrt{1 - 1/(2Q)^2} & \text{for: } Q > 1/2 \text{ (complex poles)} \end{cases} \tag{2.10}$$

The poles corresponding to Eqn. 2.10 are presented in Fig. 2-5. The poles are real for $Q < 1/2$ ($R > 2\sqrt{L/C}$), confounded for $Q = 1/2$ ($R = 2\sqrt{L/C}$) and complex for $Q > 1/2$ ($R < 2\sqrt{L/C}$).

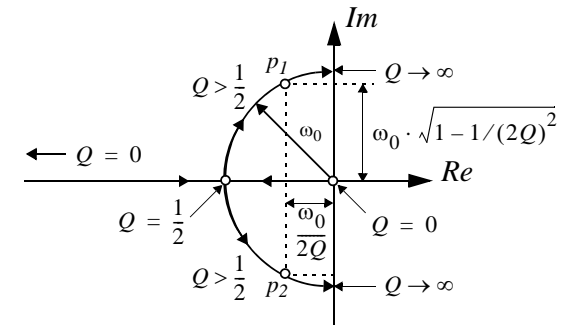


Fig 2-5: Poles of the transfer function.

The harmonic response is obtained by replacing s by $j\omega$ in Eqn. 2.9:

$$A_v(j\omega) = \frac{j\frac{\omega}{\omega_0 Q}}{1 - \left(\frac{\omega}{\omega_0}\right)^2 + j\frac{\omega}{\omega_0 Q}} = \frac{1}{1 + jQ\left(\frac{\omega}{\omega_0} - \frac{\omega_0}{\omega}\right)} = \frac{1}{1 + jQx} \tag{2.11}$$

where x is the misalignment. For $\Delta\omega \equiv (\omega - \omega_0) \ll \omega_0$ the misalignment is approximately equal to $2\Delta\omega/\omega_0$ and therefore proportional to the distance of the frequency from the resonance.

BANDWIDTH

The power dissipated in the resistor is given by:

$$P_R = \frac{V_{out}^2}{R} = |A_v(j\omega)|^2 \frac{V_{in}^2}{R} = |A_v(j\omega)|^2 P_{max} \quad (2.12)$$

It is maximum when $|A_v(j\omega)|^2 = 1$, meaning at the resonance. We therefore define the frequencies at -3 dB as those for which the power dissipated in the resistor is equal to half of the maximum power P_{max} , which corresponds to the frequencies ω_1 and ω_2 for which $|A_v(j\omega)| = 1/\sqrt{2}$ or where $x = \pm 1/Q$:

$$x_1 \equiv \frac{\omega_1 - \omega_0}{\omega_0} = -\frac{1}{Q} \quad x_2 \equiv \frac{\omega_2 - \omega_0}{\omega_0} = +\frac{1}{Q} \quad (2.13)$$

Due to the geometric symmetry of $|A_v(j\omega)|$ around ω_0 , the frequencies at -3 dB, ω_1 and ω_2 , are such that:

$$\omega_1 \omega_2 = \omega_0^2 \quad (2.14)$$

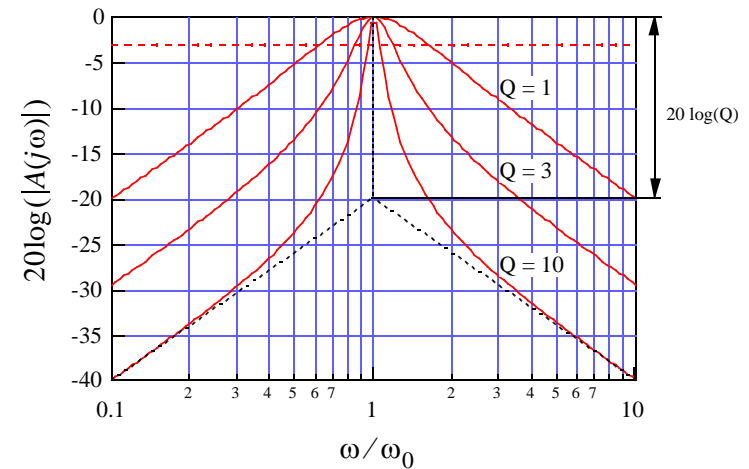
ω_1 and ω_2 can be calculated from:

$$\frac{\omega_0^2}{\omega_2} = \omega_1 \quad \text{et:} \quad \omega_2 - \frac{\omega_0^2}{\omega_2} = \omega_2 - \omega_1 = \frac{\omega_0}{Q} \quad (2.15)$$

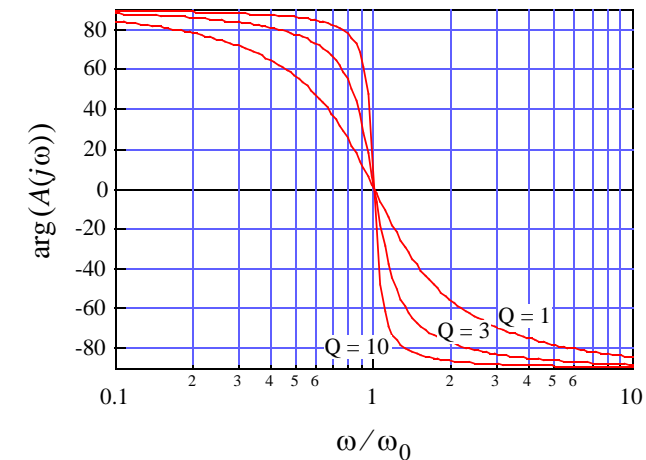
The difference between the frequencies at -3 dB is defined as the bandwidth at -3 dB:

$$B_{-3dB} \equiv \omega_2 - \omega_1 = \frac{\omega_0}{Q} = \omega_0^2 \cdot RC = \frac{R}{L} \quad (2.16)$$

HARMONIC RESPONSE



a) Amplitude.



b) Phase.

Fig 2-6: Transfer function $A(j\omega)$.

FILTERING OF HARMONICS

The attenuation of a sinusoidal signal which is a harmonic frequency of the resonant frequency $\omega = n \cdot \omega_0$ can be calculated from:

$$|A(n\omega_0)| = \frac{1}{\sqrt{1 + Q^2(n - 1/n)^2}} \underset{Q \gg 1}{\cong} \frac{n}{Q(n^2 - 1)} \underset{n \gg 1}{\cong} \frac{1}{Qn} \quad (2.17)$$

The attenuation of harmonics is better when the quality factor is higher. This criterion can help when choosing the quality factor of a resonant circuit.

VOLTAGE AT THE TERMINALS OF THE CAPACITOR AT RESONANCE

One interesting property of the series resonant circuit is that the voltage at the terminals of the capacitor can become much higher than the applied voltage. The transfer function between the input voltage and the voltage at the capacitor terminals is given by:

$$A_C(j\omega) \equiv \frac{V_C}{V_{in}} = \frac{1}{1 - \left(\frac{\omega}{\omega_0}\right)^2 + j\frac{1}{Q}} \quad (2.18)$$

At resonance, the gain is equal to the quality factor:

$$|A_C(\omega = \omega_0)| = Q \quad (2.19)$$

At resonance, the voltage at the capacitor terminals is thus equal to Q times the input voltage. Since the reactances of the inductor and the capacitor are equal at resonance, the voltage at the inductor terminals will also be Q times larger than the input voltage.

EFFECT OF THE SOURCE RESISTANCE

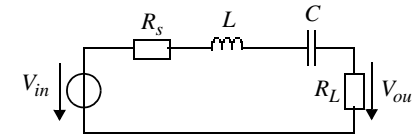


Fig 2-7: Series resonant circuit with source resistance.

In the case in which the source resistance R_s is not negligible with respect to the load resistance R_L , the transfer function of the circuit in Fig. 2-7 is given by:

$$A_v(s) \equiv \frac{V_{out}(s)}{V_{in}(s)} = A_0 \cdot \frac{\frac{s}{\omega_0 Q}}{\left(\frac{s}{\omega_0}\right)^2 + \frac{s}{\omega_0 Q} + 1} \quad (2.20)$$

The transfer function given by Eqn. 2.9 is multiplied by the attenuation factor $A_0 = R_L / (R_s + R_L)$ introduced by the resistive divider operating at resonance. The quality factor is degraded by the presence of the source resistance:

$$Q = \frac{\omega_0 L}{R_s + R_L} \quad (2.21)$$

The addition of a series resistance decreases the quality factor without changing the resonant frequency which remains equal to $\omega_0 = 1/\sqrt{LC}$.

PARALLEL RESONANT CIRCUIT

The parallel resonant circuit shown in Fig. 2-8 is the dual of the series resonant circuit of Fig. 2-4. It has, therefore, all the properties stated for the series resonant circuit. In this case, the admittance has a minimum when the susceptance of the inductor is equal to that of the capacitor. Again, this equality is only true at the resonant frequency given by Eqn. 2.8. The gain in current $A_i(s) \equiv I_{out}/I_{in}$ is identical to Eqn. 2.9.

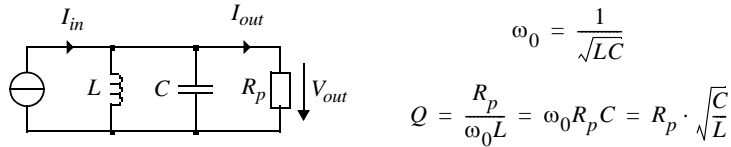


Fig 2-8: Resonant parallel circuit.

The quality factor is simply given by:

$$Q = \frac{R_p}{\omega_0 L} = \omega_0 R_p C = R_p \cdot \sqrt{\frac{C}{L}} \quad (2.22)$$

In contrast to the series resonant circuit, the quality factor of the parallel resonant circuit is proportional to the parallel resistance. The higher this resistance, the higher the quality factor. The impedance of the parallel resonant circuit is simply:

$$Z(s) \equiv \frac{V_{out}}{I_{in}} = R_p \cdot A_i(s) = R_p \cdot \frac{s \frac{L}{R_p}}{s^2 LC + s \frac{L}{R_p} + 1} = R_p \cdot \frac{\frac{s}{\omega_0 Q}}{\left(\frac{s}{\omega_0}\right)^2 + \frac{s}{\omega_0 Q} + 1} \quad (2.23)$$

As with the voltage at the terminals of the capacitor and the inductor of the series resonant circuit, the currents through those same elements of the parallel resonant circuit are Q times higher than the input current I_{in} at resonance.

PARALLEL RESONANT CIRCUIT WITH LOSSES

The impedance of the circuit in Fig. 2-9 is given by:

$$Z(s) = r_s \cdot \frac{s \frac{L}{r_s} + 1}{s^2 LC + sr_s C + 1} \cong r_s \cdot \frac{s \frac{L}{r_s}}{s^2 LC + sr_s C + 1} \quad \text{for: } \omega \gg \frac{r_s}{L} \quad (2.24)$$

For $\omega \gg r_s/L$, the zero can be considered to be practically at the origin and Eqn. 2.24 is identical to Eqn. 2.23 of the parallel resonant circuit, as long as $L/R_p = r_s C$ or:

$$R_p = \frac{L}{r_s C} = \frac{(\omega_0 L)^2}{r_s} = r_s \cdot Q_L^2 \quad (2.25)$$

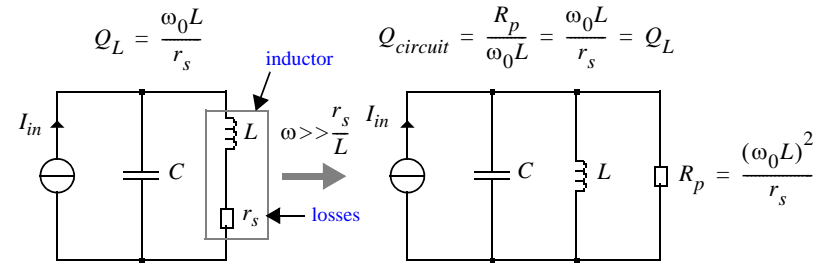


Fig 2-9: Approximation of the resonant circuit with losses.

Therefore, for $\omega \gg r_s/L$, the resonant circuit with a resistance r_s in series with the inductor can be replaced by a parallel resonant circuit with a parallel resistance R_p given by Eqn. 2.25. This approximation is almost always valid because one does not choose an inductor with a mediocre quality factor to make a circuit with a high quality factor. It is interesting to note that the quality factor of the parallel equivalent circuit defined as $Q = R_p / (\omega_0 L)$ is identical to the quality factor of the inductor $Q_L = (\omega_0 L) / r_s$. This quality factor is often called the unloaded quality factor (without load). The addition of a parallel load resistance will reduce the quality factor of the circuit.

COUPLING PARALLEL RESONANT CIRCUITS

For a given resonant frequency, the quality factor sets the bandwidth, but the sharpness of the filter is uniquely determined by the filter's order, that is to say by the number of reactive components. To obtain a filter with a form factor SF close to one (cf Fig. 2-10), several coupled resonant circuits must therefore be used (cf Fig. 2-11).

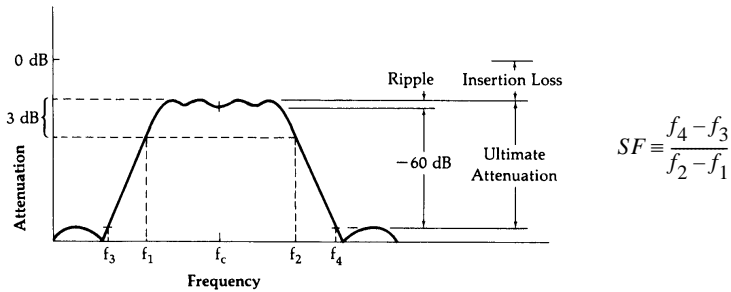


Fig 2-10: Definitions related to filter response.

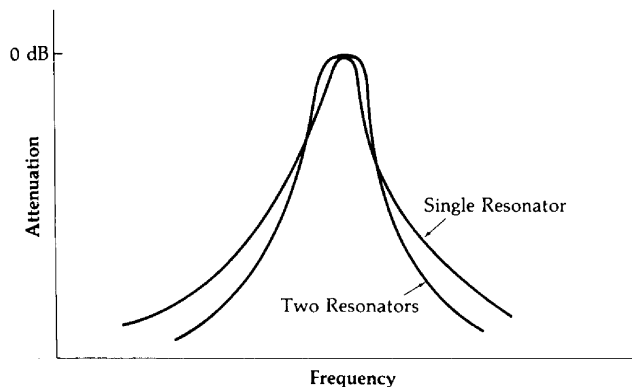


Fig 2-11: Selectivity with one or two coupled resonant circuits.

CRITICAL COUPLING

The intensity of the coupling between two resonant circuits will strongly influence the transfer function of the resulting filter. We distinguish three situations:

- a) Undercoupling: too little coupling leads to high insertion losses (cf Fig. 2-10 and 2-12);
- b) Overcoupling: too much coupling will misalign the two resonant circuits, which results in peaks at the extremities of the passband and a dip in the passband;
- c) Critical coupling: the two circuits are just coupled enough to avoid insertion losses while keeping a sufficient pass-band.

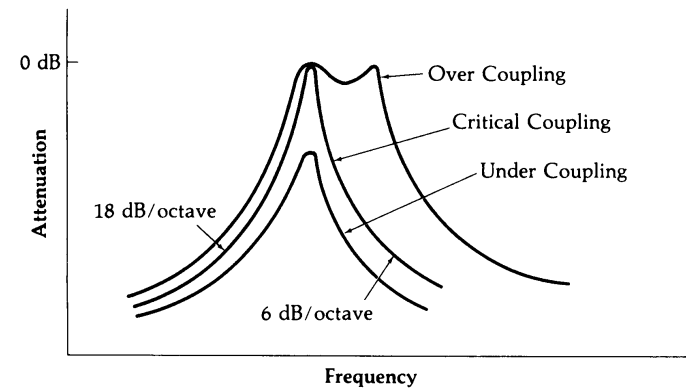


Fig 2-12: The different coupling situations.

There are three ways to couple two resonant circuits:

- 1) Capacitive coupling;
- 2) Inductive coupling;
- 3) Coupling by transformer.

Another more sophisticated way to couple resonant circuits is that of LC ladder filters.

CAPACITIVE COUPLING (1/2)

The circuit corresponding to the capacitive coupling of two resonant circuits is presented in Fig. 2-13. The coupling is realized by the capacitor C_c whose value determines whether the coupling is under, at, or over the critical level.

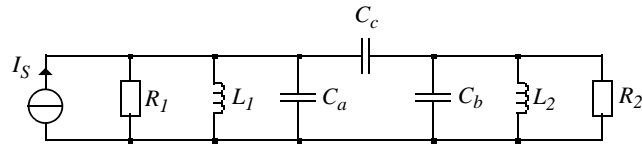


Fig 2-13: Capacitive coupling of two resonant circuits. The circuit in Fig. 2-13 can be modified by considering that the coupling admittance (of C_c) can be replaced by the equivalent circuit of Fig. 2-14.

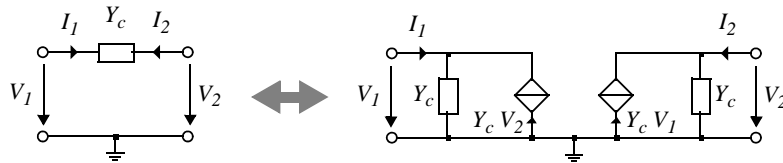


Fig 2-14: Equivalent circuit of the coupling admittance. Applying this substitution to the circuit of Fig. 2-13 we obtain the circuit in Fig. 2-15 in which we clearly see two parallel resonant circuits with admittance Y_1 and Y_2 , along with the coupling by the dependent current sources.

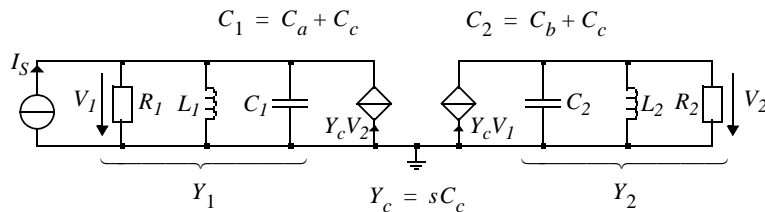


Fig 2-15: Equivalent circuit for circuit in Fig. 2-13.

CAPACITIVE COUPLING (2/2)

Each resonant circuit in Fig. 2-15 is characterized by its resonant frequency and its quality factor:

$$\omega_{0i} \equiv 1/\sqrt{L_i C_i} \quad Q_i \equiv R_i/(\omega_{0i} L_i) = \omega_{0i} R_i C_i \quad i = 1, 2 \quad (2.26)$$

The admittance of each of the resonant circuits is given by:

$$Y_i = \frac{1}{R_i} \cdot \left[1 + jQ_i \left(\frac{\omega}{\omega_{0i}} - \frac{\omega_{0i}}{\omega} \right) \right] = \frac{1}{R_i} \cdot [1 + jQ_i x_i] \quad i = 1, 2 \quad (2.27)$$

The transimpedance is thus given by:

$$Z_m(j\omega) \equiv \frac{V_2}{I_S} = \frac{Y_c}{Y_1 Y_2 - Y_c^2} \quad (2.28)$$

Considering that the resonant frequencies are equal, $\omega_{01} = \omega_{02} = \omega_0$, we get:

$$Z_m(j\omega) = \frac{\frac{j\omega}{\omega_0} KR}{1 - \left(\frac{j\omega}{\omega_0} K\right)^2 - (Qx)^2 + j2qQx} \quad (2.29)$$

$$R \equiv \sqrt{R_1 R_2} \quad Q \equiv \sqrt{Q_1 Q_2} \quad q \equiv \frac{1(Q_1 + Q_2)}{2\sqrt{Q_1 Q_2}} \quad k \equiv \frac{C_c}{\sqrt{C_1 C_2}} \quad K \equiv kQ = \omega_0 R C_c$$

Q is the average quality factor, and q the quality factor disparity coefficient which is minimum and equal to one for $Q_1 = Q_2$. It is represented in Fig. 2-16 as a function of the ratio Q_2/Q_1 . k is the coupling coefficient which is always less than one because C_1 and C_2 are both greater than C_c (cf Fig. 2-15).

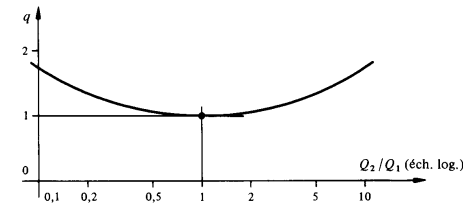


Fig 2-16: Quality factor disparity coefficient.

INDUCTIVE COUPLING

The coupling between two parallel resonant circuits can also be carried out by using a coupling inductor L_c , as shown in Fig. 2-17 a).

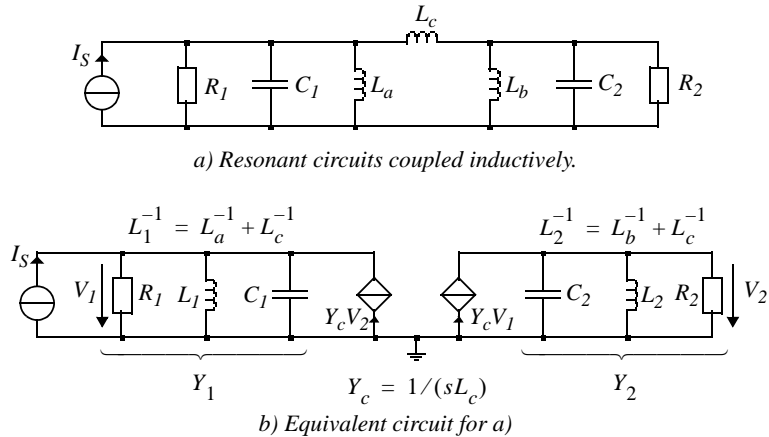


Fig 2-17: Resonant circuits coupled inductively. Eqn. 2.28 remains true with $Y_c = 1/(sL_c)$. In the case in which the resonant frequencies are equal, we get:

$$Z_m(j\omega) = \frac{\frac{\omega_0}{j\omega} KR}{1 - \left(\frac{\omega_0}{j\omega} K\right)^2 - (Qx)^2 + j2qQx} \quad (2.30)$$

All the magnitudes defined in (2.29) remain valid except K which becomes $K \equiv kQ = R/(\omega_0 L_c)$ where k is given by:

$$k = \frac{\sqrt{L_1 L_2}}{L_c} \quad (2.31)$$

COUPLING BY TRANSFORMER

The coupling of two parallel resonant circuits can also be carried out by using a transformer as shown in Fig. 2-18.

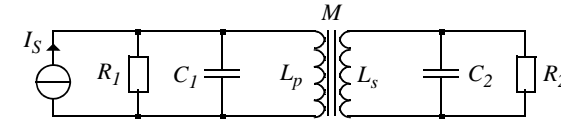


Fig 2-18: Resonant circuits coupled by a transformer. The circuit of Fig. 2-18 can be modified by using the equivalence relation shown in Fig. 2-19. The circuit in Fig. 2-18 is thus returned to that of Fig. 2-17.

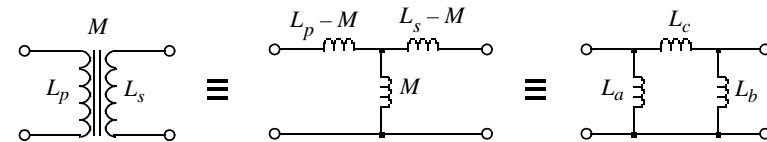


Fig 2-19: Equivalent circuit of a coupling transformer. The relationships obtained for the circuit with inductive coupling are therefore also valid for coupling by transformer, by using the following equalities:

$$\begin{aligned} L_1 &\equiv L_a // L_c = L_p(1 - k^2) \\ L_2 &\equiv L_b // L_c = L_s(1 - k^2) \\ L_c &= \frac{\sqrt{L_p L_s}(1 - k^2)}{k} = \frac{\sqrt{L_1 L_2}}{k} \\ k &= \frac{M}{\sqrt{L_p L_s}} = \frac{\sqrt{L_1 L_2}}{L_c} \end{aligned} \quad (2.32)$$

CRITICAL AND TRANSITIONAL COUPLING (1/2)

The value of the transimpedance Z_m at resonance is obtained by setting $\omega = \omega_0$ in equations (2.29) and (2.30):

$$Z_m(\omega_0) = \pm j \frac{KR}{1+K^2} = \pm j Z_{max} \frac{2K}{1+K^2} \tag{2.33}$$

The + sign corresponds to capacitive coupling and the - sign to inductive (or transformer). The magnitude of the transimpedance at resonance $|Z_m|$ depends on the coupling factor K . Critical coupling results for the value of K which maximizes $|Z_m|$, which is $K = 1$:

$$Z_{max} \equiv |Z_m|_{K=1} = R/2 \tag{2.34}$$

In fact, it corresponds to the maximum transfer of power to the resistor R_2 and therefore to impedance matching. When the coupling factor K is higher than a certain value called the transitional coupling K_t , the magnitude of the transimpedance shows two peaks at the frequencies ω_{-M} and ω_{+M} as indicated in Fig. 2-20.

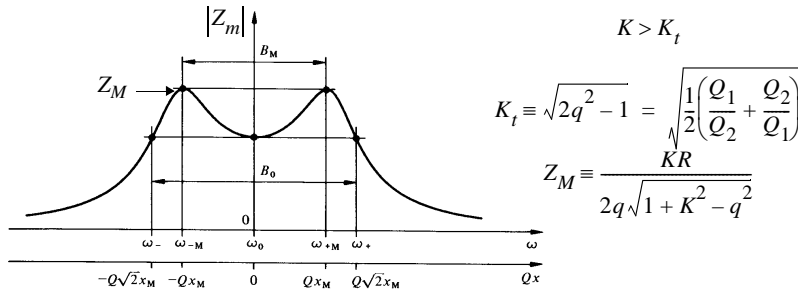


Fig 2-20: Peaks due to overcoupling. The value of the maxima Z_m is given by:

$$Z_M = \frac{KR}{2q\sqrt{1+K^2-q^2}} \tag{2.35}$$

One remarks that $Z_M = Z_{max}$ for $q = 1$ or for $Q_1 = Q_2$.

CRITICAL AND TRANSITIONAL COUPLING (2/2)

Fig. 2-21 a) shows the magnitude of Z_m/Z_{max} as a function of misalignment Qx for different values of the normalized coupling coefficient K for the case in which $Q_1 = Q_2$. We remark that for $K > K_t = 1$, the curves show maxima where Z_M equals Z_{max} . Fig. 2-21 b) shows the magnitude of Z_m/Z_{max} for the case in which the quality factors are different. We remark that the value Z_M of the maxima decreases as K increases. According to Eqn. 2.35, it tends toward $R/(2q)$ as $K \rightarrow \infty$.

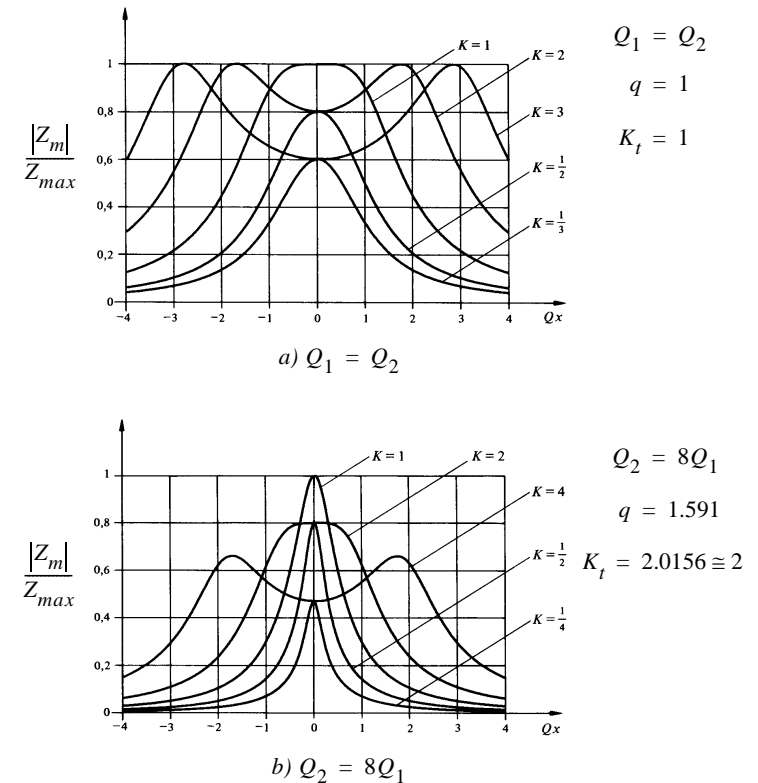


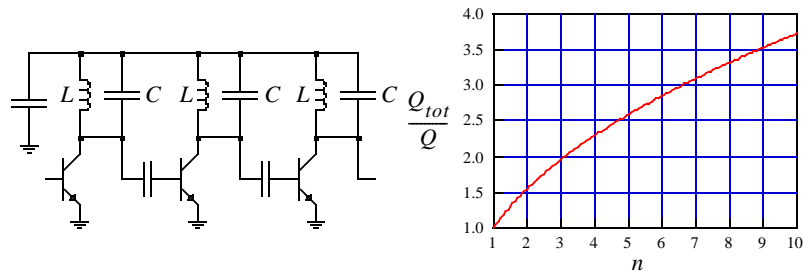
Fig 2-21: Magnitude of the transimpedance as a function of Qx

ACTIVE COUPLING

It is also possible to couple resonant circuits using active devices such as transistors. An example of such a coupling is shown in Fig. 2-22 a). In the case in which all the resonant circuits in the diagram in Fig. 2-22 a) are identical (same frequency and quality factor), the global quality factor Q_{tot} of the circuit is approximately given by:

$$Q_{tot} = \frac{Q}{\sqrt{2^{1/n} - 1}} \quad (2.36)$$

where Q is the quality factor of each of the resonant circuits and n the number of resonant circuits.



a) Example.

b) Global quality factor as a function of the number of resonant circuits (Eqn. 2.36).

Fig 2-22: Active coupling of resonant circuits.

Fig. 2-22 b) shows the global quality factor normalized to the quality factor of one single resonant circuit as a function of the number of stages. Notice that Q_{tot} increases relatively slowly and therefore that the gain in selectivity is only interesting for a reduced number of resonant stages (typically 3 or 4).

CHAPTER 3

DEFINITION OF MATCHING (1/2)

The active power provided by a source represented by its Thevenin equivalent, of internal impedance $Z_S \equiv R_S + jX_S$ with a load impedance $Z_L \equiv R_L + jX_L$ is given by:

$$P = R_L |I|^2 = R_L \left(\frac{V_S}{|Z_S + Z_L|} \right)^2 = \frac{R_L V_S^2}{(R_S + R_L)^2 + (X_S + X_L)^2} \quad (3.1)$$

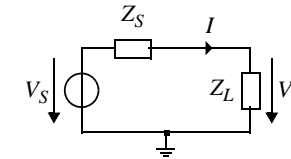


Fig 3-1: Source connected to a load.

For a given source impedance, the power dissipated in R_L is maximum when:

$$\begin{aligned} \frac{\partial P}{\partial X_L} = 0 &\Rightarrow X_L = -X_S \\ \frac{\partial P}{\partial R_L} = 0 &\Rightarrow R_S^2 - R_L^2 + (X_S + X_L)^2 = 0 \Rightarrow R_L = R_S \end{aligned} \quad (3.2)$$

and thus when:

$$\boxed{Z_L = Z_S^*} \quad (3.3)$$

The power transfer from a source to a load is therefore maximum when the load impedance is equal to the complex conjugate of the source impedance. This situation corresponds to matching.

IMPEDANCE MATCHING

DEFINITION OF MATCHING (2/2)

When the load impedance is matched to the source impedance, the load reactance has the opposite sign from the source reactance, and thus they mutually compensate each other. The resulting circuit corresponds to a series connection of the source and load resistances, which are equal, permitting a maximum transfer of power from the source to the load. If the source reactance is that of an inductance, the load reactance should be that of a capacitance, and vice versa. This matching is only valid at the resonance frequency of the inductance and capacitance in series.

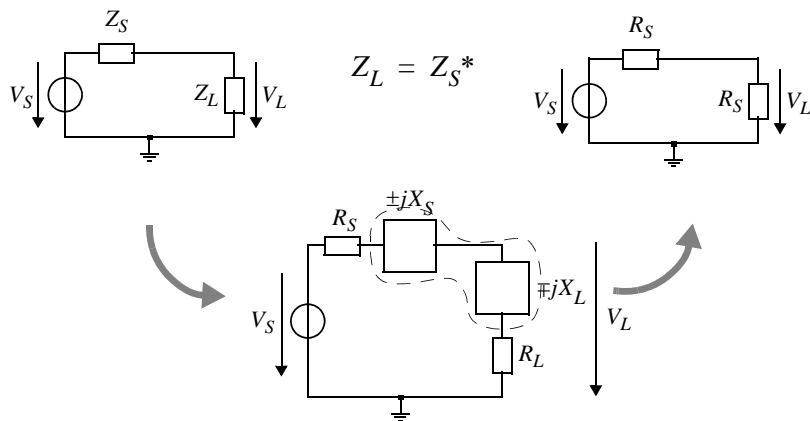


Fig 3-2: Matching the load.

Impedance matching is thus only strictly realized at a single frequency, which is the resonant frequency of the series resonant circuit. The matching worsens as the frequency gets farther from the resonant frequency, which can cause problems for circuits with a large passband. There are methods for increasing the band of frequencies for which there is matching and therefore maximum power transfer. These methods generally use circuits with a low quality factor.

PRINCIPLE OF IMPEDANCE MATCHING

Impedance matching consists of synthesizing a non-dissipating circuit (thus containing only inductors and capacitors) inserted between the source and the load, such that the impedance as seen from the source is equal to the complex conjugate of the source impedance. Of course there are an infinite number of circuits, more or less complex, that satisfy this criterion.

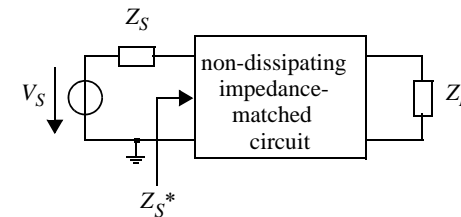


Fig 3-3: Principle of impedance matching.

All of the following methods are based on the equivalence between the series and parallel circuits illustrated in Fig. 3-4. The unloaded Q is the quality factor of the impedance-matched circuit associated either with the source or the load resistance. The loaded Q is the quality factor of the complete circuit (with the source and load). Since $R_S = R_L$, the loaded quality factor is equal to half of the unloaded quality factor.

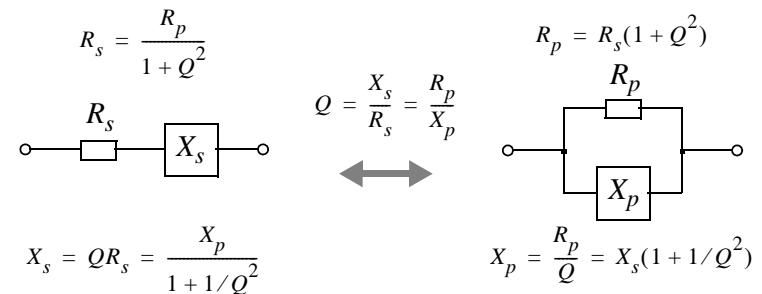


Fig 3-4: Series / parallel equivalence.

L NETWORKS (1/4)

When the source and load impedances are purely resistive and $R_L > R_S$, it is necessary to lower the impedance seen from the source by placing a reactance (inductor or capacitor) in parallel with the load. One must then compensate the reactance of the shunt element just added by placing a reactance with the opposite sign in series. In the case shown in Fig. 3-5 there is a capacitor C in parallel with the load R_L .

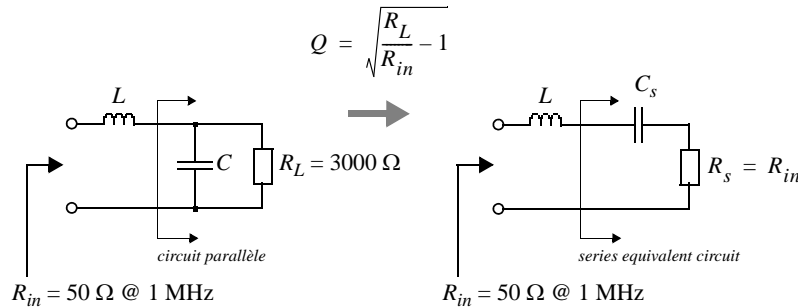


Fig 3-5: Example of an L circuit, impedance step-down. This parallel circuit can be transformed to an equivalent series circuit in which the series resistance will be equal to the source resistance, in this case 50 Ω. The two have the same quality factor:

$$R_s = \frac{R_L}{1 + Q^2} \Rightarrow Q = \sqrt{\frac{R_L}{R_s} - 1} = \sqrt{\frac{3000}{50} - 1} = 7.7 \quad (3.4)$$

from which we calculate the reactance of the inductor and the capacitor:

$$X_L = X_{C_s} = QR_s = QR_{in} = 7.7 \times 50 = 384 \Omega$$

$$X_C = R_L/Q = 3000/7.7 = 391 \Omega$$

and thus:

$$L = X_L/(2\pi f) = 384/(2\pi \times 10^6) = 69 \mu H$$

$$C = 1/(2\pi f X_C) = 1/(2\pi \times 10^6 \times 391) = 407.5 pF$$

L NETWORKS (2/4)

The amplitude of the impedance of the circuit in Fig. 3-5 is represented in Fig. 3-6. We note that the reactance of Z_{in} cancels out at the resonant frequency for which the input impedance is equal to 50 Ω. Notice that the circuit in Fig. 3-5 performs low-pass filtering. In certain cases, a high-pass characteristic is preferable, and is obtained by simply switching the capacitor and the inductor.

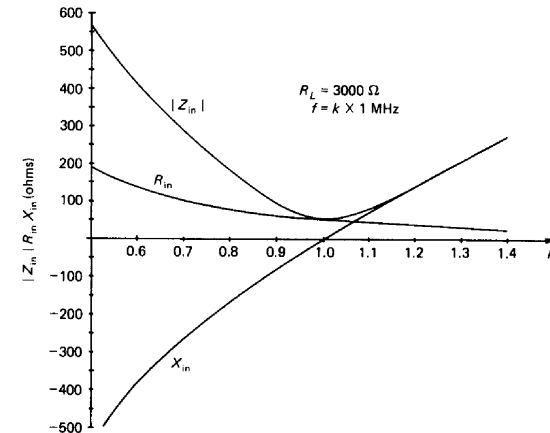


Fig 3-6: Input impedance of the circuit in Fig. 3-5. Since the two reactances must be of opposite signs, one of the components will be an inductor and the other a capacitor. There are therefore only two L networks which lower the impedance as seen from the source. They are shown in Fig. 3-7.

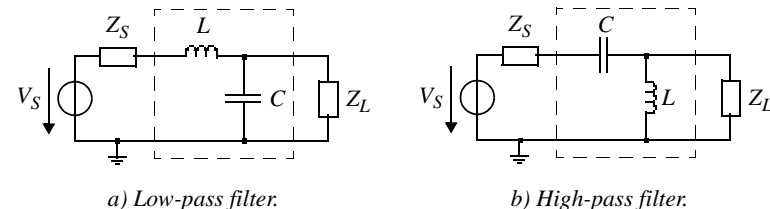


Fig 3-7: L networks, impedance step-down ($R_L > R_S$).

L NETWORKS (3/4)

When the source and load impedances are purely resistive and $R_L < R_S$, it is necessary to increase the impedance seen from the source by placing a reactance (inductor or capacitor) in series with the load. One must then compensate the reactance of the series element just added by placing a reactance of opposite sign in parallel. In the case shown in Fig. 3-8, an inductor L has been placed in series with the load R_L .

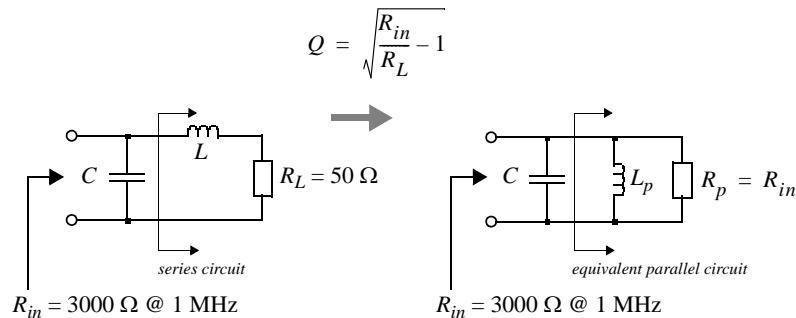


Fig 3-8: Example of L network, impedance step-up. The series circuit can be transformed to its parallel equivalent according to:

$$R_p = R_L(1 + Q^2) \Rightarrow Q = \sqrt{\frac{R_p}{R_L} - 1} = \sqrt{\frac{R_{in}}{R_L} - 1} = 7.7 \quad (3.5)$$

One can thus calculate the reactance of the inductor and the capacitor:

$$X_C = X_{Lp} = R_p / Q = R_{in} / Q = 3000 / 7.7 = 391 \Omega$$

$$X_L = QR_L = 7.7 \times 50 = 384 \Omega$$

and the values of the components for the desired frequency:

$$C = 1 / (2\pi f X_C) = 1 / (2\pi \times 10^6 \times 391) = 407.5 \text{ pF}$$

$$L = X_L / (2\pi f) = 384 / (2\pi \times 10^6) = 61.1 \mu\text{H}$$

L NETWORKS (4/4)

The amplitude of the impedance of the circuit in Fig. 3-8 is represented in Fig. 3-9. We note once again that the reactance of Z_{in} cancels out at the resonant frequency for which the input impedance is equal to 3000Ω . The circuit in Fig. 3-8 performs low-pass filtering, which can be changed to high-pass filtering by simply switching the inductor and the capacitor.

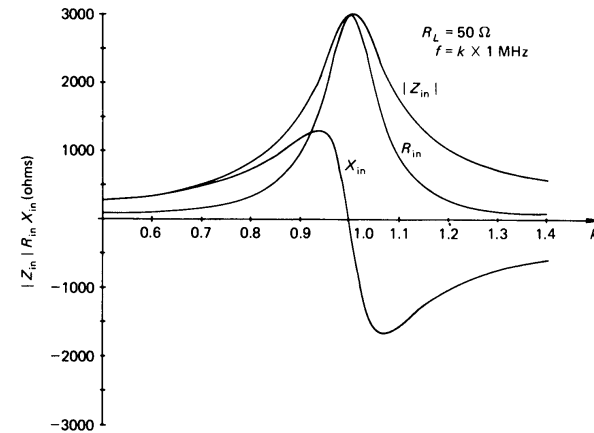


Fig 3-9: Input impedance for the circuit in Fig. 3-8. There are two L networks which allow us to increase the impedance as seen from the source. They are shown in Fig. 3-10.

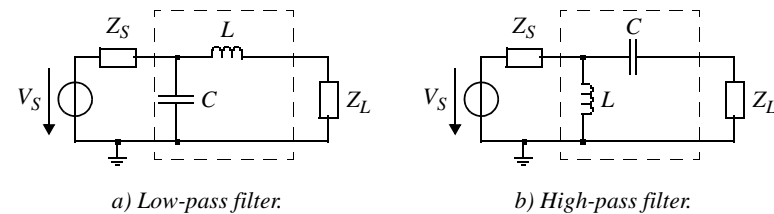


Fig 3-10: L networks, impedance step-up ($R_L < R_S$).

COMPLEX SOURCE AND LOAD IMPEDANCES (1/4)

In the preceding examples, we supposed that the source and load impedances were real. In reality, they are rarely real. For example, the input and output impedances of a bipolar transistor are always complex. There are two methods for handling the reactances of the source and load:

- absorption:** the reactances of the source and load can be taken into account in the impedance matching network by placing the components such that the functional capacitors of the network are in parallel with the parasitic capacitances and the functional inductors in series with the parasitic inductances.
- resonance:** cancel out the effect of the reactances of the source and load by placing a reactance of the opposite sign in parallel or in series.

Note that absorption is only possible when the value of the parasitic element is smaller than that of the functional element from which it must be subtracted. These two techniques can naturally be combined.

By way of example we synthesize an impedance matching network using the absorption method for the circuit in Fig. 3-11.

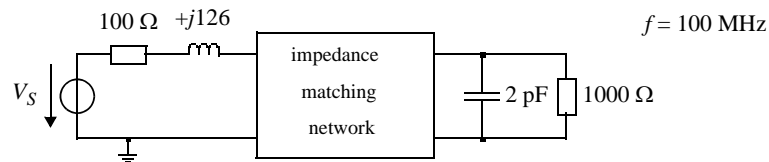


Fig 3-11: Complex source and load impedances.

At first we ignore the source and load reactances. The load resistance being larger than the source resistance, we choose the L network of Fig. 3-7 a).

COMPLEX SOURCE AND LOAD IMPEDANCES (2/4)

The quality factor is given by:

$$Q = \sqrt{R_L/R_S - 1} = 3$$

from which we get:

$$X_s = QR_S = 3 \times 100 = 300 \Omega \Rightarrow L = \frac{X_s}{2\pi f} = \frac{300}{2\pi \times 10^8} = 477 \text{ nH}$$

$$X_p = \frac{R_p}{Q} = \frac{R_L}{Q} = \frac{1000}{3} = 333 \Omega \Rightarrow C = \frac{1}{2\pi f X_p} = \frac{1}{2\pi \times 10^8 \times 333} = 4.8 \text{ pF}$$

We thus obtain the diagram shown in Fig. 3-12 a). By then subtracting the value of the 477 nH series source inductance and the value of the 4.8 pF parallel load capacitance, we obtain the diagram in Fig. 3-12 b).

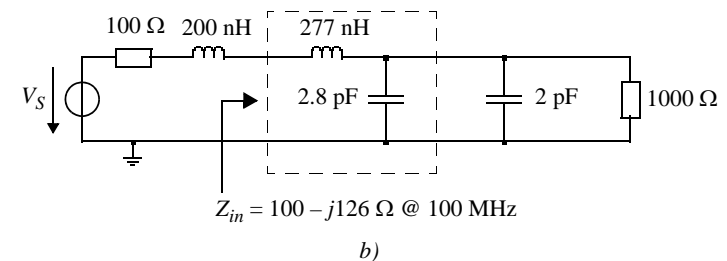
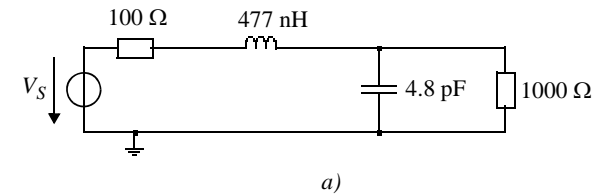


Fig 3-12: Illustration of the absorption method.

COMPLEX SOURCE AND LOAD IMPEDANCES (3/4)

Another example, illustrating the load resonance technique, is given in Fig. 3-13 a). We want to synthesize a high-pass impedance-matching circuit. The fact that the load resistance is larger than the source resistance means that we must use the circuit shown in Fig. 3-7 b). But before calculating the elements of the L network, we must rid ourselves of the load capacitance by connecting a parallel inductor whose value is calculated according to:

$$L = \frac{1}{(2\pi f)^2 C_L} = \frac{1}{(2\pi \times 75 \times 10^6)^2 \times 40 \times 10^{-12}} = 112.6 \text{ nH}$$

We therefore get the circuit of Fig. 3-13 b) from which we can calculate the elements of the L network:

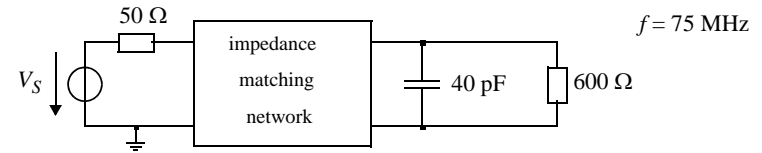
$$Q = \sqrt{\frac{R_L}{R_S} - 1} = \sqrt{\frac{600}{50} - 1} = 3.32$$

$$X_s = QR_s = 3.32 \times 50 = 166 \Omega \Rightarrow C = \frac{1}{2\pi f X_s} = \frac{1}{2\pi \times 75 \times 10^6 \times 166} = 12.78 \text{ pF}$$

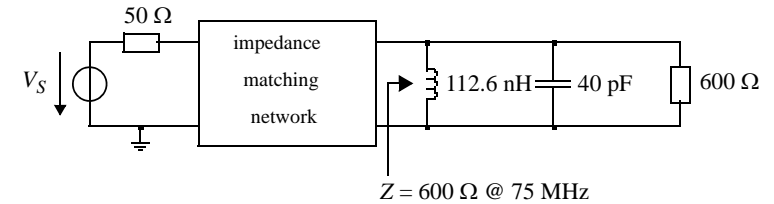
$$X_p = \frac{R_p}{Q} = \frac{R_L}{Q} = \frac{600}{3.32} = 181 \Omega \Rightarrow L = \frac{X_p}{2\pi f} = \frac{181}{2\pi \times 75 \times 10^6} = 384 \text{ nH}$$

We thus obtain the circuit in Fig. 3-13 c) which can be simplified further by calculating the equivalent inductance for the two parallel inductances connected to the load. Finally, we obtain the circuit in Fig. 3-13 d).

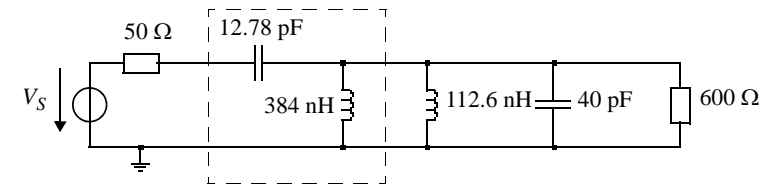
COMPLEX SOURCE AND LOAD IMPEDANCES (4/4)



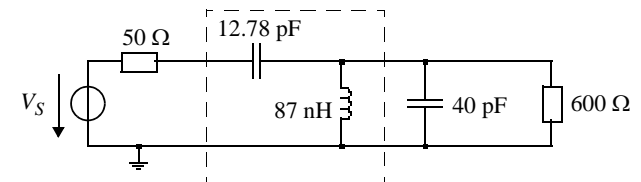
a) Circuit with complex load.



b) Addition of an inductor to compensate the load capacitance by resonance.



c) Synthesis of an L network for a resistive load.



d) Final circuit.

Fig 3-13: Illustration of the resonance technique.

THREE-ELEMENT MATCHING NETWORKS

The disadvantage of L networks comes from the fact that when the source and load resistances are specified, the quality factor and therefore the selectivity of the impedance-matching network are likewise specified (cf Eqn. 3.4 and 3.5). There are then not enough degrees of freedom to choose the quality factor independently, which can be irritating for certain applications in which we want selectivity. To compensate for this problem, it is possible to add an element and thus a degree of freedom permitting us to set the quality factor. This Q will necessarily be larger than the quality factor corresponding to an L network. The L network is thus the impedance-matching network having the minimum quality factor.

There are two types of three-element matching networks (cf Fig. 3-14):

- 1) Π networks;
- 2) T networks;

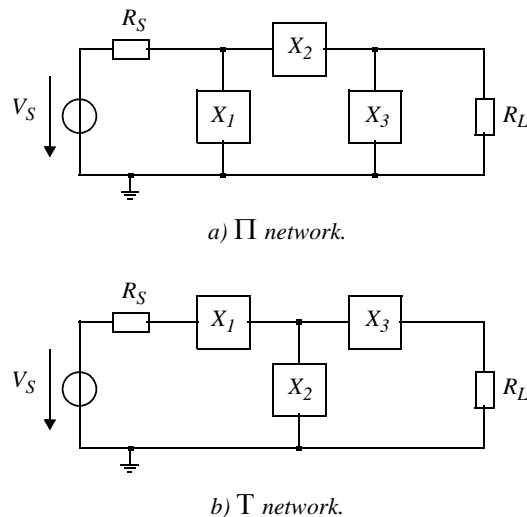


Fig 3-14: 3-element matching networks.

Π NETWORKS

One can describe the Π network as the connection of two L networks with a virtual resistance as shown in the diagram in Fig. 3-15. This virtual resistance is just used to dimension the elements of the L networks. The reactances X_{s1} and X_{p1} as well as X_{s2} and X_{p2} must be of different types (if for example X_{s1} corresponds to a capacitance, X_{p1} must correspond to an inductance).

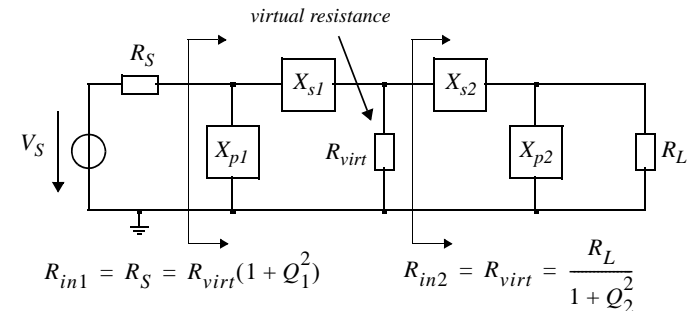


Fig 3-15: Π network represented as two L networks.

The virtual resistance R_{virt} represents the resistance seen from the center point $R_{in2} = R_{virt} = R_L / (1 + Q_2^2)$ with $Q_2 = R_L / X_{p2}$, from which we get $Q_2 = \sqrt{R_L / R_{virt} - 1}$. In addition, the resistance seen from the source must be equal to R_S , imposing $R_{in1} = R_S = R_{virt}(1 + Q_1^2)$ with $Q_1 = X_{s1} / R_{virt}$ and therefore $Q_1 = \sqrt{R_S / R_{virt} - 1}$. We remark that for the quality factors Q_1 and Q_2 to exist, the virtual resistance must be less than R_S or R_L . The quality factor of the Π network is associated to that of the L network section having the larger quality factor, and the section having the larger quality factor is on the side with the higher terminating impedance. This gives us the definition of the quality factor of a Π network:

$$Q_{\Pi} \equiv \sqrt{\frac{R_{max}}{R_{virt}} - 1} \tag{3.6}$$

where R_{max} represents the larger of the resistances R_S or R_L .

Π NETWORK EXAMPLE (1/2)

As an example, we will match a load resistance of $50\ \Omega$ to a source resistance of $3000\ \Omega$ by using a Π network, conserving a quality factor of 10 (cf Fig. 3-16).

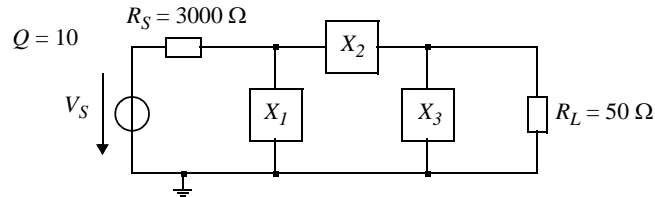


Fig 3-16: Example of designing a Π network. The frequency is equal to 1 MHz. R_{virt} is calculated from Eqn. 3.6 with $R_{max} = R_S = 3000\ \Omega$:

$$R_{virt} = \frac{R_{max}}{1 + Q^2} = \frac{3000}{1 + 10^2} = 29.703\ \Omega$$

The reactances of the first section are thus given by:

$$X_{p1} = R_S / Q = 3000 / 10 = 300\ \Omega$$

$$X_{s1} = QR_{virt} = 10 \times 29.7 = 297.03\ \Omega$$

The quality factor of the second L network section is then set by the resistances R_{virt} and R_L :

$$Q_2 = \sqrt{\frac{R_L}{R_{virt}}} - 1 = \sqrt{\frac{50}{29.703}} - 1 = 0.8266$$

The resistance R_L must now be matched to the virtual resistance. Since it appears in a parallel branch, we have:

$$X_{s2} = Q_2 R_{virt} = 0.8266 \times 29.7 = 24.55\ \Omega$$

$$X_{p2} = R_L / Q_2 = 50 / 0.8266 = 60.49\ \Omega$$

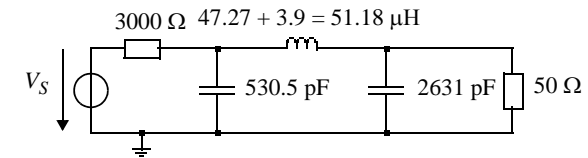
As a result of choosing inductors for the series branches, the shunt branches will therefore be capacitors:

$$C_1 = \frac{1}{2\pi f X_{p1}} = 530.5\ \text{pF} \quad L_1 = X_{s1} / (2\pi f) = 47.27\ \mu\text{H}$$

$$C_2 = \frac{1}{2\pi f X_{p2}} = 2631\ \text{pF} \quad L_2 = X_{s2} / (2\pi f) = 3.9\ \mu\text{H}$$

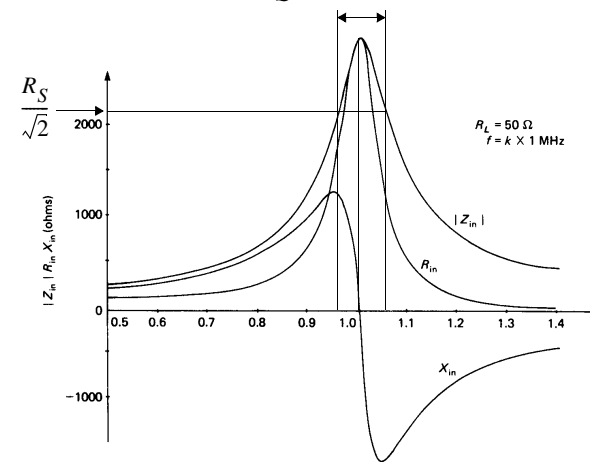
Π NETWORK EXAMPLE (2/2)

We finally obtain the circuit shown in Fig. 3-17 a), for which the magnitude of the input impedance is shown as a function of the frequency in Fig. 3-17 b). We notice that the imposed quality factor corresponds well to the bandwidth at -3 dB and that the form factor is larger than that of Fig. 3-6, because this is a 3rd order filter.



a) Final circuit.

$$B = \frac{f_0}{Q} = \frac{1\ \text{MHz}}{10} = 100\ \text{kHz}$$



b) Input impedance of the circuit in Fig. 3-17 a).

Fig 3-17: Example of the design of a Π network.

T NETWORKS

The T network can be described as two back-to-back L networks of which the shunt branches are in parallel, as shown in Fig. 3-18. The difference with respect to the Π network is that in the T network, the virtual resistance is larger than both the source and load resistances. The T network is often used for matching small impedances with a high quality factor.

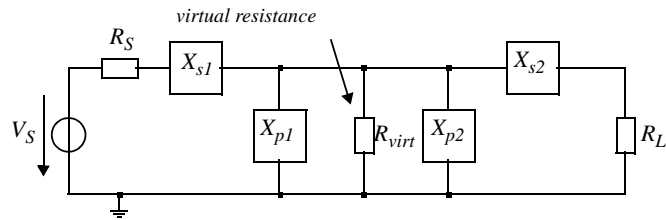


Fig 3-18: The T network represented as two L networks. The quality factor of the T network is determined by the L network section with the higher quality factor. By definition, the section with the higher quality factor is at the side with the smaller terminating resistor. Q is determined by the formula:

$$Q_T \equiv \sqrt{\frac{R_{virt}}{R_{min}} - 1} \tag{3.7}$$

where R_{min} is the smaller terminating resistor.

T NETWORK EXAMPLE

As an example, we would like to design a T network to match a source resistance of 10Ω to a load resistance of 50Ω with a quality factor of 10. We would like to use a minimum number of inductors, and we want the resulting filter to be of type pass-band.

The virtual resistance is calculated from Eqn. 3.7:

$$R_{virt} = R_{min}(Q^2 + 1) = R_S(Q^2 + 1) = 10 \times 101 = 1010\Omega$$

The section with the higher quality factor is on the source side. The reactances of the corresponding L network section are:

$$X_{s1} = QR_S = 10 \times 10 = 100\Omega \quad X_{p1} = R_{virt}/Q = 1010/10 = 101\Omega$$

The quality factor of the L network section on the load side is determined by the resistances R_{virt} and R_L :

$$Q_2 = \sqrt{R_{virt}/R_L - 1} = \sqrt{1010/50 - 1} = 4.4$$

$$X_{p2} = R_{virt}/Q_2 = 1010/4.4 = 230\Omega \quad X_{s2} = Q_2 R_L = 4.4 \times 50 = 220\Omega$$

One possible design in which there is only one inductor and the filtering characteristic is of type passband is shown in Fig. 3-19.

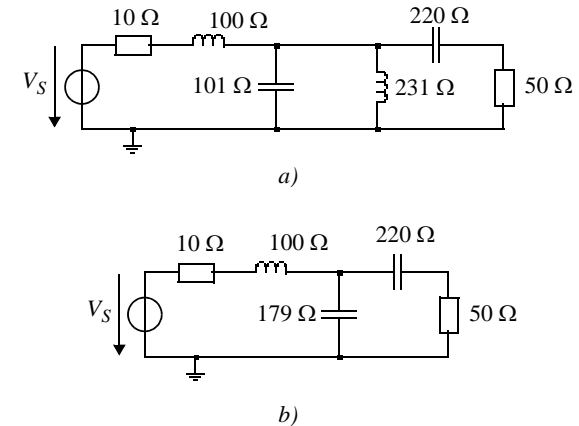
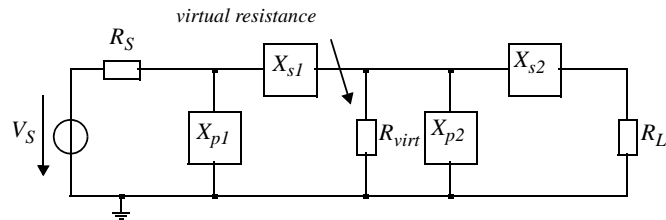


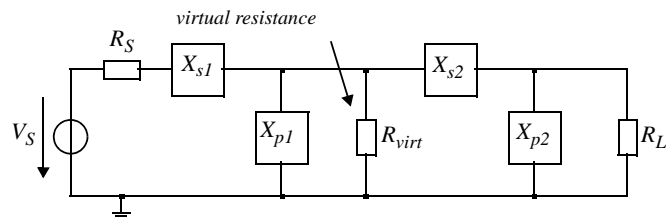
Fig 3-19: Example of T network.

WIDEBAND IMPEDANCE MATCHING (1/2)

Up until now we have seen L networks for which the quality factor was determined by the source and load resistances, and Π and T networks which allow us to choose a quality factor independently of the source and load, as long as it is higher than that of the L network. These circuits are thus appropriate for narrow-band impedance matching. To match impedances over a wider band (or to have a quality factor smaller than that of the simple L network), we can use two cascaded L networks like those presented in Fig. 3-20. In these configurations, the value of the virtual resistance must be between those of the termination resistances, with the result that the quality factor goes from that of an L network to that of a Π or T network.



a) It can be proved that R_L must be smaller than R_S to use this configuration.



b) It can be proved that R_L must be larger than R_S to use this configuration.

Fig 3-20: Low quality factor (wideband) matching network.

WIDEBAND IMPEDANCE MATCHING (2/2)

The minimum quality factor and therefore the maximum bandwidth are obtained when:

$$R_{virt} = \sqrt{R_S R_L} \quad (3.8)$$

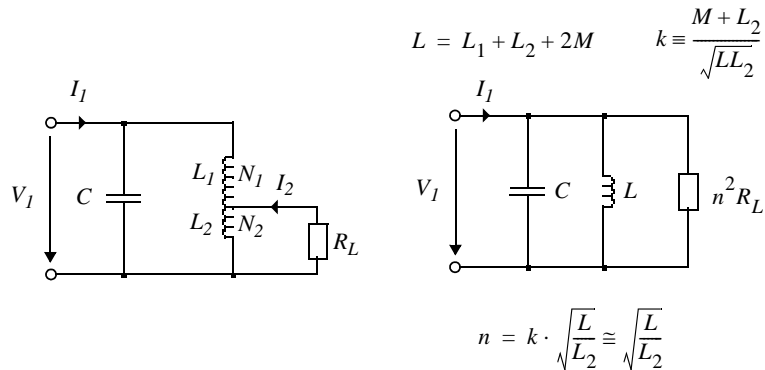
The quality factor is thus defined by:

$$Q \equiv \sqrt{\frac{R_{virt}}{R_{min}} - 1} = \sqrt{\frac{R_{max}}{R_{virt}} - 1} \quad (3.9)$$

where R_{virt} is the virtual resistance and R_{min} and R_{max} are, respectively, the smaller and larger terminating resistances.

MATCHING WITH AN AUTOTRANSFORMER

The impedance matching of two circuits can also be carried out by using an inductor with a central lead (or autotransformer) or a capacitive divider. These matching networks are useful when one wants to create, for example, a parallel resonant circuit with a high quality factor, loaded with a small impedance.



a) Autotransformer.

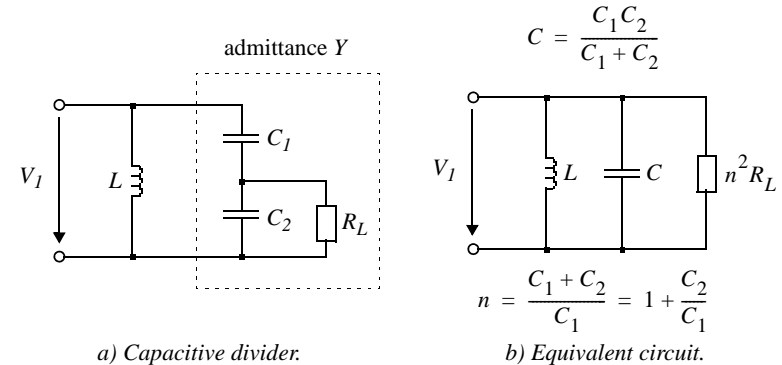
b) Equivalent circuit.

Fig 3-21: Impedance matching by autotransformer. The equivalent resistance in parallel with the LC circuit is equal to the load resistance R_L multiplied by a factor n^2 :

$$R'_L = n^2 \cdot R_L \cong \frac{L}{L_2} \cdot R_L \quad (3.10)$$

IMPEDANCE MATCHING WITH A CAPACITIVE DIVIDER

It is also possible to do impedance matching with a capacitive divider, as shown in Fig. 3-22.



a) Capacitive divider.

b) Equivalent circuit.

Fig 3-22: Impedance matching with a capacitive divider. The admittance Y appearing in parallel with the inductance L in the diagram in Fig. 3-22 a) has the value:

$$Y(s) = sC_1 \cdot \frac{1 + sR_L C_2}{1 + sR_L(C_1 + C_2)} = G_p + j \cdot X_p \quad (3.11)$$

For frequencies $\omega \gg (R_L C_2)^{-1} > [R_L(C_1 + C_2)]^{-1}$, this admittance can be broken up into a parallel conductance

$$G_p \cong \frac{1}{R'_L} = \frac{(\omega C_1)^2 R_L}{1 + (\omega R_L(C_1 + C_2))^2} \cong \frac{1}{R_L [1 + C_2/C_1]^2} \quad (3.12)$$

and a capacitance C equal to the series connection of C_1 and C_2 . The resistance seen at the terminals of the circuit at the resonant frequency of the parallel LC is thus equal to the load resistance multiplied by a factor n^2 :

$$R'_L = n^2 \cdot R_L = \left[1 + \frac{C_2}{C_1} \right]^2 \cdot R_L \quad (3.13)$$

SMITH CHARTS

The Smith Chart is probably one of the most useful graphical tools for the conception of HF circuits, and specifically for the synthesis of impedance matching networks. It was invented in the 1930's by an engineer at Bell Labs named Phillip Smith. The Smith Chart is a bilinear transformation of the plane of normalized impedances z to the plane of the reflection coefficient Γ :

$$\Gamma = \frac{z-1}{z+1} = \frac{Z/Z_0-1}{Z/Z_0+1} = \frac{Z-Z_0}{Z+Z_0} \quad (3.14)$$

where Z_0 is the normalization impedance, usually 50Ω . The Smith Chart lets us find the impedance z when we know the reflection coefficient Γ or vice versa.

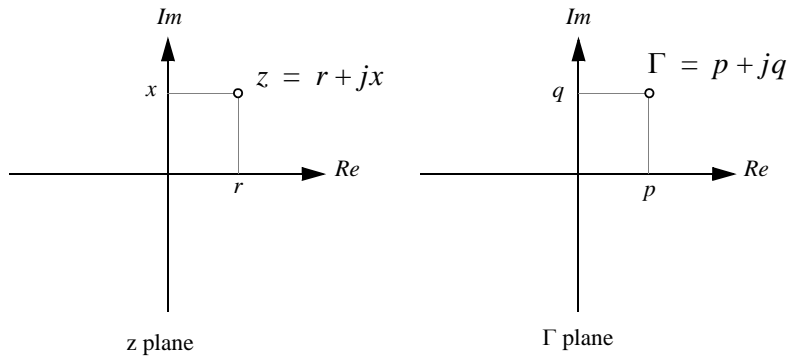


Fig 3-23: Transformation of the z plane to the Γ plane. By setting $z = r + jx$ and $\Gamma = p + jq$, and knowing r and x , p and q must be determined from the following relationship:

$$\Gamma = p + jq = \frac{(r-1) + jx}{(r+1) + jx} \quad (3.15)$$

SMITH CHART CONSTRUCTION (1/2)

Constant resistance circles

By setting the real and imaginary parts of Eqn. 3.15 to be equal, we find the equations which describe the curves of constant r :

$$\left(p - \frac{r}{r+1}\right)^2 + q^2 = \left(\frac{1}{r+1}\right)^2 \quad (3.16)$$

as well as those of constant x :

$$(p-1)^2 + \left(q - \frac{1}{x}\right)^2 = \left(\frac{1}{x}\right)^2 \quad (3.17)$$

The curves for $r = const$ defined by Eqn. 3.16 are circles with radius $1/(r+1)$ of which the center is located on the real axis at the point $r/(r+1)$. The two intersections with the real axis are located at $(r-1)/(r+1)$ and 1 . For r varying from 0 to 10, we obtain the network of circles shown in Fig. 3-24. Each point on one of these circles has the same (normalized) resistance.

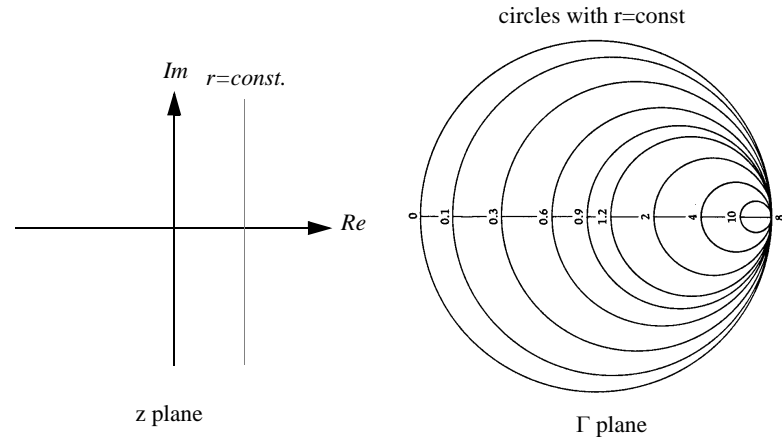


Fig 3-24: Constant resistance circles

SMITH CHART CONSTRUCTION (2/2)

Constant reactance circles

The curves with $x = \text{const}$ defined by Eqn. 3.17 are also circles, with radius $1/x$ of which the center is located at coordinates $(1, 1/x)$. For x varying from 0.1 to 10, we get the network of circles shown in Fig. 3-25. Each point of one of these circles has the same (normalized) reactance.

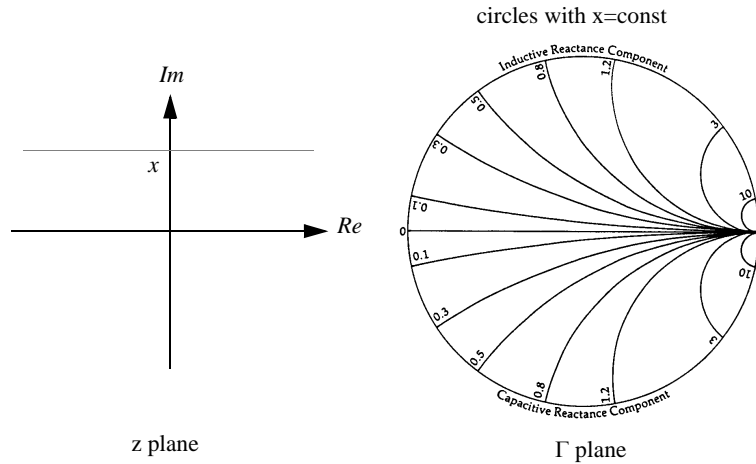


Fig 3-25: Constant reactance circles.

IMPEDANCE CHARTS

The superposition of constant resistance and constant reactance circles gives the complete Smith Chart of impedances, as shown in Fig. 3-26. The exterior circle corresponds to zero resistance or a purely imaginary impedance. The upper part corresponds to a positive reactance and thus to an inductance, while the lower part corresponds to a negative reactance and thus to a capacitance. The horizontal diameter corresponds to zero reactance and thus to a purely resistive impedance.

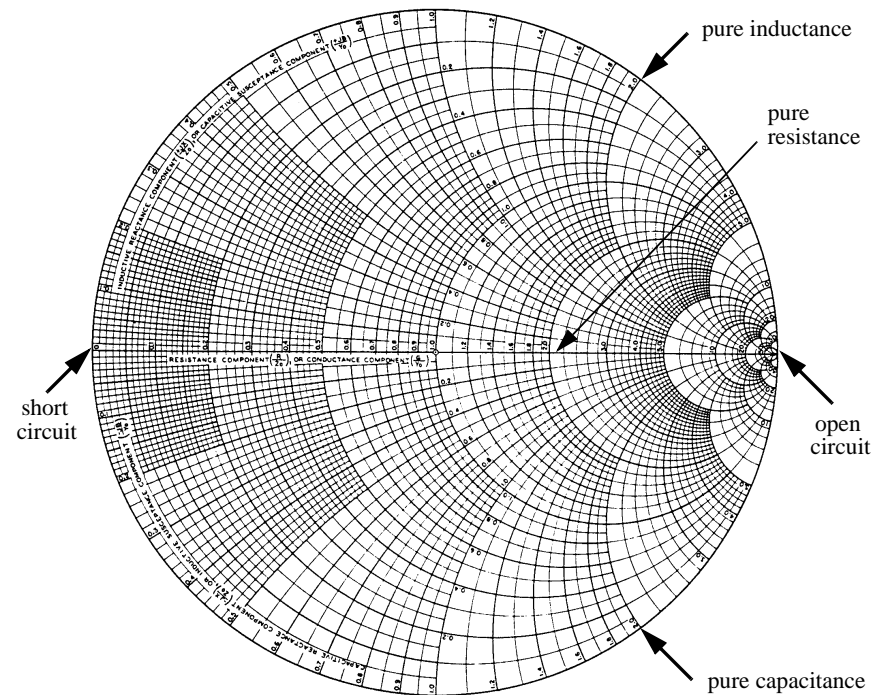


Fig 3-26: Impedance chart.

ADDITION OF A SERIES CAPACITOR

Fig. 3-27 represents the effect of the series addition of a normalized negative reactance $-j1.0$ (corresponding to a capacitance) with a normalized impedance $z = 0.5 + j0.7$. The resulting impedance is thus given by $z = 0.5 + j0.7 - j1.0 = 0.5 - j0.3$. The series addition of this capacitor corresponds graphically to moving around the constant resistance circle $r = 0.5$ counter-clockwise.

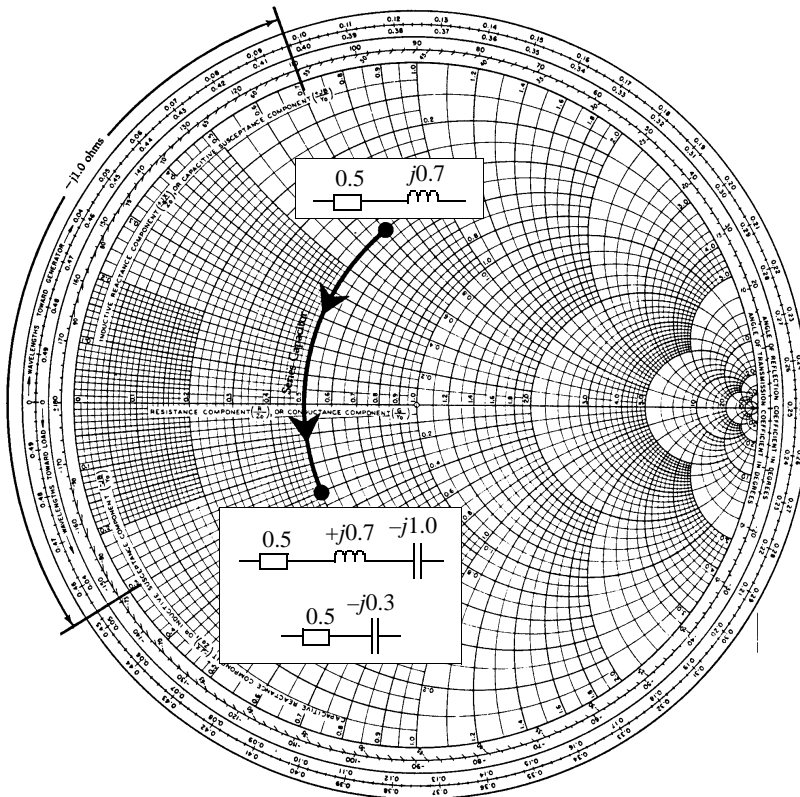


Fig 3-27: Addition of a series capacitor.

ADDITION OF A SERIES INDUCTOR

Fig. 3-28 represents the effect of the series addition of a positive reactance $j1.8$ (corresponding to an inductance) with a normalized impedance $z = 0.8 - j1.0$. The resulting impedance is equal to $z = 0.8 - j1.0 + j1.8 = 0.8 + j0.8$. The series addition of this inductor corresponds graphically to moving around the constant resistance circle 0.8 clockwise.

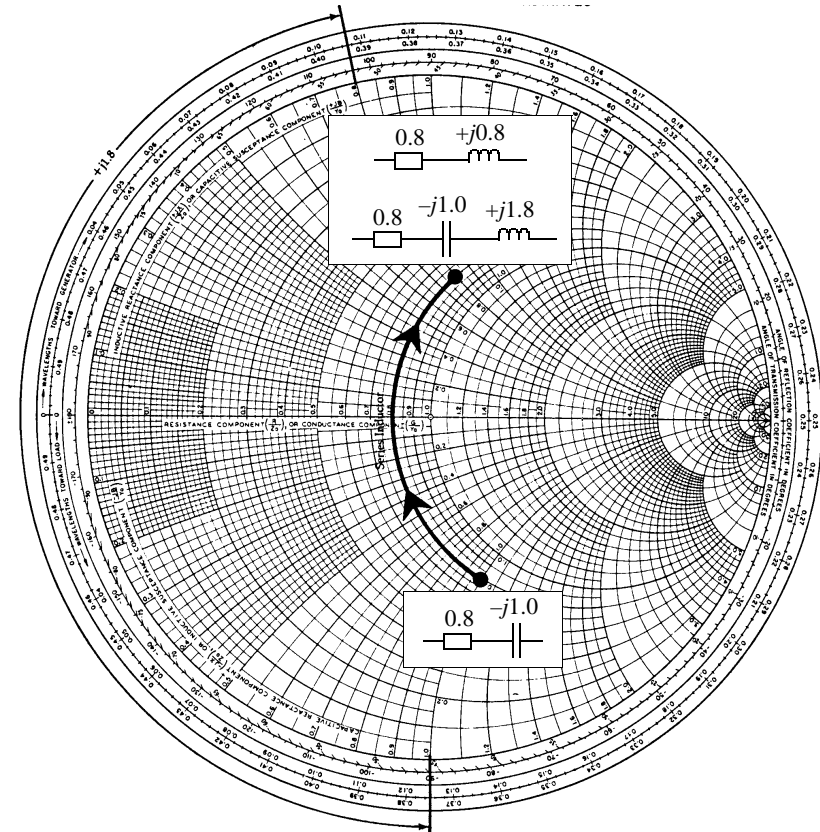


Fig 3-28: Addition of a series inductor.

CONVERTING IMPEDANCE TO ADMITTANCE

The Smith Chart can be used to convert an impedance z to an admittance $y = 1/z = g \pm jb$. Let's look at $z = 1 + j$, for example. The corresponding admittance is $y = 1/z = 0.5 - j0.5$. The two corresponding points are shown in Fig. 3-29. Note that they are the same distance d from the origin, but in opposite directions. On the Smith Chart, one easily finds the admittance corresponding to an impedance by moving the distance between z and the origin, but in the opposite direction.

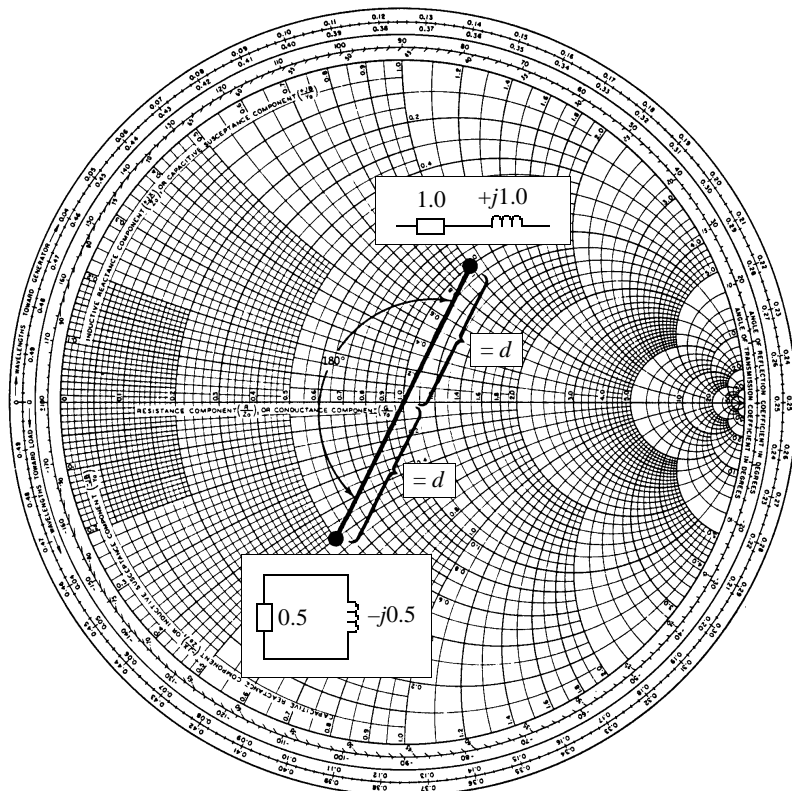


Fig 3-29: Conversion of impedance to admittance.

COMBINED IMPEDANCE AND ADMITTANCE CHART

By rotating the impedance chart by 180° , we obtain the admittance chart. Fig. 3-30 shows the superposition of these two charts. One single point now simultaneously corresponds to an impedance and its admittance, of which the values can be read from the respective charts. Notice that because the admittance chart is found by the 180° rotation of the impedance chart, the upper half corresponds to negative susceptances (inductances) and the lower half to positive susceptances (capacitances).

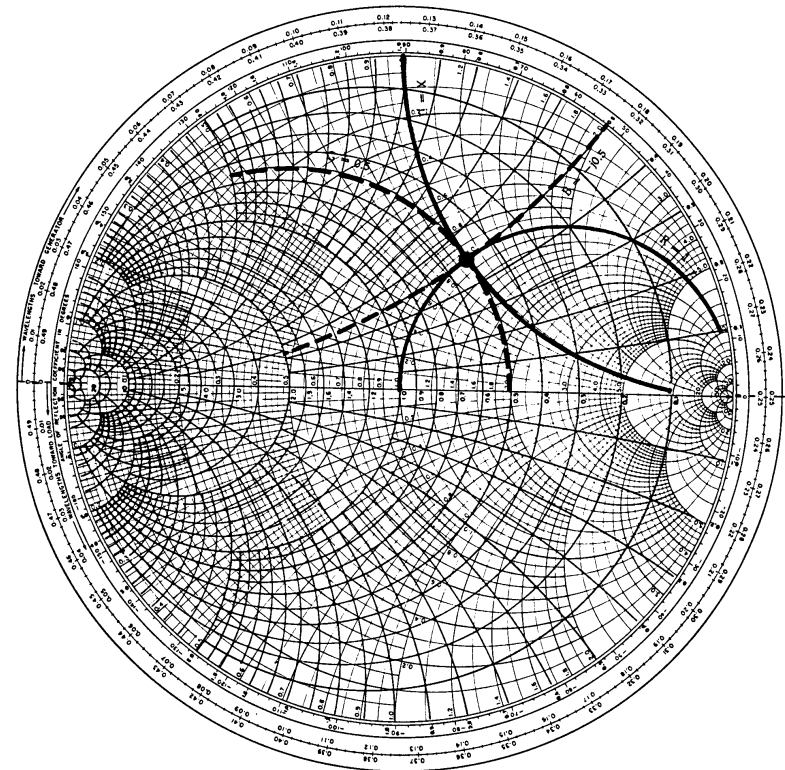


Fig 3-30: The complete Smith chart.

ADDITION OF A SHUNT CAPACITOR

Fig. 3-31 shows the effect of the series addition of a positive susceptance $+j0.8$ (capacitance) to an admittance of $y = 0.2 - j0.5$, resulting in an admittance $y = 0.2 + j0.3$. From a graphical point of view, the parallel addition of a capacitor corresponds to moving around a constant conductance circle clockwise.

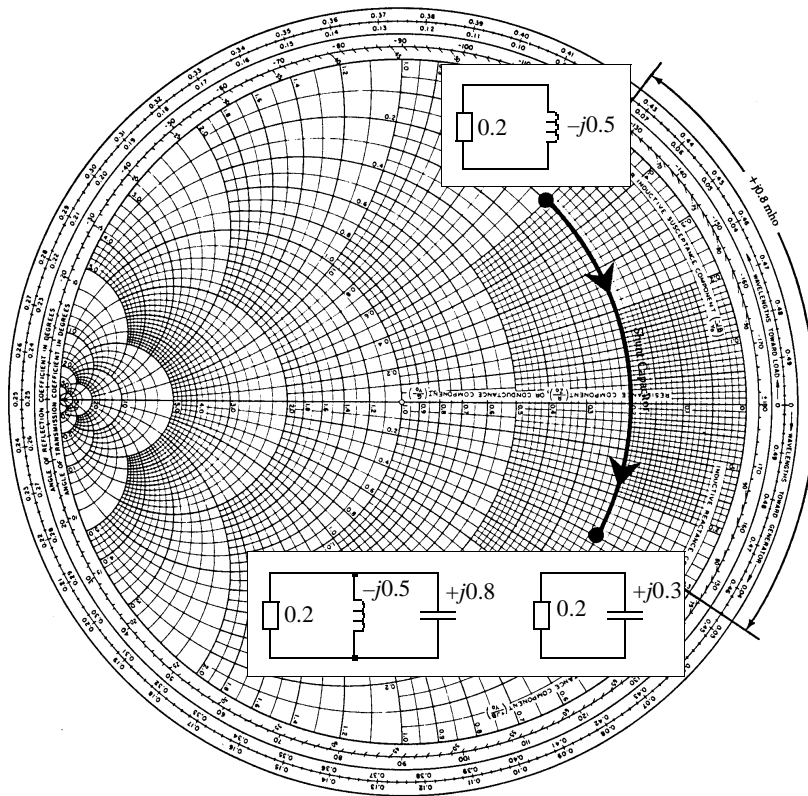


Fig 3-31: Addition of a shunt capacitor.

ADDITION OF A SHUNT INDUCTOR

Fig. 3-32 shows the effect of the parallel addition of a negative susceptance $-j1.5$ (inductance) to an admittance $y = 0.7 + j0.8$. The resulting admittance is $y = 0.7 - j$. This operation corresponds graphically to moving around a constant conductance circle counter-clockwise.

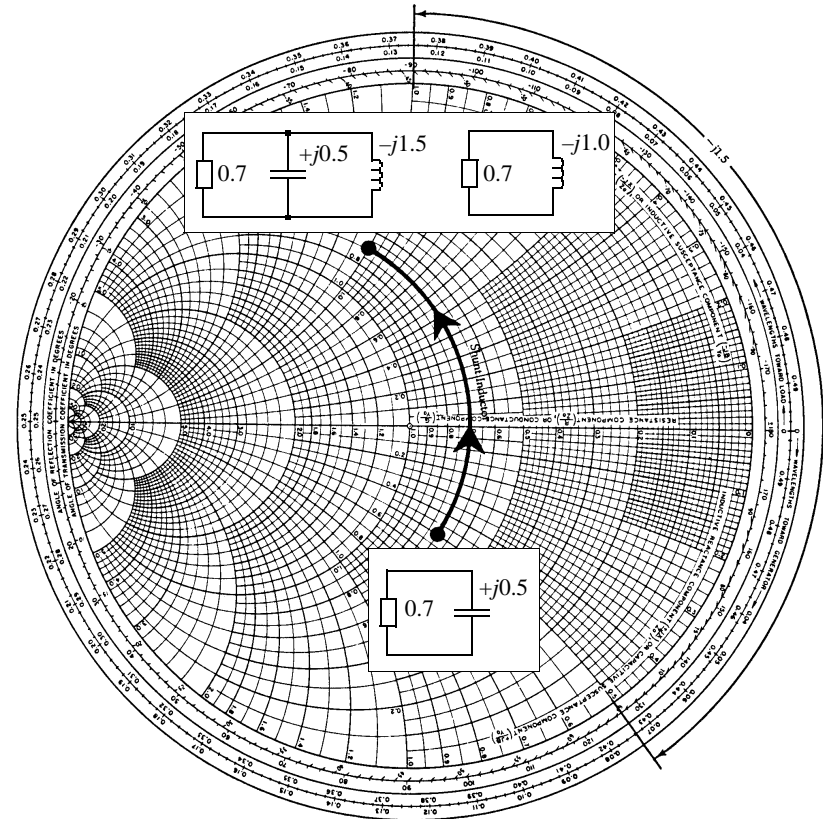


Fig 3-32: Addition of a shunt inductor.

SUMMARY OF SMITH CHART MANIPULATION

Fig. 3-32 presents a summary of the effect of the addition of components on a Smith Chart.

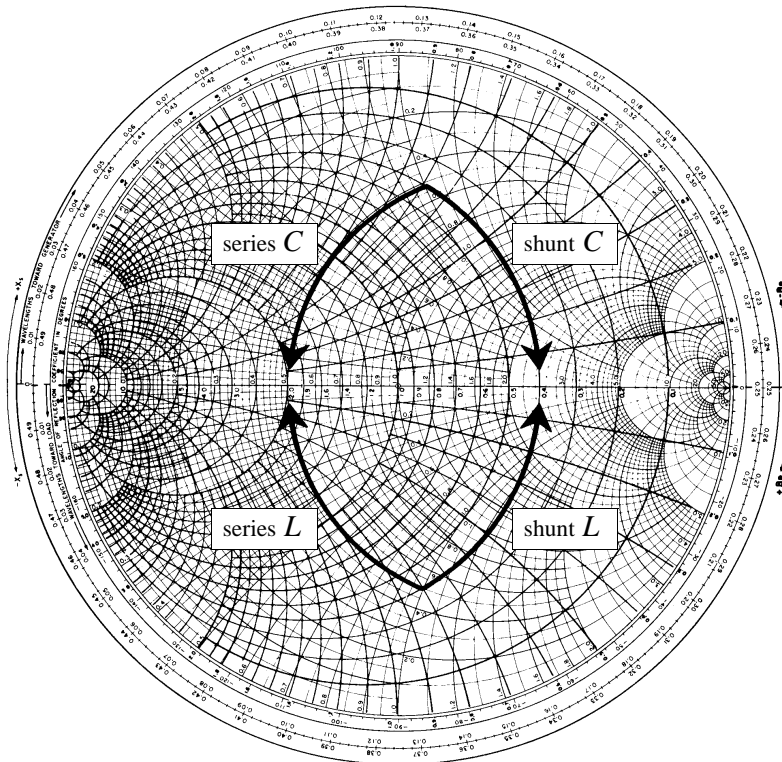


Fig 3-33: Summary of the manipulation of components on the Smith Chart.

EXAMPLE 1 (1/2)

Design a two-element circuit to impedance-match a source impedance $Z_S = 25 - j15$ to a load impedance $Z_L = 100 - j25$ for a frequency of 60 MHz. The transfer function should be of type low-pass.

The impedance that must be seen by the source is its complex conjugate, $Z_S^* = 25 + j15$. Thus, we must transform the load impedance to an impedance Z_S^* . We choose to normalize the impedance to $R_0 = 50\Omega$, so: $z_S^* = 0.5 + j0.3$ and $z_L = 2 - j0.5$. These two normalized impedances are represented respectively at point A (load) and at point C (source). We must link these two points by introducing series and parallel elements. The constraint of needing a low-pass characteristic, forces us to have a series inductor combined with a parallel capacitor. The only way to connect point A to point C while satisfying this demand is represented in Fig. 3-34. The arc AB corresponds to a shunt capacitor with normalized susceptance $+b = 0.73$. The arc BC corresponds to a series inductor with normalized reactance $+x = 1.2$. We find the values of the components by denormalizing according to the following equations:

$$\begin{array}{ll} \text{series:} & \text{parallel:} \\ C = \frac{1}{\omega x R_0} & C = \frac{b}{\omega R_0} \\ L = \frac{x R_0}{\omega} & L = \frac{R_0}{\omega b} \end{array} \quad (3.18)$$

$$C = \frac{b}{\omega R_0} = \frac{0.73}{2\pi 60 \times 10^6 \times 50} = 38.7 \text{ pF}$$

from which:

$$L = \frac{x R_0}{\omega} = \frac{1.2 \times 50}{2\pi 60 \times 10^6} = 159 \text{ nH}$$

EXAMPLE 1 (2/2)

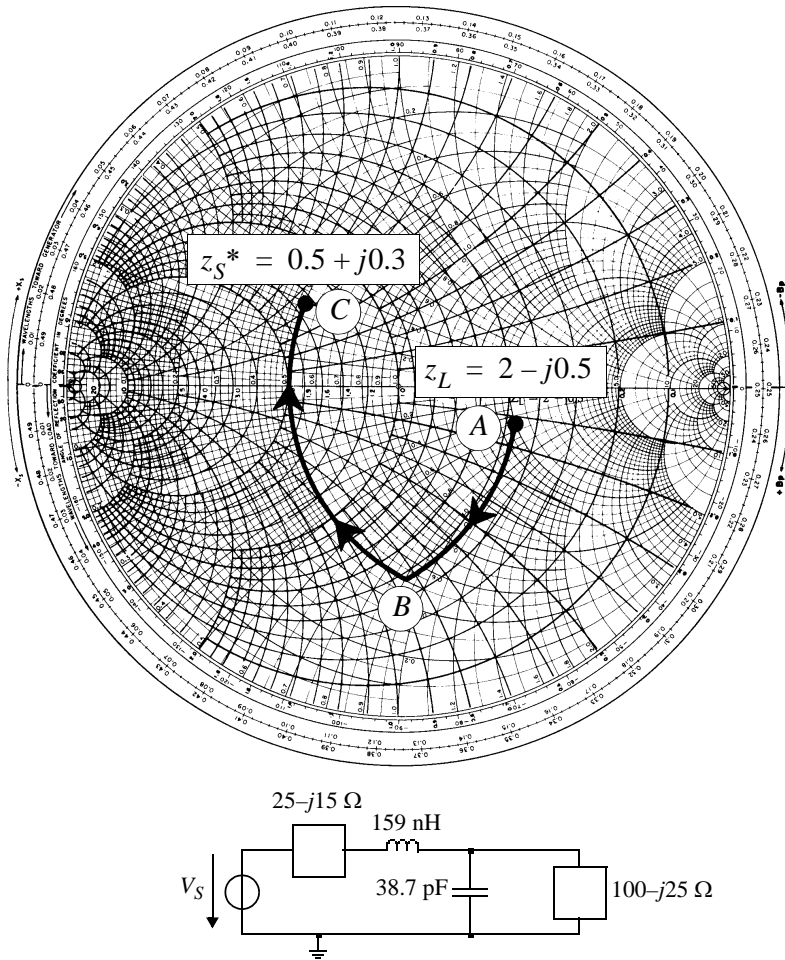


Fig 3-34: Example of two-element impedance matching.

CONSTANT-Q ARCS

We have seen that when matching networks of more than two elements, it is possible to choose the quality factor of the circuit. Fig. 3-35 represents the set of points with quality factor 5. These are situated on two arcs. The higher the quality factor, the more the arcs approach the circumference of the exterior circle representing an infinite quality factor.

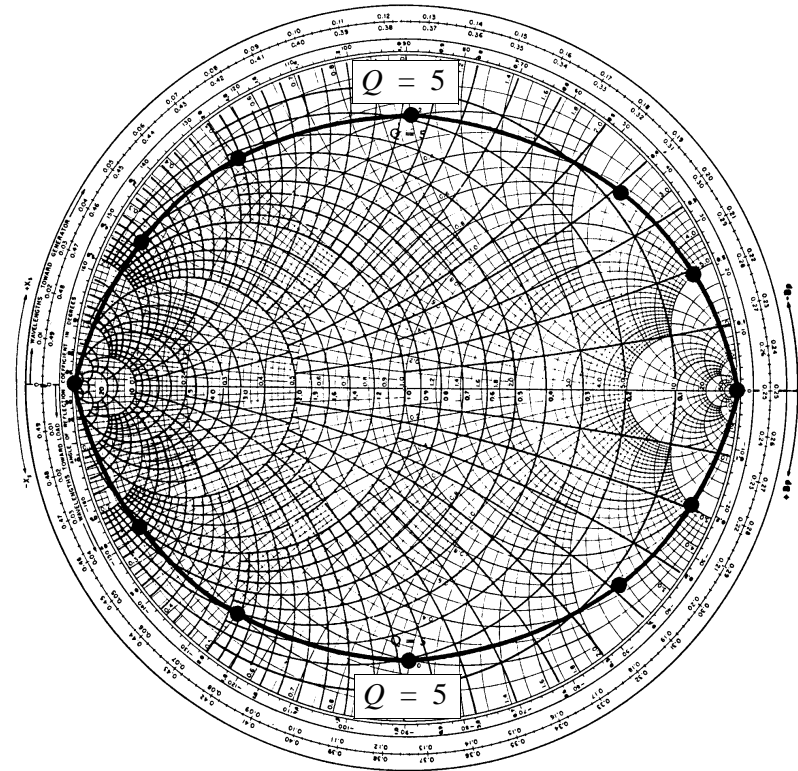


Fig 3-35: Constant-Q arcs.

THREE-ELEMENT NETWORKS

The design procedure using the Smith Chart for three-element matching circuits is as follows:

- 1) Draw the arcs corresponding to the specified quality factor;
- 2) Plot the normalized load impedance and the normalized source impedance;
- 3) Determine which of the terminating resistors will set the quality factor of the circuit: the smaller for T networks, and the larger for Π networks;

4) For T networks:

$R_S > R_L$: from the load, move along a constant resistance circle to the intersection with the constant-Q arc. This arc will determine the value of the first element. Reach the point z_s^* by first adding a shunt element and then a series element;

$R_S < R_L$: find the intersection I of the constant-R circle of the source, with the constant-Q arc. Reach the point I from the load by using two elements: first a series element followed by a shunt element. Reach the point z_s^* by moving around the constant-R circle with the help of another series element.

5) For Π networks:

$R_S > R_L$: find the intersection I of the constant conductance circle of the source with the constant-Q arc. Leave from the load towards the point I first with a shunt element followed by a series element. Go toward the point z_s^* on the constant-G circle by using another shunt element;

$R_S < R_L$: leave from the load on the constant-G circle until reaching the intersection with the constant-Q arc. The length of this arc determines the value of the first shunt element. Go to the point z_s^* by adding first a series element, followed by a shunt element.

EXAMPLE 2 (1/2)

We would like to design a T network to impedance-match a source $Z_S = (15 + j15)\Omega$ with a load impedance $Z_L = 225\Omega$ for a frequency of 30 MHz and a quality factor of 5.

We normalize with $R_0 = 75\Omega$ and find $z_s^* = 0.2 - j0.2$ and $z_L = 3$. Since we want a T network, in this case it is the source termination that determines the quality factor. Following the procedure for $R_S < R_L$, it is first necessary to determine the intersection I of the constant-R circle that passes through z_s^* and the constant-Q arc. Then we must leave from the load to go to this point I , first with a series inductor L_3 with reactance $x_3 = 2.5$ and a shunt capacitor C_2 with susceptance $b_2 = 1.15$. Then we move around the constant-R circle with a series inductor L_1 with reactance $x_1 = 0.8$. We calculate the values of the elements according to:

$$L_3 = \frac{x_3 R_0}{\omega} = \frac{2.5 \times 75}{2\pi 30 \times 10^6} = 995 \text{ nH}$$

$$C_2 = \frac{b_2}{\omega R_0} = \frac{1.15}{2\pi 30 \times 10^6 \times 75} = 81 \text{ pF} \quad (3.19)$$

$$L_1 = \frac{x_1 R_0}{\omega} = \frac{0.8 \times 75}{2\pi 30 \times 10^6} = 318 \text{ nH}$$

The resulting circuit and the design process are shown in Fig. 3-36.

EXAMPLE 2 (2/2)

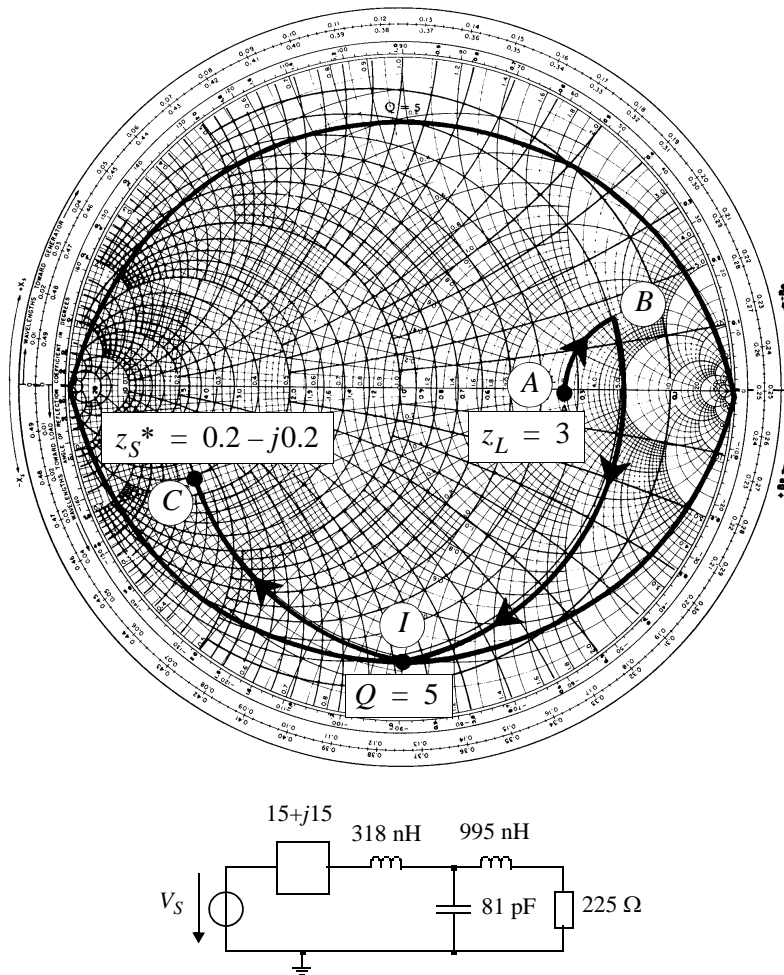


Fig 3-36: Example of three-element impedance matching.

CHAPTER 4

TYPES OF HF FILTERS

Among the multiple ways of making filters, only the following are useable for HF (3 MHz to 30 MHz) and VHF (30 MHz to 300 MHz):

- 1) LC filters;
- 2) Continuous time g_m -C filters;
- 3) Mechanical filters;
- 4) Ceramic filters;
- 5) Quartz filters;
- 6) Surface Acoustic Wave (SAW) filters.

With the exception of g_m -C filters, all these filters are realized with discrete components. The g_m -C filters are the only ones that can be integrated on a chip while maintaining good enough performance at high frequency (< 300 MHz).

HF FILTERS

ATTENUATION, PHASE, AND GROUP DELAY

A filter is a linear circuit that discriminates between different frequencies. The frequencies that are not affected by the filter make up the passband, while the attenuated frequencies make up the stopband. Since the filter is linear, the transfer function can be defined:

$$H(j\omega) \equiv \frac{\text{output signal}}{\text{input signal}} = H_0 \cdot \frac{\prod_{k=1}^M (s - z_k)}{\prod_{k=1}^N (s - p_k)} = |H(j\omega)| \cdot e^{-j\phi(\omega)} \quad (4.1)$$

where z_k are the transmission zeros, p_k are the transmission poles and $\phi(\omega)$ is the phase shift. The input and output signals are generally voltages, but more rarely currents. It is common in filter theory to use attenuation, defined by:

$$A(j\omega) \equiv -20\log(|H(j\omega)|) \quad (4.2)$$

which thus corresponds to the log of the inverse of the transfer function. The values ω_k for which $A(j\omega_k) = 0$ are the attenuation zeros and the frequencies ω_k for which $A(j\omega_k) \rightarrow \infty$ are the attenuation poles, which correspond to the transmission zeros situated on the imaginary axis.

In certain cases, the filter has a phase shift corresponding to a certain constant delay for the passband frequencies. We then specify the group delay by:

$$\tau(\omega) \equiv \frac{d\phi(\omega)}{d\omega} \quad (4.3)$$

CLASSES OF TRANSFER FUNCTIONS

Filters can be classified according to their attenuation characteristics:

- 1) Low-Pass Filter = LPF;
- 2) High-Pass Filter = HPF;
- 3) Band-Pass Filter = BPF;
- 4) Band-Reject Filter = BRF.

Diagrams of these four types of attenuation characteristics are presented in Fig. 4-1.

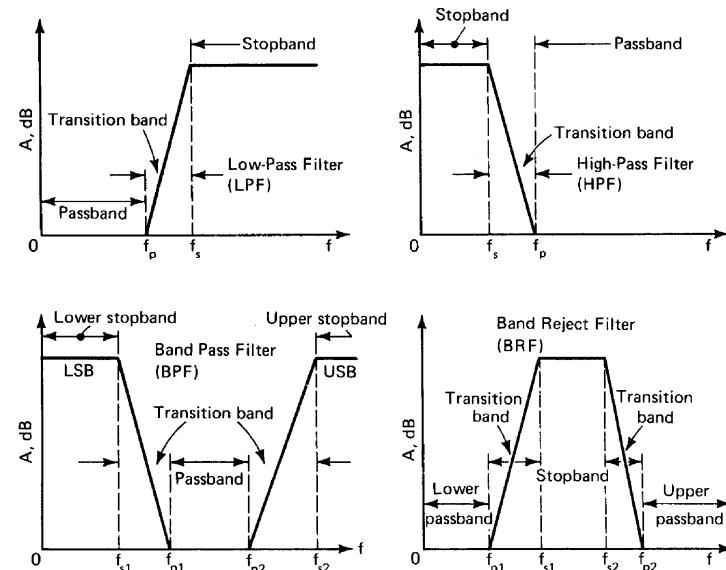


Fig 4-1: The principal attenuation characteristics.

Each of these characteristics contains one or several passbands and stopbands, separated by transition bands in which the attenuation varies. The narrower these transition bands, the more selective the filter. This requires a high-order transfer function and implies a complex realization and high cost.

FILTER SPECIFICATIONS

Within the set of specifications of a filter, such as the dimensions, the power consumption, the functional temperature range, etc., the most important is certainly the specification of the attenuation characteristics or in certain cases the group delay. This is usually done given the attenuation or group delay tolerance limits (cf Fig. 4-2). It is useful to remember that the attenuation characteristics and the phase shift cannot be specified independently so that the causality of the filter is assured.

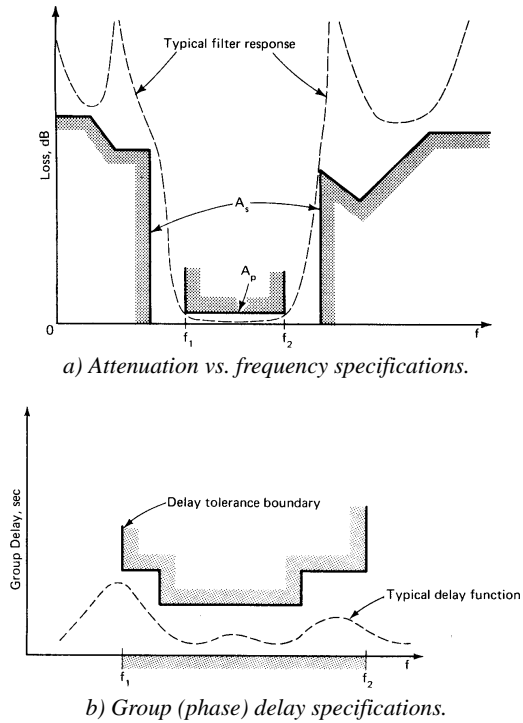


Fig 4-2: Different specifications of a filter.

NORMALIZATION AND LOW-PASS PROTOTYPE

The design of a filter can be broken into two steps: the approximation step followed by the realization (or implementation). The approximation step involves the search for a transfer function that satisfies the imposed specifications, while the realization step involves the synthesis of a circuit (either active or passive) having the transfer function defined during the approximation step. In the case in which the specification is simple (constant and equal attenuation in the stopbands), tabulated analytical approximations can be used. These tables generally correspond to a low-pass filter with a stopband normalized to 1 rad/s (cf Fig. 4-3).

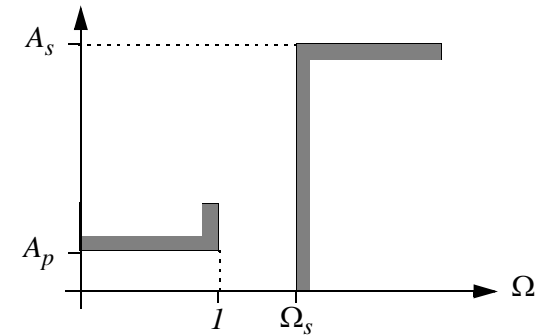


Fig 4-3: Normalized tolerance plot.

These tables can also be applied to high-pass, band-pass, or band-reject filter design, by using the appropriate frequency or circuit transformations.

LOW-PASS ↔ HIGH-PASS TRANSFORMATION

It is easy to transform a low-pass filter to high-pass by the simple inversion of the frequency axis, which corresponds to the following frequency transformation:

$$j\Omega = \omega_p / (j\omega) \tag{4.4}$$

where Ω is the normalized frequency corresponding to the low-pass prototype (LPP) filter and ω is the frequency of the high-pass (HP) filter to be realized, expressed in rad/s. The low-pass prototype filter is simply obtained by carrying out the transformations indicated in Fig. 4-4.

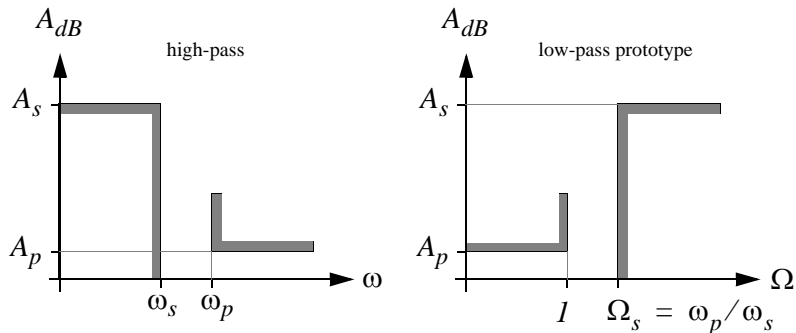


Fig 4-4: Obtaining the LPP from the HP tolerance plot. Circuit transformations correspond to this frequency transformation. In particular, for LC filters, the (denormalized) high-pass filter is obtained by applying the transformation rules shown in Fig. 4-5.

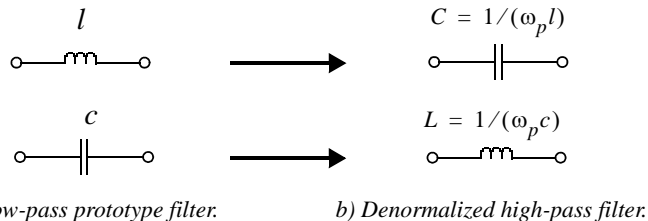


Fig 4-5: Transformation of elements of the LPP filter.

LOW-PASS ↔ BANDPASS TRANSFORMATION (1/4)

In the case in which the tolerance plot of a bandpass filter specifies a constant and equal attenuation in the stopbands, the transformation low-pass ↔ bandpass can be used:

$$s = \frac{p^2 + \omega_0^2}{p \cdot B} \tag{4.5}$$

where $s = j\Omega$ is the Laplace variable in the domain of the low-pass prototype filter and $p = j\omega$ is the Laplace variable in the domain of the bandpass filter. Eqn. 4.5 transforms the frequency $s = 0$ to $p = \pm j\omega_0$, which is then the center frequency of the bandpass filter. The frequencies $s = \pm j\Omega$ are transformed to two positive frequencies $\omega_{1,2} = \mp \frac{1}{2}B\Omega + \sqrt{\omega_0^2 + \frac{1}{4}(B\Omega)^2}$ such that:

$$\omega_1 \omega_2 = \omega_0^2 \tag{4.6}$$

This signifies that each frequency of the tolerance plot of the low-pass prototype filter corresponding to a given attenuation is transformed to two frequencies having the same attenuation and located according to geometrical symmetry around the center frequency. In addition, the passband edges transform into two frequencies $\omega_{p1,p2} = \mp \frac{1}{2}B + \sqrt{\omega_0^2 + \frac{1}{4}B^2}$ and therefore:

$$\omega_{p2} - \omega_{p1} = B \tag{4.7}$$

where B is the filter bandwidth (in rad/s). The frequencies $s = \pm j\Omega_s$ map into two positive frequencies ω_{s1} and ω_{s2} such that:

$$\omega_{s2} - \omega_{s1} = B\Omega_s \tag{4.8}$$

These properties of the low-pass ↔ bandpass transformation are illustrated in an example in Fig. 4-6. The method to obtain the tolerance plot of the LPP from the bandpass filter specifications is described on page 4-10.

LOW-PASS ↔ BANDPASS TRANSFORMATION (2/4)

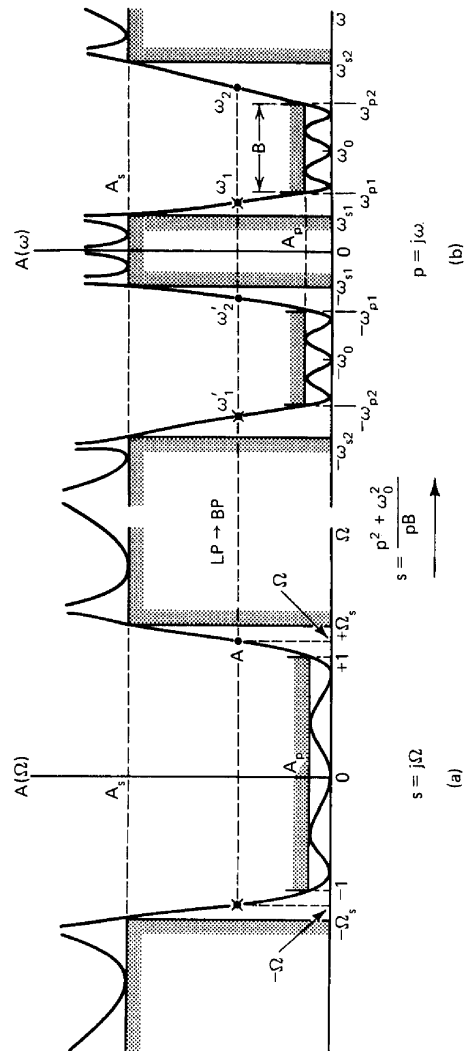


Fig 4-6: Low-pass ↔ bandpass transformation.

LOW-PASS ↔ BANDPASS TRANSFORMATION (3/4)

Consider the tolerance plot of the bandpass filter shown in Fig. 4-7 a).

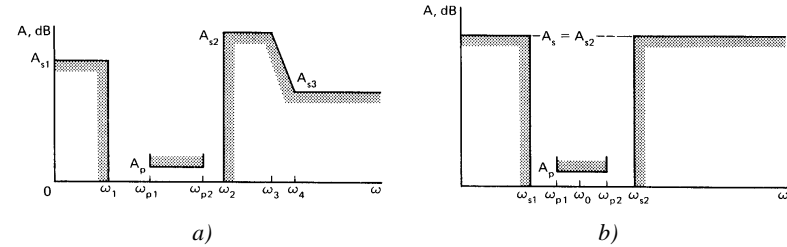


Fig 4-7: Modification of the initial tolerance plot of the bandpass filter for the establishment of the specifications of the low-pass prototype filter.

In order to be able to apply the low-pass ↔ bandpass transformation, the tolerance plot must be modified as follows:

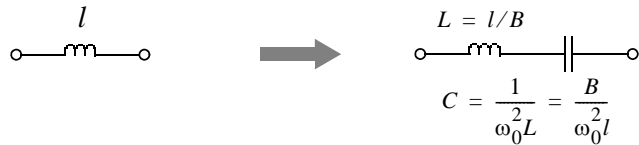
- 1) The attenuation in the stopbands must be leveled to the maximum attenuation (cf Fig. 4-7 b));
- 2) The stopband edges must be modified such that they satisfy the geometric symmetry property of the transformation. To do this, we first calculate the center frequency $\omega_0 = \sqrt{\omega_{p1} \omega_{p2}}$ and then evaluate $\omega_{s1} = \omega_0^2 / \omega_2$. If $\omega_{s1} > \omega_1$, the stopband edges are ω_{s1} and ω_2 . If $\omega_{s1} < \omega_1$, we must calculate $\omega_{s2} = \omega_0^2 / \omega_1$ and define the stopband edges as ω_1 and ω_{s2} .

We can now derive the tolerance plot of the low-pass prototype (LPP) filter by remarking that the attenuations A_p and A_s remain unchanged, while the frequency Ω_s is given by:

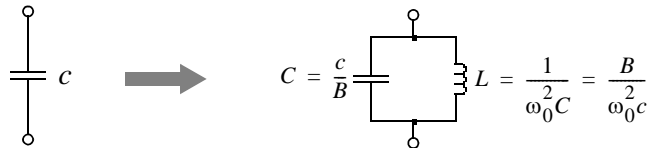
$$\Omega_s = \frac{\omega_{s2} - \omega_{s1}}{\omega_{p2} - \omega_{p1}} = \frac{\omega_{s2} - \omega_{s1}}{B} \tag{4.9}$$

LOW-PASS ↔ BANDPASS TRANSFORMATION (4/4)

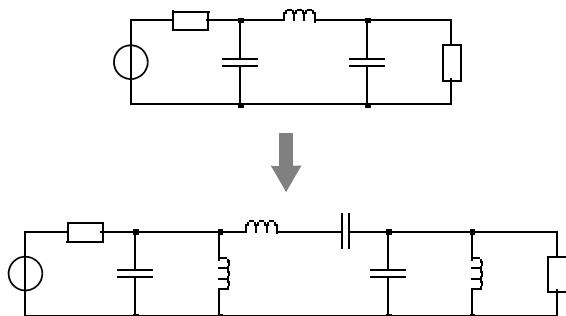
The low-pass ↔ bandpass transformation described by Eqn. 4.5 corresponds to a reactance transformation that can be directly applied to an LC filter. Knowing the center frequency ω_0 and the bandwidth B of the bandpass filter, one can then replace the inductors by series resonant circuits and the capacitors by parallel resonant circuits, all tuned to the same resonant frequency ω_0 expressed in rad/s.



a) Transformation of an inductor (normalized).



b) Transformation of a capacitor (normalized).



c) Transformation of a third-order all-pole filter.

Fig 4-8: Application of the low-pass ↔ bandpass transformation.

TYPES OF APPROXIMATIONS

There are several types of approximations, each having their own features. The best-known are:

- 1) The Butterworth approximation: offers a very flat attenuation in the passband with a monotonically increasing attenuation in the stopband. The transition from the passband to the stopband is controlled. The phase characteristic is nonlinear, and the group delay has a bump at the passband edge.
- 2) The Chebyshev approximation: offers a more rapid transition from the passband to the stopband than the Butterworth, but has ripples in the passband. The attenuation increases monotonically in the stopband. The phase characteristic is highly nonlinear and the group delay has peaks at the passband edge.
- 3) The Bessel approximation: offers a linear phase delay and therefore a constant group delay in the passband. However, the transition from the passband to the stopband is very gradual.
- 4) The Cauer or Elliptic approximation: offers a very steep transition from the passband to the stopband, but has ripples in the passband as well as the stopband. The phase characteristic and the group delay are highly nonlinear and rippled.

BUTTERWORTH APPROXIMATION (1/3)

The Butterworth function is certainly the simplest of the analytical approximations. The typical shape of the Butterworth transfer function is shown in Fig. 4-9.

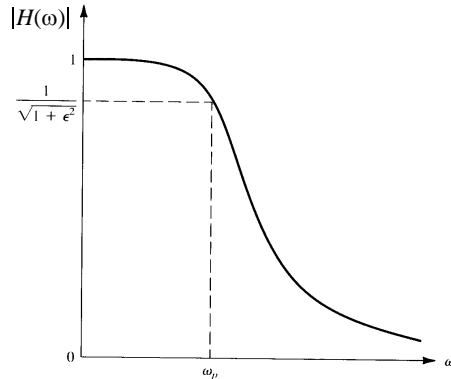


Fig 4-9: Magnitude of the Butterworth transfer function.

The magnitude of the Butterworth transfer function of order N and the corresponding attenuation are given respectively by:

$$|H(\omega)| \equiv \frac{1}{\sqrt{1 + \varepsilon^2 \left(\frac{\omega}{\omega_p}\right)^{2N}}} = \frac{1}{\sqrt{1 + \varepsilon^2 \Omega^{2N}}} \quad (4.10)$$

$$A_{dB} \equiv 20 \log\left(\frac{1}{|H(\Omega)|}\right) = 10 \log(1 + \varepsilon^2 \Omega^{2N}) \quad (4.11)$$

where $\Omega \equiv \omega/\omega_p$ is the frequency normalized to the cutoff frequency ω_p which is the frequency which corresponds to an attenuation A_p . In the particular case where $\varepsilon = 1$, ω_p corresponds to the frequency at -3 dB ($A_p = 3dB$). The parameter ε is thus determined by the maximum variation of the attenuation tolerated in the passband, given A_p :

$$\varepsilon = \sqrt{10^{A_p/10} - 1} \quad (4.12)$$

BUTTERWORTH APPROXIMATION (2/3)

The function given by Eqn. 4.10 is plotted for $\varepsilon = 1$ and for different values of N in Fig. 4-10.

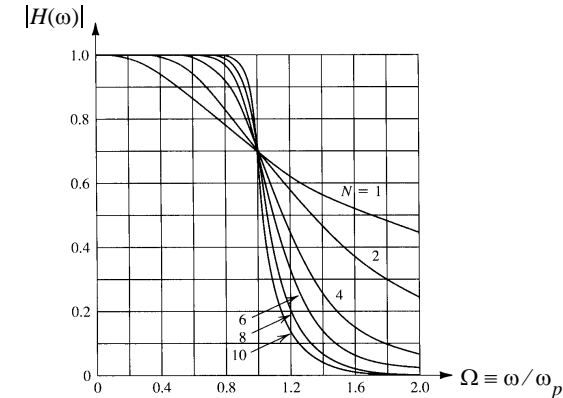


Fig 4-10: Magnitude of the transfer function for $\varepsilon = 1$.

It can be shown that the $2N-1$ derivatives of Eqn. 4.10 with ω cancel out at the origin, which explains the increasingly flat appearance of the characteristics near the origin when the filter's order increases. The order of the filter that satisfies a certain tolerance plot can be determined by noting that the attenuations at the passband and stopband edges are given by:

$$A_p = 10 \log(1 + \varepsilon^2) \quad A_s = 10 \log(1 + \varepsilon^2 \Omega_s^{2N}) \quad (4.13)$$

from which one gets the minimum value of the order N that satisfies the tolerance plot:

$$N \geq \frac{\log\left(\frac{10^{A_s/10} - 1}{10^{A_p/10} - 1}\right)}{2 \cdot \log(\Omega_s)} \quad (4.14)$$

If the expression on the right side of Eqn. 4.14 is not a whole number, we must choose the next highest whole number.

BUTTERWORTH APPROXIMATION (3/3)

It can be shown that the poles of the transfer function $H(\Omega)$ are located on a circle as indicated in Fig. 4-11.

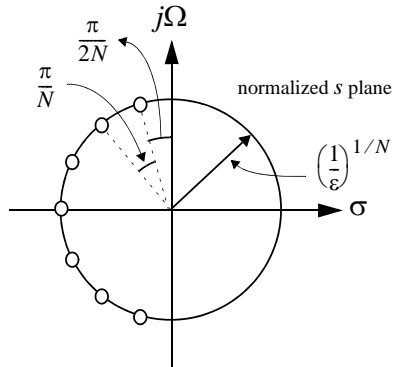


Fig 4-11: Poles of the Butterworth transfer function in the normalized s plane (7th order).

The complex conjugate poles can be grouped by pairs, and the transfer function can be factored into a product of a possible 1st degree function and 2nd order functions each having the same normalized resonant frequency Ω_0 and quality factors Q_k given by:

$$\Omega_0 \equiv \frac{\omega_0}{\omega_p} = \left(\frac{1}{\epsilon}\right)^{1/N} \quad Q_k = \frac{1}{2 \sin\left(\frac{2k-1}{2N}\pi\right)} \quad k = 1, 2, \dots, N \quad (4.15)$$

The procedure for synthesizing a Butterworth filter is summarized below:

- 1) Normalize the tolerance plot by dividing the frequency by the filter's cutoff frequency. This permits Ω_s to be determined;
- 2) Determine the order according to Eqn. 4.14;
- 3) Calculate the value of ϵ using Eqn. 4.12.

CHEBYSHEV APPROXIMATION (1/3)

Fig. 4-12 shows the typical shape of the magnitude of the transfer function of even-order and odd-order Chebyshev filters. In contrast with the Butterworth filter, the Chebyshev filter has ripples in the passband, followed by a monotonic decrease in the stopband. Notice that the number of maxima and minima in the positive passband corresponds to $(N+1)$ where N is the order of the filter.

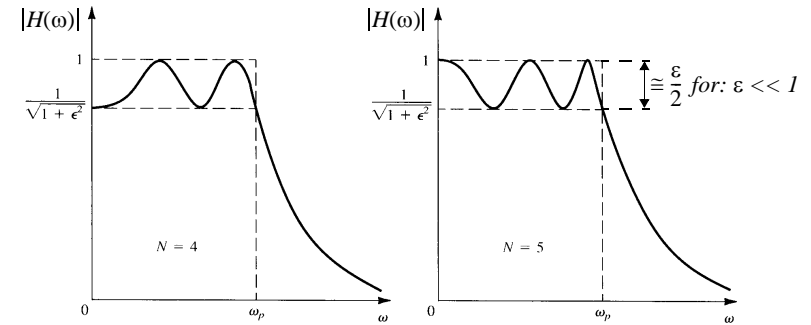


Fig 4-12: Typical transfer function shapes for a Chebyshev filter. The transfer function is given by:

$$|H(\omega)| \equiv \frac{1}{\sqrt{1 + \epsilon^2 C_N^2\left(\frac{\omega}{\omega_p}\right)}} = \frac{1}{\sqrt{1 + \epsilon^2 C_N^2(\Omega)}} \quad (4.16)$$

$$A_{dB} \equiv 20 \log\left(\frac{1}{|H(\Omega)|}\right) = 10 \log(1 + \epsilon^2 C_N^2(\Omega)) \quad (4.17)$$

where $C_N^2(\Omega)$ is the Chebyshev polynomial of order N defined by:

$$C_N(\Omega) \equiv \begin{cases} \cos(N \cdot \arccos(\Omega)) & \Omega \leq 1 \\ \cosh(N \cdot \operatorname{acosh}(\Omega)) & \Omega > 1 \end{cases} \quad (4.18)$$

CHEBYSHEV APPROXIMATION (2/3)

These polynomials satisfy the following recursive formula:

$$C_{n+1}(\Omega) = 2\Omega C_n(\Omega) - C_{n-1}(\Omega) \quad (4.19)$$

The first polynomials given below are shown in Fig. 4-13.

$$\begin{aligned} C_0(\Omega) &= 1 & C_1(\Omega) &= \Omega \\ C_2(\Omega) &= 2\Omega^2 - 1 & C_3(\Omega) &= 4\Omega^3 - 3\Omega \\ C_4(\Omega) &= 8\Omega^4 - 8\Omega^2 + 1 \end{aligned} \quad (4.20)$$

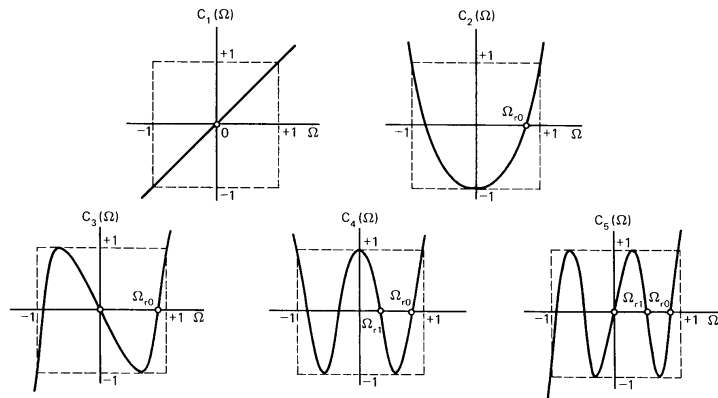


Fig 4-13: Chebyshev polynomials.

The attenuation of a Chebyshev filter of order N at the stop-band edge is given by:

$$A_s \equiv A_{dB}(\Omega = \Omega_s) = 10\log(1 + \varepsilon^2 C_N^2(\Omega_s)) \cong 20\log(\varepsilon C_N(\Omega_s)) \quad (4.21)$$

Which gives:
$$A_s + 20\log\left(\frac{1}{\varepsilon}\right) = 20\log(C_N(\Omega_s)) \quad (4.22)$$

CHEBYSHEV APPROXIMATION (3/3)

The right side of Eqn. 4.22 is constant for a given order N and value Ω_s . Once the order has been chosen, the attenuation can be split up between the two left-hand terms of Eqn.4.22 according to the specifications. An increase of the attenuation in the stopband implies an increase of ε and therefore of the ripple in the passband. Eqn. 4.22 is represented in Fig. 4-14. Knowing A_p , A_s and Ω_s , the chart in Fig. 4-14 can be used to determine the order necessary to satisfy the tolerance plot.

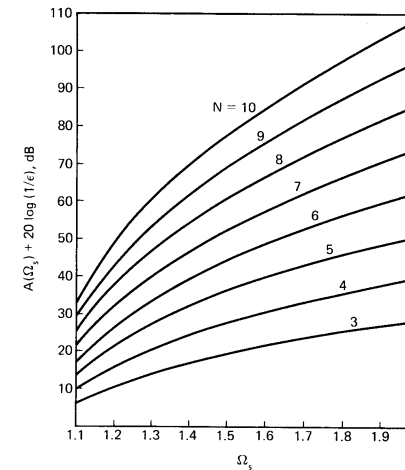


Fig 4-14: Chart for choosing the Chebyshev filter order.

The order necessary to satisfy the tolerance plot can also be determined by using the following formula:

$$N \geq \frac{A_s + 20\log\left(\frac{1}{\varepsilon}\right) + 6}{8.68 \operatorname{acosh}(\Omega_s)} \quad (4.23)$$

COMPARISON OF BUTTERWORTH AND CHEBYSHEV APPROXIMATIONS

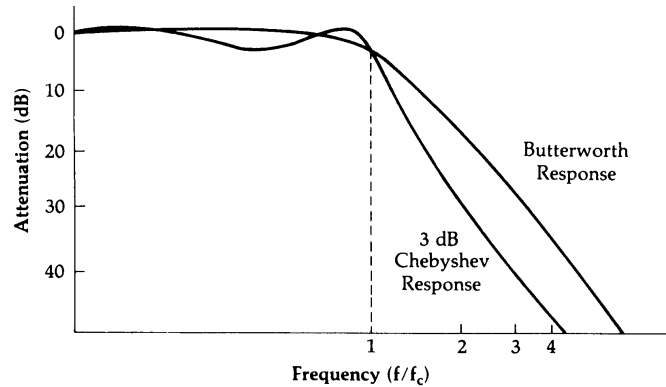


Fig 4-15: Comparison of the attenuation of 3rd order Butterworth and Chebyshev filters.

ALL-POLE LOW-PASS LC FILTER (1/3)

For both Butterworth and Chebyshev approximations, there are direct relationships between the values of the reactive components and the characteristic parameters ϵ and N for the low-pass prototype filters in Fig. 4-16 and 4-17. In general, we would choose one of the filters with the minimum number of inductors in Fig. 4-16.

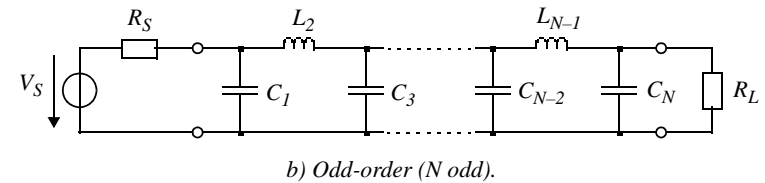
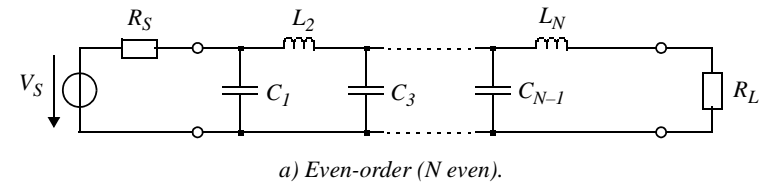


Fig 4-16: All-pole low-pass LC filters with minimum inductors.

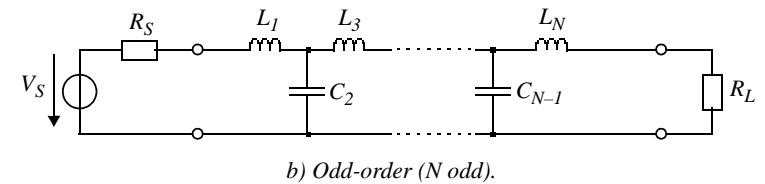
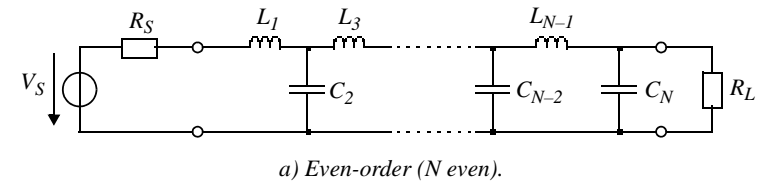


Fig 4-17: All-pole low-pass LC filters with minimum capacitors.

ALL-POLE LOW-PASS LC FILTER (2/3)

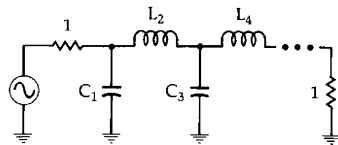
Butterworth

For the Butterworth approximation, the values of the reactive elements (capacitors et inductors) of the filters in Fig. 4-16 having equal resistive terminations equal to 1 Ω and a cutoff frequency ω_p equal to 1 rad/s, are simply given by:

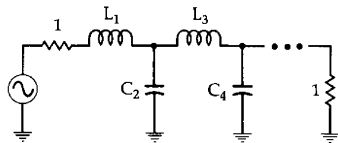
$$C_k, L_k = 2\varepsilon^{1/N} \sin\left(\frac{2k-1}{2N}\pi\right) \quad k = 1, 2, \dots, N \quad (4.24)$$

Note that Eqn. 4.24 is only valid for filters with identical terminations R_S = R_L = 1Ω. The values calculated from Eqn. 4.24 are tabulated in Table 4-1 for ε = 1. For the case in which R_S ≠ R_L, it is necessary to use Table 4-2.

Table 4-1: Butterworth prototype filter (R_S = R_L = 1Ω) and ω_p = 1 rad/s.



n	C ₁	L ₂	C ₃	L ₄	C ₅	L ₆	C ₇
2	1.414	1.414					
3	1.000	2.000	1.000				
4	0.765	1.848	1.848	0.765			
5	0.618	1.618	2.000	1.618	0.618		
6	0.518	1.414	1.932	1.932	1.414	0.518	
7	0.445	1.247	1.802	2.000	1.802	1.247	0.445
n	L ₁	C ₂	L ₃	C ₄	L ₅	C ₆	L ₇



ALL-POLE LOW-PASS LC FILTER (3/3)

Chebyshev

The relationships for a Chebyshev approximation are a little more complicated. First we must determine the constants h and ξ using the value of ε:

$$h \equiv \left(\frac{1}{\varepsilon} + \sqrt{1 + \frac{1}{\varepsilon^2}}\right)^{1/N} \quad \text{and:} \quad \xi \equiv h - \frac{1}{h} \quad (4.25)$$

The cutoff frequency ω_p is equal to 1 rad/s. The values of the reactive elements are then given by:

$$C_1 = \frac{4 \sin\left(\frac{\pi}{2N}\right)}{\xi R_S} \quad (4.26)$$

$$C_{2k-1} \cdot L_{2k} = \frac{16 \sin\left(\frac{4k-3}{2N}\pi\right) \sin\left(\frac{4k-1}{2N}\pi\right)}{\xi^2 + \left(2 \sin\left(\frac{2k-1}{N}\pi\right)\right)^2} \quad (4.27)$$

$$C_{2k+1} \cdot L_{2k} = \frac{16 \sin\left(\frac{4k-1}{2N}\pi\right) \sin\left(\frac{4k+1}{2N}\pi\right)}{\xi^2 + \left(2 \sin\left(\frac{2k}{N}\pi\right)\right)^2}$$

$$N \text{ odd:} \quad C_N = \frac{4 \sin\left(\frac{\pi}{2N}\right)}{\xi R_L} \quad (4.28)$$

$$N \text{ even:} \quad L_N = \frac{4R_L \sin\left(\frac{\pi}{2N}\right)}{\xi}$$

The calculation must begin with Eqn. 4.26 if we have the value of R_S or in the reverse order, that is to say with Eqn. 4.28 if we have the value of R_L. Note that contrary to Butterworth filters, where the terminations can be identical, in the case of even-order Chebyshev filters, they must be different. The element values are tabulated in Tables 4-3 to 4-6 for different ripple values in the passband.

EXAMPLE: CALCULATION OF A THIRD-ORDER CHEBYSHEV PROTOTYPE FILTER

We would like to find the values of the reactive elements of a 3rd order Chebyshev filter having a ripple in the passband of less than 0.1 dB, a cutoff frequency of 1 rad/s and a source resistance $R_S = 1\Omega$.

From Eqn. 4.12 we get $\varepsilon = 0.1526204$. From Eqn. 4.25 we have $h = 2.36215$ and $\xi = 1.938812$. Knowing that $R_S = 1\Omega$, we can calculate C_1 from Eqn. 4.26:

$$C_1 = \frac{4 \sin(\pi/6)}{\xi} = 1.03156F$$

$$C_1 L_2 = \frac{16 \sin(\pi/6) \sin((3\pi)/6)}{\xi^2 + (2 \sin(\pi/3))^2} = 1.183609$$

From which: $L_2 = 1.1473966H$

$$C_3 L_2 = \frac{16 \sin((3\pi)/6) \sin((5\pi)/6)}{\xi^2 + (2 \sin((2\pi)/3))^2} = 1.183609$$

From which: $C_3 = 1.03156F$

Note that according to Eqn. 4.28, R_L is equal to R_S .

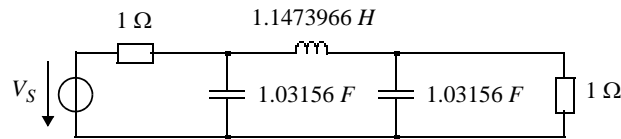


Fig 4-18: Example of the calculation of a 3rd order Chebyshev prototype filter.

SURFACE ACOUSTIC WAVE (SAW) FILTERS (1/2)

Surface Acoustic Waves (SAWs) are a special type of elastic wave that propagates along discontinuities such as the free surface of a solid (or the separation surface between two different elastic media). They were discovered theoretically by Lord Rayleigh, in 1885, during his studies of earthquakes. The amplitude of the mechanical deformations decreases exponentially inside the solid when getting farther from the surface such that the mechanical energy carried by the wave is confined, in a region about the thickness of the wavelength λ , under the surface (cf Fig. 4-19).

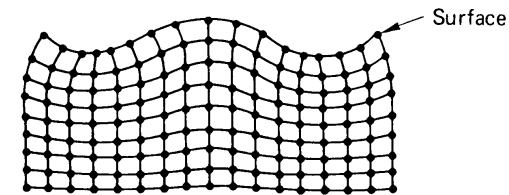


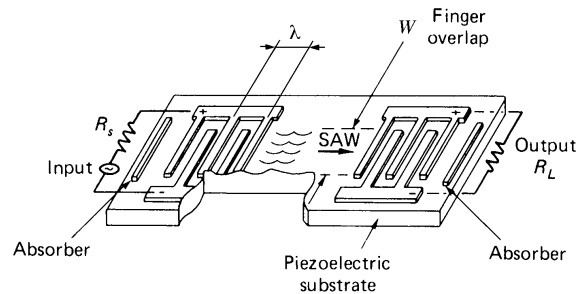
Fig 4-19: Propagation of a surface wave.

These waves, nondispersive, are characterized by slow propagation (average speed $v = 3 \text{ km/s}$) and a generally weak attenuation (on the order of $10^{-4} \text{ dB}/\lambda$, i.e. $0,01 \text{ dB}/\mu\text{s}$ for lithium niobate YZ at 100 MHz).

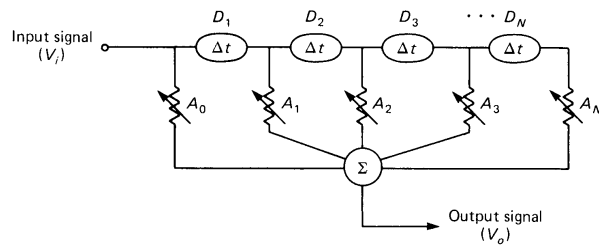
Since the signals to be filtered are usually electrical, the use of elastic phenomena requires transformations from mechanical energy to electrical energy and vice versa. Piezoelectric crystals in which there is a natural coupling between elastic and electrical phenomena are thus the material used. Indeed, if the substrate is piezoelectric, the deformations produced by the elastic wave induce local electric fields, which accompany the mechanical wave during its propagation. The electric field interacts with all the metal electrodes placed on the surface, which can also be connected to exterior circuits.

SURFACE ACOUSTIC WAVE (SAW) FILTERS (2/2)

The surface waves are generated and detected with transducers made of interdigitated metallic combs deposited on the substrate (cf Fig. 4-20 a)). The classic technology uses photolithography of a thin metallic layer, usually aluminum about 2000 Å thick, deposited on a polished monocrystal: one single mask level is usually enough and the fabrication yield is excellent.



a) Setup of a SAW filter.



b) Corresponding transversal filter.

Fig 4-20: Diagram of a SAW filter.

The surface acoustic wave filter corresponds to the transversal filter (FIR filter) whose diagram is shown in Fig. 4-20 b). The delay Δt is due to the spacing between each finger of the transducers, and the weighting factor A of the delayed signal is determined by the length W of each finger.

TRANSFER FUNCTION OF A SAW FILTER

For a regular comb, the elastic excitations due to different finger pairs add together to give a synchronous frequency $f_0 = v/\lambda$. If the frequency moves away from this value, the interference is no longer completely constructive and the resulting signal diminishes: the passband of a regular transducer is narrower when it has more fingers. If N is the total number of fingers, the frequency response is given by:

$$H(x) = \frac{\sin(x)}{x} \quad \text{with } x \equiv (N-1) \frac{\pi f - f_0}{2 f_0} \quad (4.29)$$

Other responses can be obtained either by changing the amplitude by appropriately weighting finger length (apodization) (cf Fig. 4-21 a)), or by changing the phase by weighting finger spacing (cf Fig. 4-21 b).

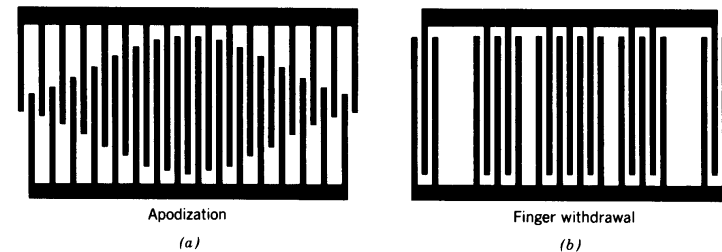


Fig 4-21: Weighting the impulse response.

The global transfer function is equal to the product of the relative functions of the emitter and receiver transducers. If one of the transducers has few fingers (meaning a wide passband), the transfer function is determined uniquely by the design of the other. In addition, if the second transducer with uniform aperture has few fingers, it will have high insertion loss. If the number of fingers increases, its frequency response, in $\sin x/x$, will "round out" the global response of the filter. The use of two apodized transducers complicates the problem of synthesis.

TRANSDUCER EQUIVALENT CIRCUIT

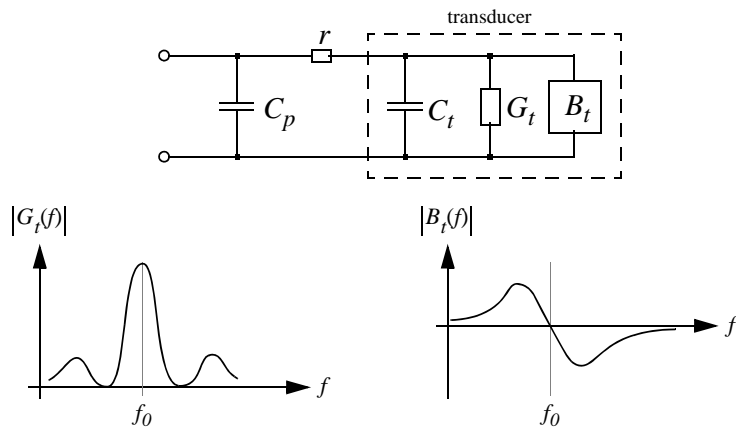


Fig 4-22: *Transducer equivalent circuit.*

The equivalent circuit of a transducer is shown in Fig. 4-22. The input admittance of the transducer (within the dotted lines of Fig. 4-22) is composed of three parallel elements given by:

$$C_t \equiv \frac{N-1}{2} \varepsilon W$$

$$G_t(f) \equiv G_{max} \left[\frac{\sin(x)}{x} \right]^2 \quad (4.30)$$

$$B_t(f) \equiv G_{max} \frac{\sin(2x) - 2x}{2x^2}$$

with:

$$G_{max} \equiv G_t(f_0) = 8k^2 f_0 C_t \frac{N-1}{2} \quad (4.31)$$

where k^2 is the electromechanical coupling coefficient of the piezoelectric material, ε its permittivity and W the length of the transducer fingers. Two parasitic elements have been added: the resistance r of the electrodes and the capacitance C_p associated with the setup.

REFLECTIONS AND INSERTION LOSSES

Secondary effects change the ideal response of interdigitated transducers. The most important are related either to diffraction, the waveform spreading out if its opening is too small, or to reflections from the crystal edges and particularly from the other electrodes. Intratransducer reflections can be minimized by using double-finger electrodes, in which each finger is replaced by a pair of fingers of thickness $\lambda/8$ instead of $\lambda/4$ (cf Fig. 4-23).

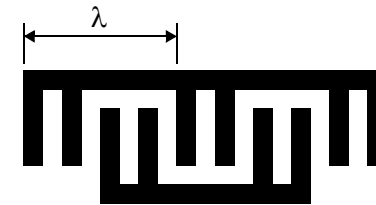


Fig 4-23: *Reduction of intratransducer reflections.*

The reflections from the two ports, due to the regeneration of elastic waves by the voltage created on the transducer electrodes, cause "triple transit" echoes that are as strong as the losses are weak. This effect can be reduced by slightly changing the device so that the insertion losses are equal or greater than 20 dB or by using double or unidirectional multiphased transducers at the price of a reduced bandwidth.

The insertion losses of surface acoustic wave filters stem mainly from the bidirectionality of the transducers and from the electrical mismatching, but also, especially at high frequency, from the parasitic resistance of the fingers and from the propagation losses in the substrate. In addition, by tolerating reasonable losses, one can only obtain, from a given material, a limited relative passband $\Delta f/f_0$, on the order of k , the square root of the electromechanical coupling coefficient.

LIMITS AND APPLICATIONS OF SAW FILTERS

Under 10 MHz, crystal dimensions lead to filters with modest performance. Above 1 GHz, major technological problems arise. But it is in the VHF and UHF ranges that SAW filters are the most advantageous. Limited by the dimensions of the crystals (several cm), the transition band of transversal filters remains higher than 100 kHz. It can be reduced by the use of resonators. It is difficult to give characteristic numbers, for insertion losses or for ripples in the band, because performance varies enormously both with the quality of the design and realization and also as a function of the filter design specifications. Thus a narrow-band filter can have just 2 or 3 dB of losses if the unidirectional structure is realized well, while a wide-band filter with small ripples in the band will have insertion losses of about 20 dB. A major advantage of SAW filters is that they don't require any frequency adjustment.

They are commonly used to realize the IF filters in TV receivers (cf Fig. 4-24).

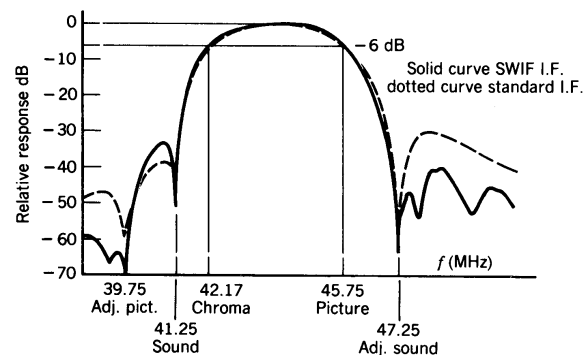


Fig 4-24: Response of a SAW filter for IF TV.

OTHER SAW FILTER STRUCTURES

The preceding description of surface wave filters implies an ideal model in which the waves propagate freely, without reflection. In practice, we seek to design devices in which these conditions are roughly satisfied. Nevertheless, there is another approach in which the deviation from the model of free waves is deliberately emphasized in order to take advantage of these effects.

The surface motion reflects from mechanical and electrical discontinuities. If we exclude the reflections from the crystal boundaries, difficult to control and usually avoided by using an absorber (cf Fig. 4-20), we mostly use reflections from arrays:

a) arrays of mechanical grooves: Regular grooves can be etched by ions on a crystal surface; an array made of ZnO or silica, or even metal can also be deposited. Thus, each line of discontinuity will be the source of a reflected wavelet. If the reflected wavelets from the different lines are in phase, the effect will be cumulative.

b) conductor arrays: Reflections from arrays of conductors are more subtle. The incident waves induce a current in the conductors, which then behave as transducers whose excitation is caused by the incident wave. The waves re-emitted in this way by the transducer are interpreted as "electrically" reflected (or diffused) waves. The amplitude of this diffusion depends strongly on the load: open circuit, short circuit, matched circuit, etc. One can even obtain a re-emission that is geometrically separated from the incident wave, which leads to multiple band couplers.

SAW RESONATOR FILTERS

By placing two transducers inside a surface wave cavity closed by two reflectors of one of the types described above, we obtain a resonator filter.

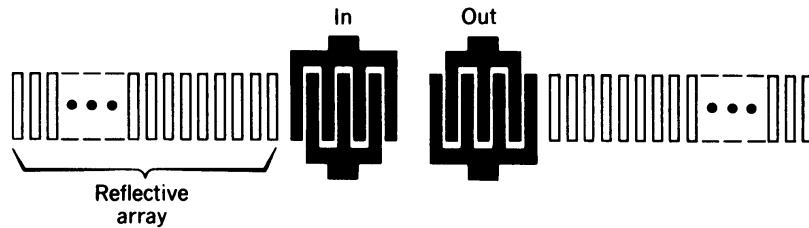


Fig 4-25: Example of a SAW resonator filter.

We can thus achieve quality factors on the order of 10^4 . It is also possible to place the transducers outside the cavity, which makes their position less critical but increases insertion losses. We can also couple multiple cavities, for example by using multiple-band couplers, but this process is rarely used for more than two cavities.

MULTISTRIP ARRAY FILTERS

A multiple band coupler placed astride over an input track and an output track has the simple effect of shifting the phase of the piezoelectric waves. On the other hand, if the pitch of the array is modulated on both tracks, we get a selective reflection at certain frequencies, which allows the realization of electric diffusion filters. We can also use this procedure by reversing the propagation direction with reflection (MRA or multistrip reflective array) or on the contrary, by preserving the propagation direction with transmission (MTA or multistrip transmissive array).

REFLECTIVE ARRAY COMPRESSOR SAW FILTERS

Fig. 4-26 represents a double-reflection filter on two etched arrays, turned approximately 45° from the axis of propagation of the input and output waves. This process is very convenient for realizing dispersive filters (used in modern radar) in which the bandwidth \times transmission time product reaches 10^4 . A similar process which uses points instead of grooves has also been proposed.

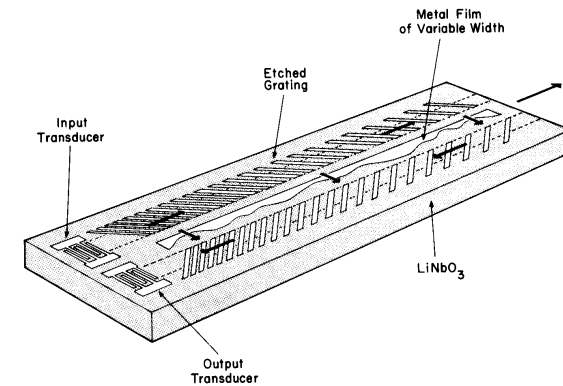


Fig 4-26: Reflective array dispersive filter.

ACTIVE SAW FILTERS

Finally, we would like to point out the possibility of looping back a line of surface waves on itself through an amplifier which almost completely compensates the losses. We thus obtain extremely narrow-band filters (overvoltage = several 10^4) that can be made tunable by inserting an electronic phase-shifter in the loop.

Table 4-2: Butterworth prototype filter ($R_S \neq R_L$, $\varepsilon = 1$).

n	R_S/R_L	C_1	L_2	C_2	L_3	C_3	L_4	C_4	L_5	C_5	L_6	C_6	L_7
2	1.111	1.035	1.835										
	1.250	0.849	2.121										
	1.429	0.697	2.439										
	1.667	0.566	2.828										
	2.000	0.448	3.316										
	2.500	0.342	4.065										
	3.333	0.245	5.313										
	5.000	0.156	7.707										
	10.000	0.074	14.814										
	∞	1.414	0.707										
3	0.900	0.808	1.633	1.384	1.599								
	0.800	0.844	1.384	1.384	1.926								
	0.700	0.915	1.165	1.165	2.277								
	0.600	1.023	0.965	0.965	2.702								
	0.500	1.181	0.779	0.779	3.261								
	0.400	1.425	0.604	0.604	4.064								
	0.300	1.838	0.440	0.440	5.363								
	0.200	2.669	0.284	0.284	7.910								
	0.100	5.167	0.138	0.138	15.455								
	∞	1.500	1.333		0.500								
4	1.111	1.111	0.466	1.592	1.744	1.469	1.811						
	1.250	0.388	1.695	1.511	1.511	1.811	1.469						
	1.429	0.325	1.862	1.291	1.291	2.175	1.607						
	1.667	0.269	2.103	1.082	1.082	2.613	2.175						
	2.000	0.218	2.452	0.883	0.883	3.187	2.836						
	2.500	0.169	2.986	0.691	0.691	4.009	3.826						
	3.333	0.124	3.684	0.531	0.531	5.338	5.338						
	5.000	0.080	5.383	0.387	0.387	7.940	7.940						
	10.000	0.054	8.959	0.282	0.282	15.642	15.642						
	∞	1.331	1.574		1.082	0.383	0.383						
n	R_S/R_L	L_1	C_2	L_3	C_3	L_4	C_4	L_5	C_5	L_6	C_6	L_7	C_7
5	0.900	0.442	1.027	0.866	1.261	1.910	1.756	1.389	1.738				
	0.800	0.517	0.731	0.609	0.928	2.061	1.544	1.738	1.389				
	0.700	0.586	0.609	0.496	0.388	2.285	1.333	1.333	2.108				
	0.600	0.686	0.496	0.388	0.301	2.600	1.126	1.126	2.582				
	0.500	0.838	0.388	0.301	0.224	3.051	0.924	0.924	3.133				
	0.400	1.094	0.285	0.224	0.166	3.736	0.727	0.727	3.965				
	0.300	1.608	0.186	0.166	0.122	4.884	0.537	0.537	5.307				
	0.200	3.512	0.091	0.122	0.089	7.185	0.352	0.352	7.935				
	0.100	15.45	0.045	0.089	0.073	14.095	0.173	0.173	15.710				
	∞	1.545	1.694	1.382	0.894	1.382	0.894	0.309	0.309				
6	1.111	0.289	1.040	1.116	1.322	2.054	1.744	1.550	1.335				
	1.250	0.245	0.866	1.116	1.126	1.126	2.239	1.550	1.335				
	1.429	0.207	0.731	1.236	0.957	0.957	2.499	1.346	1.346				
	1.667	0.173	0.609	1.407	0.801	0.801	2.858	1.143	1.143				
	2.000	0.141	0.496	1.653	0.654	0.654	3.369	0.942	0.942				
	2.500	0.111	0.388	2.028	0.514	0.514	4.141	0.745	0.745				
	3.333	0.082	0.285	2.656	0.379	0.379	5.433	0.552	0.552				
	5.000	0.054	0.166	3.917	0.248	0.248	8.020	0.363	0.363				
	10.000	0.028	0.089	7.1705	0.122	0.122	15.738	0.179	0.179				
	∞	1.353	1.789	1.353	1.202	1.202	0.894	0.309	0.309				
7	0.900	0.299	0.711	1.040	1.278	2.125	1.727	1.527	1.296				
	0.800	0.322	0.606	1.116	1.157	1.404	1.489	1.346	1.346				
	0.700	0.357	0.515	1.236	1.091	1.091	1.618	1.150	1.150				
	0.600	0.408	0.432	1.407	0.917	0.917	1.974	0.951	0.951				
	0.500	0.480	0.354	1.653	0.751	0.751	2.507	0.754	0.754				
	0.400	0.599	0.278	2.028	0.582	0.582	3.304	0.560	0.560				
	0.300	0.826	0.206	2.656	0.437	0.437	4.582	0.382	0.382				
	0.200	1.179	0.163	3.917	0.307	0.307	8.020	0.252	0.252				
	0.100	3.538	0.089	7.1705	0.157	0.157	15.738	0.132	0.132				
	∞	1.437	1.789	1.437	1.397	1.397	0.894	0.309	0.309				

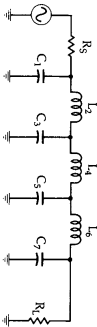
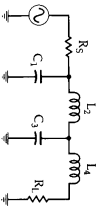
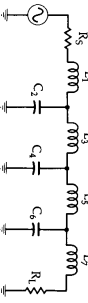
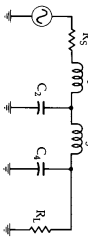


Table 4-3: Chebyshev prototype filter ($A_p \leq 0.01$ dB).

n	R_S/R_L	C_1	L_2	C_3	L_4	C_5	L_6	C_7	L_8	C_9	L_{10}	C_{11}	L_{12}	C_{13}	L_{14}	C_{15}	L_{16}	C_{17}	L_{18}	C_{19}	L_{20}	C_{21}	L_{22}	C_{23}	L_{24}	C_{25}	L_{26}	C_{27}	L_{28}	C_{29}	L_{30}	C_{31}	L_{32}	C_{33}	L_{34}	C_{35}	L_{36}	C_{37}	L_{38}	C_{39}	L_{40}	C_{41}	L_{42}	C_{43}	L_{44}	C_{45}	L_{46}	C_{47}	L_{48}	C_{49}	L_{50}	C_{51}	L_{52}	C_{53}	L_{54}	C_{55}	L_{56}	C_{57}	L_{58}	C_{59}	L_{60}	C_{61}	L_{62}	C_{63}	L_{64}	C_{65}	L_{66}	C_{67}	L_{68}	C_{69}	L_{70}	C_{71}	L_{72}	C_{73}	L_{74}	C_{75}	L_{76}	C_{77}	L_{78}	C_{79}	L_{80}	C_{81}	L_{82}	C_{83}	L_{84}	C_{85}	L_{86}	C_{87}	L_{88}	C_{89}	L_{90}	C_{91}	L_{92}	C_{93}	L_{94}	C_{95}	L_{96}	C_{97}	L_{98}	C_{99}	L_{100}	C_{101}	L_{102}	C_{103}	L_{104}	C_{105}	L_{106}	C_{107}	L_{108}	C_{109}	L_{110}	C_{111}	L_{112}	C_{113}	L_{114}	C_{115}	L_{116}	C_{117}	L_{118}	C_{119}	L_{120}	C_{121}	L_{122}	C_{123}	L_{124}	C_{125}	L_{126}	C_{127}	L_{128}	C_{129}	L_{130}	C_{131}	L_{132}	C_{133}	L_{134}	C_{135}	L_{136}	C_{137}	L_{138}	C_{139}	L_{140}	C_{141}	L_{142}	C_{143}	L_{144}	C_{145}	L_{146}	C_{147}	L_{148}	C_{149}	L_{150}	C_{151}	L_{152}	C_{153}	L_{154}	C_{155}	L_{156}	C_{157}	L_{158}	C_{159}	L_{160}	C_{161}	L_{162}	C_{163}	L_{164}	C_{165}	L_{166}	C_{167}	L_{168}	C_{169}	L_{170}	C_{171}	L_{172}	C_{173}	L_{174}	C_{175}	L_{176}	C_{177}	L_{178}	C_{179}	L_{180}	C_{181}	L_{182}	C_{183}	L_{184}	C_{185}	L_{186}	C_{187}	L_{188}	C_{189}	L_{190}	C_{191}	L_{192}	C_{193}	L_{194}	C_{195}	L_{196}	C_{197}	L_{198}	C_{199}	L_{200}	C_{201}	L_{202}	C_{203}	L_{204}	C_{205}	L_{206}	C_{207}	L_{208}	C_{209}	L_{210}	C_{211}	L_{212}	C_{213}	L_{214}	C_{215}	L_{216}	C_{217}	L_{218}	C_{219}	L_{220}	C_{221}	L_{222}	C_{223}	L_{224}	C_{225}	L_{226}	C_{227}	L_{228}	C_{229}	L_{230}	C_{231}	L_{232}	C_{233}	L_{234}	C_{235}	L_{236}	C_{237}	L_{238}	C_{239}	L_{240}	C_{241}	L_{242}	C_{243}	L_{244}	C_{245}	L_{246}	C_{247}	L_{248}	C_{249}	L_{250}	C_{251}	L_{252}	C_{253}	L_{254}	C_{255}	L_{256}	C_{257}	L_{258}	C_{259}	L_{260}	C_{261}	L_{262}	C_{263}	L_{264}	C_{265}	L_{266}	C_{267}	L_{268}	C_{269}	L_{270}	C_{271}	L_{272}	C_{273}	L_{274}	C_{275}	L_{276}	C_{277}	L_{278}	C_{279}	L_{280}	C_{281}	L_{282}	C_{283}	L_{284}	C_{285}	L_{286}	C_{287}	L_{288}	C_{289}	L_{290}	C_{291}	L_{292}	C_{293}	L_{294}	<
-----	-----------	-------	-------	-------	-------	-------	-------	-------	-------	-------	----------	----------	----------	----------	----------	----------	----------	----------	----------	----------	----------	----------	----------	----------	----------	----------	----------	----------	----------	----------	----------	----------	----------	----------	----------	----------	----------	----------	----------	----------	----------	----------	----------	----------	----------	----------	----------	----------	----------	----------	----------	----------	----------	----------	----------	----------	----------	----------	----------	----------	----------	----------	----------	----------	----------	----------	----------	----------	----------	----------	----------	----------	----------	----------	----------	----------	----------	----------	----------	----------	----------	----------	----------	----------	----------	----------	----------	----------	----------	----------	----------	----------	----------	----------	----------	----------	----------	----------	----------	----------	-----------	-----------	-----------	-----------	-----------	-----------	-----------	-----------	-----------	-----------	-----------	-----------	-----------	-----------	-----------	-----------	-----------	-----------	-----------	-----------	-----------	-----------	-----------	-----------	-----------	-----------	-----------	-----------	-----------	-----------	-----------	-----------	-----------	-----------	-----------	-----------	-----------	-----------	-----------	-----------	-----------	-----------	-----------	-----------	-----------	-----------	-----------	-----------	-----------	-----------	-----------	-----------	-----------	-----------	-----------	-----------	-----------	-----------	-----------	-----------	-----------	-----------	-----------	-----------	-----------	-----------	-----------	-----------	-----------	-----------	-----------	-----------	-----------	-----------	-----------	-----------	-----------	-----------	-----------	-----------	-----------	-----------	-----------	-----------	-----------	-----------	-----------	-----------	-----------	-----------	-----------	-----------	-----------	-----------	-----------	-----------	-----------	-----------	-----------	-----------	-----------	-----------	-----------	-----------	-----------	-----------	-----------	-----------	-----------	-----------	-----------	-----------	-----------	-----------	-----------	-----------	-----------	-----------	-----------	-----------	-----------	-----------	-----------	-----------	-----------	-----------	-----------	-----------	-----------	-----------	-----------	-----------	-----------	-----------	-----------	-----------	-----------	-----------	-----------	-----------	-----------	-----------	-----------	-----------	-----------	-----------	-----------	-----------	-----------	-----------	-----------	-----------	-----------	-----------	-----------	-----------	-----------	-----------	-----------	-----------	-----------	-----------	-----------	-----------	-----------	-----------	-----------	-----------	-----------	-----------	-----------	-----------	-----------	-----------	-----------	-----------	-----------	-----------	-----------	-----------	-----------	-----------	-----------	-----------	-----------	-----------	-----------	-----------	-----------	-----------	-----------	-----------	-----------	-----------	-----------	---

Table 4-5: Chebyshev prototype filter ($A_p \leq 0.5$ dB).

n	R_s/R_L	C_1	L_2	C_3	L_4	C_5	L_6	C_7
2	1.984	0.983	1.950					
3	1.000	1.864	1.280	1.834				
4	1.984	0.920	2.356	1.826				
5	1.000	1.807	1.303	2.691	1.303	1.807		
6	1.984	0.905	2.577	1.368	2.713	1.299	1.796	
7	1.000	1.790	1.296	2.718	2.718	2.718	1.790	1.790

Table 4-4: Chebyshev prototype filter ($A_p \leq 0.1$ dB).

n	R_s/R_L	C_1	L_2	C_3	L_4	C_5	L_6	C_7
2	1.335	1.209	1.638					
3	1.000	1.433	1.594	1.433				
4	1.335	0.992	2.148	1.341				
5	1.000	1.301	1.556	2.241	1.556	1.301		
6	1.335	0.942	2.090	1.659	2.247	1.534	1.277	
7	1.000	1.292	1.520	2.239	2.239	2.239	1.292	1.277

Table 4-6: Chebyshev prototype filter ($A_p \leq 1$ dB).

n	R_s/R_L	C_1	L_2	C_3	L_4
2	3.000	0.572	3.132		
	4.000	0.365	4.600		
	8.000	0.157	9.658		
	∞	1.213	1.109		
3	1.000	2.216	1.068	2.216	
	0.500	4.431	0.817	2.216	
	0.333	6.647	0.726	2.216	
	0.250	8.862	0.680	2.216	
	0.125	17.725	0.612	2.216	
	∞	1.652	1.460	1.108	
4	3.000	0.653	4.411	0.814	2.535
	4.000	0.452	7.083	0.612	2.848
	8.000	0.209	17.164	0.428	3.251
	∞	1.350	2.010	1.488	1.106

n	R_s/R_L	C_1	L_2	C_3	L_4	C_5	L_6	C_7
5	1.000	2.207	1.128	3.103	1.128	2.207		
	0.500	4.414	0.565	4.653	1.128	2.207		
	0.333	6.622	0.376	6.205	1.128	2.207		
	0.250	8.829	0.282	7.786	1.128	2.207		
	0.125	17.727	0.44	13.081	1.128	2.207		
	∞	1.721	1.845	2.081	1.483	1.103		
6	3.000	0.679	3.873	0.771	4.711	0.969	2.406	
	4.000	0.481	5.644	0.476	7.351	0.949	2.582	
	0.333	0.227	12.310	0.198	16.740	0.725	2.800	
	0.250	1.378	2.204	1.690	2.074	1.494	1.102	
	0.125	2.204	1.131	3.147	1.194	3.147	1.131	2.204
	∞	1.000	0.566	6.293	0.895	3.147	1.131	2.204
	3.000	4.408	0.377	9.441	0.796	3.147	1.131	2.204
	4.000	6.612	0.377	12.588	0.747	3.147	1.131	2.204
	8.000	8.815	0.283	25.175	0.671	3.147	1.131	2.204
	0.125	17.631	0.141	2.185	1.703	2.079	1.494	1.102
	∞	1.741	1.877	2.185	1.703	2.079	1.494	1.102

n	R_s/R_L	L_1	C_2	L_3	C_4	L_5	C_6	L_7
2	3.000							
	4.000							
	8.000							
	∞							
3	1.000	2.216		2.216				
	0.500	4.431		2.216				
	0.333	6.647		2.216				
	0.250	8.862		2.216				
	0.125	17.725		2.216				
	∞	1.652		1.108				
4	3.000	0.653	4.411	0.814	2.535			
	4.000	0.452	7.083	0.612	2.848			
	8.000	0.209	17.164	0.428	3.251			
	∞	1.350	2.010	1.488	1.106			

n	R_s/R_L	L_1	C_2	L_3	C_4	L_5	C_6	L_7
5	1.000	2.207		3.103				
	0.500	4.414		4.653				
	0.333	6.622		6.205				
	0.250	8.829		7.786				
	0.125	17.727		13.081				
	∞	1.721		2.081				
6	3.000	0.679	3.873	0.771	4.711	0.969	2.406	
	4.000	0.481	5.644	0.476	7.351	0.949	2.582	
	0.333	0.227	12.310	0.198	16.740	0.725	2.800	
	0.250	1.378	2.204	1.690	2.074	1.494	1.102	
	0.125	2.204	1.131	3.147	1.194	3.147	1.131	2.204
	∞	1.000	0.566	6.293	0.895	3.147	1.131	2.204
	3.000	4.408	0.377	9.441	0.796	3.147	1.131	2.204
	4.000	6.612	0.377	12.588	0.747	3.147	1.131	2.204
	8.000	8.815	0.283	25.175	0.671	3.147	1.131	2.204
	0.125	17.631	0.141	2.185	1.703	2.079	1.494	1.102
	∞	1.741	1.877	2.185	1.703	2.079	1.494	1.102

CHAPTER 5

NOISE AND SIGNAL-TO-NOISE RATIO

NOISE AND DISTORSION

Noise can be generally defined as any undesirable signal that masks or degrades the useful signal. This definition includes deterministic noise, due to coupling with the clock signal for example, and random noise whose origin is the fluctuation of a physical quantity such as voltage or current.

Deterministic noise can usually be drastically reduced or even eliminated by techniques such as shielding, filtering, or others. By its nature, random noise cannot be predicted and therefore cannot be eliminated. It can only be manipulated and reduced by techniques such as filtering.

We will use the term noise uniquely for random noise.

Noise is important because it represents the resolution limit for many systems.

Noise, being a random signal, is described by its statistical properties such as its amplitude probability distribution at a certain instant. In most cases it is not actually necessary to know the probability density, but only the first- and second-order moments corresponding to the average and the variance.

In many cases, noise can be considered stationary.

The noise of a circuit or system must always be compared to the signal that carries the useful information. We therefore introduce the notion of Signal-to-Noise Ratio (SNR) which is the ratio between the signal power and the noise power:

$$SNR \equiv \frac{\text{Average signal power}}{\text{Average noise power}} = \frac{P_{\text{signal}}}{P_N} \quad (5.1)$$

SPECTRAL NOISE FACTOR

The spectral noise factor of a two-port network as shown in Fig. 5-1 is defined as the ratio of the Power Spectral Density (PSD) of the maximum output noise, N_o , and the PSD of the noise due to the source resistance connected to the two-port network input, N_i , measured at a temperature of 290 K:

$$F(f) \equiv \frac{\text{PSD of total noise at output}}{\text{PSD at output due to source resistance } R_s} = \frac{N_o(f)}{G(f) \cdot N_i} \quad (5.2)$$

where $G(f)$ represents the gain in power of the two-port network and N_i is the PSD of the noise at the input of the two-port network due to the source.

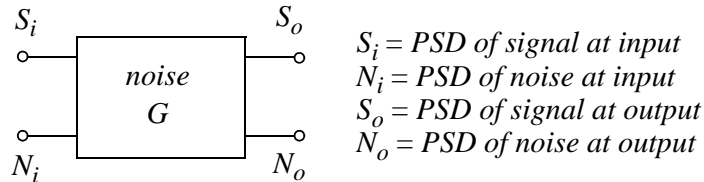


Fig 5-1: Two-port network with noise, and noise factor. The contribution of basic noise at the output of the two-port network is thus given by:

$$N_o - GN_i = FGN_i - GN_i = (F - 1)GN_i \quad (5.3)$$

This basic contribution can be shifted to the two-port network input as a PSD N_p by dividing (5.3) by the gain G :

$$N_p = (F - 1)N_i \quad (5.4)$$

where $F - 1$ is the excess noise factor. The noise factor can then be written as:

$$F = 1 + \frac{N_p}{N_i} > 1 \quad (5.5)$$

The noise factor is thus always greater than one.

NOISE FIGURE AND AVERAGE NOISE FACTOR

We define the noise figure NF by:

$$NF \equiv 10 \log(F) > 0 \text{ dB} \quad (5.6)$$

The minimum (ideal) value of F being equal to 1, the minimum noise figure is equal to 0 dB. According to the definition given by (5.2), the noise factor is a function of frequency. It is generally defined for a set frequency. We can also define an average noise factor which takes into account the bandwidth B of a system:

$$\bar{F} \equiv \frac{\int N_o df}{\int G(f)N_i df} = \frac{\int F(f)G(f)N_i df}{\int G(f)N_i df} = \frac{\int F(f)G(f) df}{\int G(f) df} \quad (5.7)$$

which reduces to the average value of F when the gain is constant in the bandwidth B :

$$\bar{F} = \frac{1}{B} \int F(f) df \quad (5.8)$$

for $G(f) = G_0 = \text{const.}$ in the bandwidth B .

NOISE FACTOR AND SIGNAL-TO-NOISE RATIO

The noise factor can also be defined as a function of the signal-to-noise ratio (SNR) at the input SNR_i and at the output SNR_o :

$$SNR_i \equiv \frac{P_{Si}}{P_{Ni}} = \frac{\int_B S_i df}{\int_B N_i df} \quad \text{and:} \quad SNR_o \equiv \frac{P_{So}}{P_{No}} = \frac{\int_B G(f)S_i df}{\int_B N_o df} \quad (5.9)$$

Eqn. 5.7 can be rewritten:

$$\bar{F} = \frac{P_{No}}{P_{Ni}} = \frac{1}{SNR_o} \frac{P_{So}}{P_{Si}} = \frac{1}{SNR_o} \frac{\int_B G(f)S_i df}{\int_B G(f)N_i df} \quad (5.10)$$

which for constant gain simplifies to:

$$\bar{F} = \frac{1}{SNR_o} \frac{\int_B S_i df}{\int_B N_i df} = \frac{SNR_i}{SNR_o} \quad (5.11)$$

The noise factor can thus be equivalently defined as the quotient of the signal-to-noise ratio at the input and the signal-to-noise ratio at the output. It is therefore a measure of the degradation of the signal-to-noise ratio at the output due to the basic noise generated by the two-port network.

NOISE TEMPERATURE

The power available from a source impedance Z_S corresponds to the maximum power that it can deliver to a load impedance Z_L . We know that this situation is achieved when the load impedance is equal to the complex conjugate of the source impedance:

$$Z_L = Z_S^* \quad (5.12)$$

In these conditions, the maximum power available from a source impedance R_S is given by:

$$P_S = \frac{V_S^2}{4R_S} \quad (5.13)$$

where V_S is the RMS source voltage. From this, we can deduce the power available from a source of thermal noise:

$$P_{Ni} = \frac{4kTR_S B}{4R_S} = kTB \quad (5.14)$$

We remark that this available thermal noise power is independent of the value of the source resistance. Thus, kTB is the maximum power available from any source that has an impedance with a resistive term. We also define the PSD available from a source in the bandwidth B as:

$$N_i = kT \quad (= 4 \times 10^{-21} J) \quad (5.15)$$

Note that this PSD is independent of the resistance value. The noise factor can then be expressed by:

$$F = 1 + \frac{N_a}{kT} \quad (5.16)$$

where T is the reference temperature (usually room temperature) and N_a the contribution of the two-port network.

NOISE TEMPERATURE

The noise factor is usually between 1 and 10. In certain cases, a larger scale is necessary. We use instead of the noise factor, the noise temperature T_r , defined by:

$$F \equiv 1 + \frac{T_r}{T} \quad (5.17)$$

From which: $T_r = (F - 1)T = N_a/k \quad (5.18)$

NOISE FACTOR OF CASCADING TWO-PORT NETWORKS

Consider the cascade connection of two 2-port networks, each characterized by its power gain and noise factor (cf Fig. 5-2).

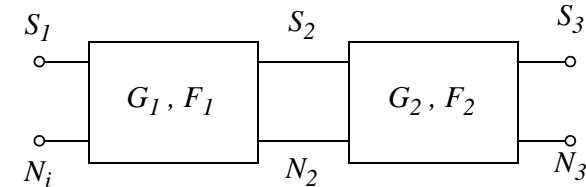


Fig 5-2: Noise factor of cascading two-port networks. The global noise factor F is defined by:

$$F = \frac{N_3}{GN_i} = \frac{N_3}{G_1 G_2 N_i} \quad (5.19)$$

The noise at the output of the first two-port network is equal to the noise at the input N_i multiplied by the gain in power G_1 plus the contribution of the first two-port network at the output $(F_1 - 1)G_1 N_i$:

$$N_2 = G_1 N_i + (F_1 - 1)G_1 N_i = F_1 G_1 N_i \quad (5.20)$$

The noise at the output of the second two-port network is equal to the noise at the input N_2 multiplied by the gain in power G_2 plus the contribution of the second two-port network at the output $(F_2 - 1)G_2 N_i$:

$$N_3 = G_2 N_2 + (F_2 - 1)G_2 N_i = G_2 F_1 G_1 N_i + (F_2 - 1)G_2 N_i \quad (5.21)$$

From which: $F = F_1 + \frac{(F_2 - 1)G_2 N_i}{G_2 G_1 N_i} = F_1 + \frac{F_2 - 1}{G_1} \quad (5.22)$

For the case in which $G_1 \gg (F_2 - 1)$, $F \cong F_1$ and the global noise factor is essentially determined by the first stage of the cascade. Eqn. 5.22 can be easily generalized for the case of n two-port networks in cascade (Friis Formula):

$$\left| F = F_1 + \frac{F_2 - 1}{G_1} + \frac{F_3 - 1}{G_1 G_2} + \dots + \frac{F_n - 1}{G_1 G_2 \dots G_{n-1}} \right| \quad (5.23)$$

SENSITIVITY AND MINIMUM DETECTABLE SIGNAL

The power of the input signal P_{Si} corresponding to a given signal-to-noise ratio at the output SNR_o is called the sensitivity of the system. The level (in dBm) corresponding to P_{Si} is called the minimum detectable signal (MDS).

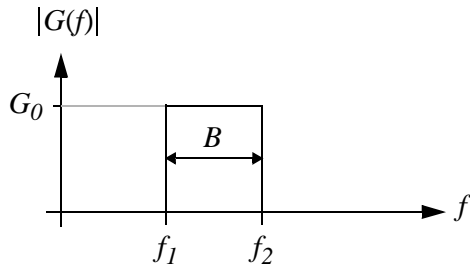


Fig 5-3: Gain in power of an ideal system. For a system whose gain is constant in a frequency bandwidth B and zero beyond this band (cf Fig. 5-3), the average noise factor is given by:

$$\bar{F} = \frac{\int_B G(f)S_i df}{SNR_o \int_B G(f)N_i df} = \frac{G_0 \int_B S_i df}{SNR_o G_0 \int_B N_i df} = \frac{P_{Si}}{SNR_o kTB} \quad (5.24)$$

From this we get the signal power for a given signal-to-noise ratio at the output SNR_o and a given average noise factor:

$$P_{Si} = \bar{F} \cdot kTB \cdot SNR_o \quad (5.25)$$

or in terms of the input signal level in dBm:

$$L_{min} \equiv 10\log\left(\frac{P_{Si}}{1mW}\right) = \bar{NF} + 10\log\left(\frac{kTB}{1mW}\right) + (SNR_o)_{dB} \quad [dBm] \quad (5.26)$$

EQUIVALENT NOISE SOURCES

A two-port network with noise can be modeled by the same two-port network without internal noise sources, and two noise sources V_N and I_N , independent of the values of the source resistance R_S and the load resistance R_L (cf Fig. 5-4).

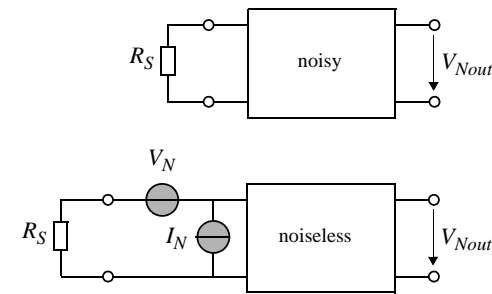


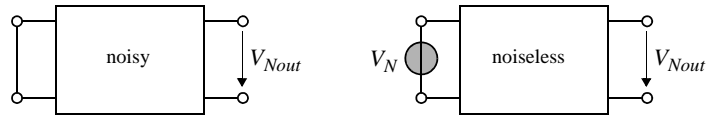
Fig 5-4: Noisy two-port network and its noiseless model, with equivalent noise sources at the input.

Note that the two noise sources are necessary in order to have a complete description of the two-port network noise for all source resistance values. In fact, when $R_S = 0$, the noise at the output V_{Nout} is due only to the noise source V_N , while if $R_S \rightarrow \infty$, it is due to the current noise source I_N . Since each of these sources considers the effects of the same physical causes of noise, internal to the two-port network, they are usually not independent. But in most cases, the correlation between V_N and I_N is weak and can be neglected.

CALCULATION OF EQUIVALENT NOISE SOURCES (1/2)

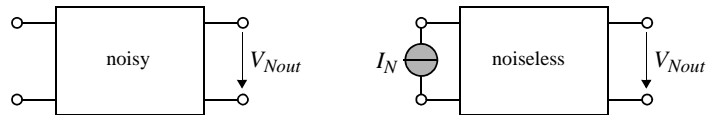
Voltage amplifier

The PSD S_{VN} of the source V_N of a voltage amplifier is calculated by evaluating the PSD of the output noise voltage of the two-port network when the input is short-circuited, and dividing it by the square of the voltage gain A_v (cf Fig. 5-5 a). The PSD S_{IN} of the source I_N is obtained by evaluating the PSD of the output noise voltage of the two-port network when the input is an open circuit, and dividing it by the square of the transimpedance Z_m (cf Fig. 5-5 b).



$$S_{VN} = \frac{S_{VNout}}{|A_v(f)|^2} \quad A_v \equiv \frac{V_{Nout}}{V_N}$$

a) Source of noise voltage.



$$S_{IN} = \frac{S_{VNout}}{|Z_m(f)|^2} \quad Z_m \equiv \frac{V_{Nout}}{I_N}$$

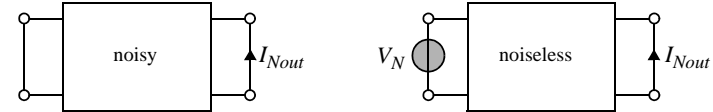
b) Source of noise current.

Fig 5-5: Calculation of PSD of equivalent noise sources of a voltage amplifier.

CALCULATION OF EQUIVALENT NOISE SOURCES (2/2)

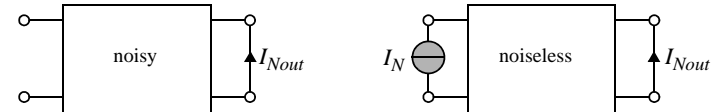
Transconductance amplifier

The PSD S_{VN} of the source V_N of a transconductance amplifier is calculated by evaluating the PSD of the output noise current of the two-port network when the input is short-circuited, and dividing it by the square of the transadmittance Y_m (cf Fig. 5-5 a). The PSD S_{IN} of the source I_N is obtained by evaluating the PSD of the output noise current of the two-port network when the input is an open circuit, and dividing by the square of the current gain A_i (cf Fig. 5-5 b).



$$S_{VN} = \frac{S_{INout}}{|Y_m(f)|^2} \quad Y_m \equiv \frac{I_{Nout}}{V_N}$$

a) Source of noise voltage.



$$S_{IN} = \frac{S_{INout}}{|A_i(f)|^2} \quad A_i \equiv \frac{I_{Nout}}{I_N}$$

b) Source of noise current.

Fig 5-6: Calculation of PSD of equivalent noise sources of a transconductance amplifier.

EQUIVALENT NOISE VOLTAGE SOURCE FOR THE BIPOLAR TRANSISTOR

The equivalent noise sources for the bipolar transistor can be calculated from the small-signal model shown in Fig. 5-7.

$$S_{VNB} = 4kTr_{bb'} \quad S_{INB} = 2qI_B + K_f \frac{I_B^{AF}}{f} \quad S_{INC} = 2qI_C$$

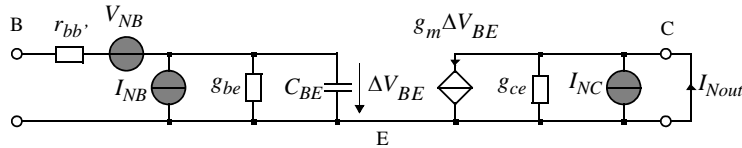


Fig 5-7: Small-signal model of the bipolar transistor, including the noise sources.

By considering that $g_{ce} \ll g_m$ and $g_{be}r_{bb'} \ll 1$, the low-frequency noise current when the input is short-circuited is given by:

$$I_{Nout} = I_{NC} + g_m \Delta V_{BE} = I_{NC} - g_m V_{NB} \quad (5.27)$$

The PSD of the current I_{Nout} is thus:

$$S_{INout} = S_{INC} + g_m^2 S_{VNB} \quad (5.28)$$

from which we find the PSD of the source V_N :

$$\begin{aligned} S_{VN} &= \frac{S_{INout}}{g_m^2} = \frac{S_{INC}}{g_m^2} + S_{VNB} = \frac{2qI_C}{g_m^2} + 4kTr_{bb'} \\ &= 4kT \left(r_{bb'} + \frac{1}{2g_m} \right) = 4kTR_N \end{aligned} \quad (5.29)$$

with:

$$R_N \equiv r_{bb'} + \frac{1}{2g_m} \quad (5.30)$$

EQUIVALENT NOISE CURRENT SOURCE FOR THE BIPOLAR TRANSISTOR

The noise current when the input is an open circuit is:

$$I_{Nout} = I_{NC} + \frac{g_m \cdot I_{NB}}{g_{be} + j\omega C_{BE}} = I_{NC} + \beta(j\omega) I_{NB} \quad (5.31)$$

Since the current gain is equal to $\beta(j\omega)$, the PSD of the source I_N is:

$$S_{IN} = S_{INB} + \frac{S_{INC}}{|\beta(j\omega)|^2} = 2q \left(I_B + \frac{I_C}{|\beta(j\omega)|^2} \right) + K_f \frac{I_B^{AF}}{f} \quad (5.32)$$

The current gain as a function of the frequency is given by:

$$\beta(f) = \frac{\beta_F}{1 + j\beta_F(f/f_T)} \quad (5.33)$$

so

$$S_{IN} = 2q \left(I_B + \frac{I_C}{\beta_F^2} \left(1 + \beta_F^2 \left(\frac{f}{f_T} \right)^2 \right) \right) + K_f \frac{I_B^{AF}}{f} \cong \quad (5.34)$$

$$2qI_C \left(\frac{1}{\beta_F} + \left(\frac{f}{f_T} \right)^2 \right) + K_f \frac{I_B^{AF}}{f}$$

The PSD of the source I_N as a function of the frequency is shown in Fig. 5-8.

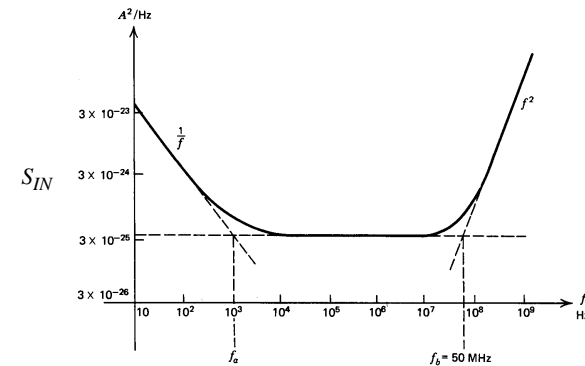


Fig 5-8: PSD of the equivalent noise current source I_N .

EQUIVALENT NOISE SOURCE OF AN AMPLIFIER CONNECTED TO A SOURCE

Amplifier noise associated with a voltage source can be modeled by a single noise source V_{Neq} (cf Fig. 5-9), including the noise from the source resistance $4kTR_S$ and the noise from the amplification device.

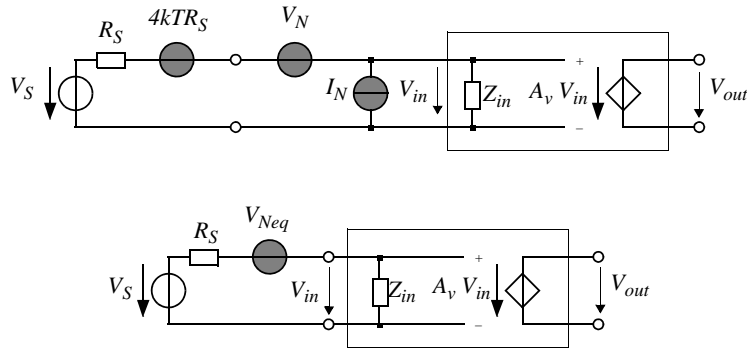


Fig 5-9: Noisy amplifier and equivalent noise sources. The PSD of the output noise is given by:

$$S_{VNout} = |A_v(f)|^2 \left\{ \underbrace{\left| \frac{Z_{in}}{Z_{in} + R_S} \right|^2 S_{VN}}_{\text{contribution of the amplifier}} + \underbrace{\left| \frac{R_S Z_{in}}{Z_{in} + R_S} \right|^2 S_{IN}}_{\text{contribution of the source}} + \underbrace{\left| \frac{Z_{in}}{Z_{in} + R_S} \right|^2 4kTR_S}_{\text{contribution of the source}} \right\} \quad (5.35)$$

The voltage gain between the source and the output being equal to $(Z_{in}/(Z_{in} + R_S))A_v(f)$, the PSD of the equivalent noise voltage source at the input is thus given by:

$$S_{VNeq} = 4kTR_S + S_{VN} + R_S^2 S_{IN} \quad (5.36)$$

This PSD is independent of the parameters Z_{in} and A_v of the amplifier, but depends on the source resistance R_S .

NOISE FACTOR OF AN AMPLIFIER AND OPTIMUM SOURCE RESISTANCE

The spectral noise factor of the amplifier in Fig. 5-9 is simply given by the ratio between S_{VNeq} and the contribution of the source $4kTR_S$:

$$F = \frac{S_{VNeq}}{4kTR_S} = 1 + \frac{S_{VN}}{4kTR_S} + \frac{S_{IN}}{4kT(1/R_S)} \quad (5.37)$$

This noise factor is independent of the amplifier parameters Z_{in} and A_v . In addition, it has a minimum for a value R_{Sopt} of the source resistance:

$$R_{Sopt} = \sqrt{\frac{S_{VN}}{S_{IN}}} \quad (5.38)$$

The corresponding minimum noise factor is thus:

$$F_{opt} = 1 + \frac{\sqrt{S_{VN} \cdot S_{IN}}}{2kT} \quad (5.39)$$

The noise figure corresponding to (5.37) is represented as a function of R_S in Fig. 5-10.

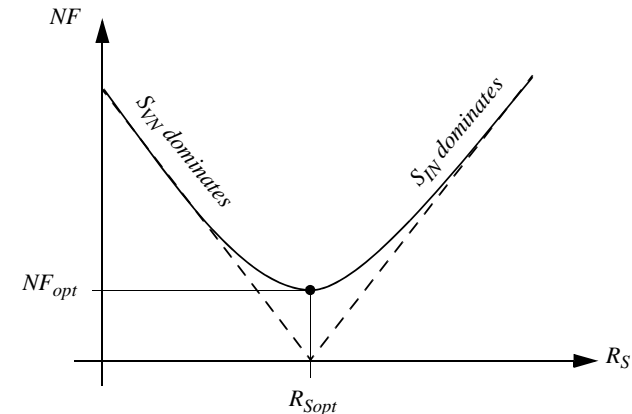


Fig 5-10: Noise figure corresponding to (5.37).

OPTIMUM SOURCE RESISTANCE OF BIPOLAR AND MOS TRANSISTORS

The optimum source resistance and the minimum noise factor for a bipolar transistor (neglecting the $1/f$ noise, that is by setting $K_f = 0$), are calculated from:

$$S_{VN} = 4kT\left(r_{bb'} + \frac{1}{2g_m}\right) \quad S_{IN} = 2qI_B \quad (5.40)$$

We find:

$$R_{Sopt} = \sqrt{\beta_F} \frac{\sqrt{1 + 2g_m r_{bb'}}}{g_m} \quad F_{opt} = 1 + \frac{\sqrt{1 + 2g_m r_{bb'}}}{\sqrt{\beta_F}} \quad (5.41)$$

From (5.41) we deduce that a low-noise bipolar transistor must have a small base resistance $r_{bb'}$ and a large current gain β_F . The optimum source resistance and the minimum noise factor for a MOS transistor (without $1/f$ noise) are calculated from the PSD of the equivalent noise sources at the input:

$$S_{VN} = 4kT \frac{Y}{g_m} \quad S_{IN} \cong 0 \quad (5.42)$$

from which: $R_{Sopt} \rightarrow \infty \quad F_{opt} \rightarrow 1 \quad (5.43)$

The MOS transistor is thus well matched for large source resistances.

In practice, for source resistances higher than $1 \text{ M}\Omega$, the MOS transistor offers a noise factor for white noise that is smaller than that of the bipolar (for the same transconductance). But the noise factor can be deteriorated by the presence of $1/f$ noise, which is generally higher in a MOS transistor.

IMPEDANCE MATCHING FOR MINIMUM NOISE

If the source resistance R_S is fixed, it is useless to try to obtain the condition $R_S = R_{opt}$ by adding series or parallel resistors. In fact, they would only worsen the noise of the system. We can, however, obtain the minimum noise factor by using an (ideal) transformer of ratio n as indicated in Fig. 5-11.

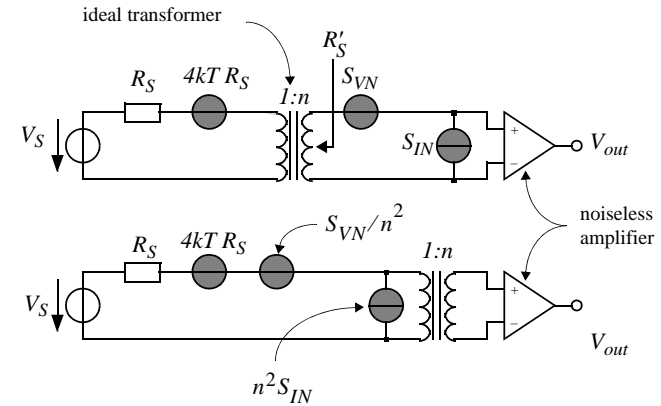


Fig 5-11: Source impedance matching for a minimum noise factor.

The PSD of the equivalent noise at the input is then given by:

$$S_{VNeq} = 4kTR_S + \frac{S_{VN}}{n^2} + n^2 \cdot R_S^2 S_{IN} \quad (5.44)$$

This PSD is minimum for a transformation ratio n_{opt} :

$$n_{opt}^2 = \frac{R'_S}{R_S} = \frac{R_{Sopt}}{R_S} = \frac{1}{R_S} \sqrt{\frac{S_{VN}}{S_{IN}}} \quad (5.45)$$

$$S_{VNeq} = 4kTR_S + 2R_S \sqrt{S_{VN} S_{IN}} = 4kTR_S \left(1 + \frac{\sqrt{S_{VN} S_{IN}}}{2kT}\right) = 4kTR_S \cdot F_{opt} \quad (5.46)$$

This optimum ratio also gives the minimum noise factor.

TOTAL EQUIVALENT INPUT NOISE FOR A RESISTIVE SOURCE

As indicated in Fig. 5-14, the block made up of an amplifier, of which the noise is modeled by two noise sources S_{VN} and S_{IN} , and an impedance source R_S , can be modeled by a single noise voltage source in series with the source V_S with PSD S_{VNeq} :

$$S_{VNeq} = 4kTR_S + S_{VN} + R_S^2 \cdot S_{IN} \quad (5.50)$$

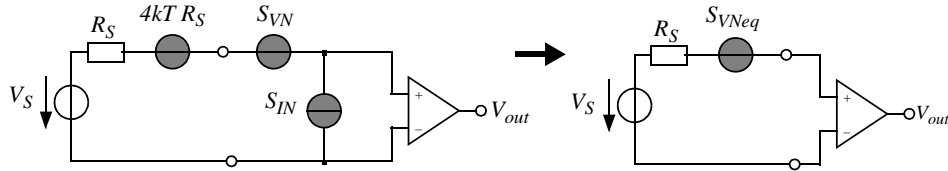


Fig 5-14: Total equivalent noise source at the input. Notice that this PSD is minimum when $R_S \rightarrow 0$ and not for $R_S = R_{opt}$, value for which the contribution of S_{VN} is equal to that of S_{IN} :

$$S_{VNeq} \Big|_{R_S=R_{Sopt}} = 4kTR_{Sopt} + 2 \cdot S_{VN} \quad (5.51)$$

Eqn. 5.50 is graphed as a function of the source resistance R_S in Fig. 5-15.

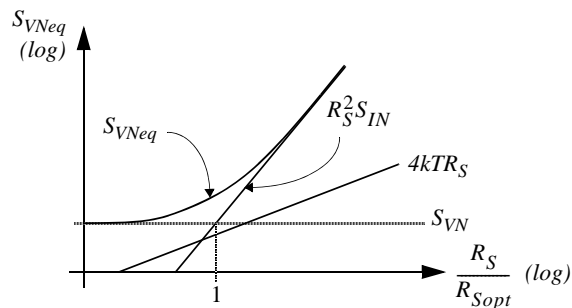


Fig 5-15: S_{VNeq} as a function of R_S .

VOLTAGE AMPLIFIER WITH RESISTIVE SOURCE (1/4)

Equivalent circuit

Consider the voltage amplifier presented in Fig. 5-16.

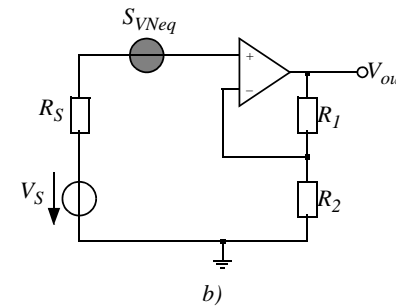
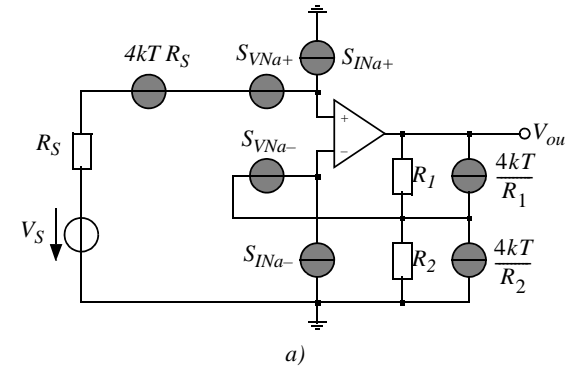


Fig 5-16: Voltage amplifier and equivalent noise model. Ignoring the correlations that exist between S_{VNa+} and S_{INa+} (S_{VNa-} and S_{INa-}), the PSD of the equivalent noise voltage at the input is given by:

$$S_{VNeq} = 4kT(R_S + R_{12}) + S_{VNa+} + S_{VNa-} + R_S^2 S_{INa+} + R_{12}^2 S_{INa-} \quad (5.52)$$

with:

$$R_{12} = R_1 \parallel R_2 \quad (5.53)$$

VOLTAGE AMPLIFIER WITH RESISTIVE SOURCE (2/4)

Bipolar input stage

For the case in which the input stage of the amplifier is realized with bipolar transistors, the PSD S_{VNa+} and S_{INa+} are given by the equations (5.29) and (5.34). Ignoring the $1/f$ noise ($K_f = 0$), we find the PSD S_{VNeq} :

$$\begin{aligned} S_{VNeq} &= 4kT \left(R_S + R_{12} + 2r_{bb'} + \frac{U_T}{I_C} \right) + (R_S^2 + R_{12}^2) 2qI_C \left(\frac{1}{\beta_F} + \left(\frac{f}{f_T} \right)^2 \right) \\ &= 4kT \left(R_S + R_{12} + 2r_{bb'} + \frac{U_T}{I_C} + (R_S^2 + R_{12}^2) \frac{I_C}{2\beta_F U_T} \right) \end{aligned} \quad (5.54)$$

for $f \ll f_T$ and $\beta_F \gg 1$. Notice that S_{VNeq} has a minimum for one particular value of the polarization current I_{Copt} :

$$I_{Copt} \equiv \sqrt{\frac{2\beta_F}{R_S^2 + R_{12}^2}} \cdot U_T \quad g_{mopt} \equiv \sqrt{\frac{2\beta_F}{R_S^2 + R_{12}^2}} \quad (5.55)$$

The minimum value of the PSD S_{VNeq} is thus given by:

$$\begin{aligned} S_{VNeqopt} &= 4kT \left(R_S + R_{12} + 2r_{bb'} + 2 \sqrt{\frac{R_S^2 + R_{12}^2}{2\beta_F}} \right) = 4kT \cdot R_{Neq} \\ &= R_{Neq} \end{aligned} \quad (5.56)$$

VOLTAGE AMPLIFIER WITH RESISTIVE SOURCE (3/4)

Optimum polarization current

The equivalent noise resistance R_{Neq} normalized to the source resistance R_S is graphed in Fig. 5-17 as a function of the polarization current for a bipolar transistor. For $r_{bb'} = R_S = R_I = 50 \Omega$ and $\beta_F = 200$, we find $I_{Copt} = 7.35 \text{ mA}$.

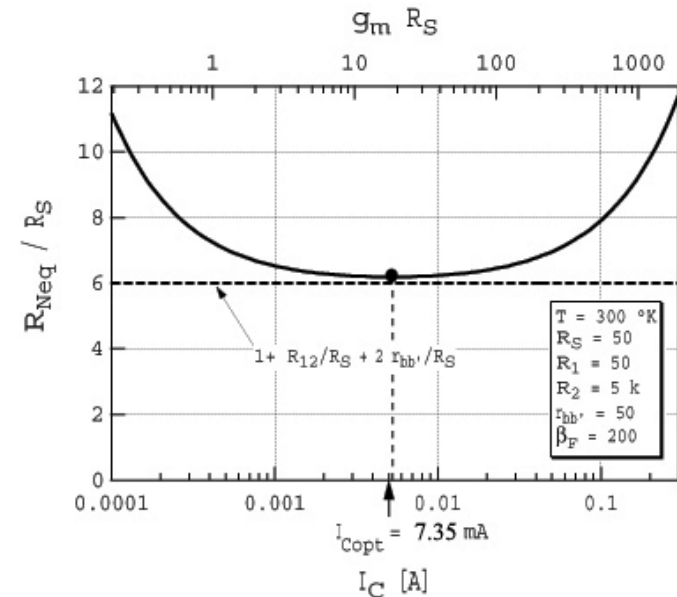


Fig 5-17: Optimum polarization current.

VOLTAGE AMPLIFIER WITH RESISTIVE SOURCE (4/4)

MOS input stage

For the case in which the input transistors are MOS transistors, we have:

$$S_{VNa+} = S_{VNa-} = 4kT \left(\frac{\gamma}{g_m} + \frac{K_f}{W L f} \right) \quad (5.57)$$

$$S_{INa+} = S_{INa-} = (\omega C_{in})^2 S_{VNa+}$$

The equivalent PSD of the input noise is thus given by:

$$S_{VNeq} = 4kT \left\{ R_S + R_{12} + \left[\frac{\gamma}{g_m} + \frac{K_f}{W L f} \right] [2 + (\omega C_{in})^2 (R_S^2 + R_{12}^2)] \right\} \quad (5.58)$$

which simplifies at low frequency ($\omega \ll 1 / (C_{in} \sqrt{R_S^2 + R_{12}^2})$) to:

$$S_{VNeq} = 4kT \left(R_S + R_{12} + 2 \left[\frac{\gamma}{g_m} + \frac{K_f}{W L f} \right] \right) \quad (5.59)$$

In this case, there is no optimum as a function of polarization. The noise contribution of the MOS transistors can be made negligible compared to the noise term due to the resistances, by reducing S_{VNa+} and S_{VNa-} . This is achieved by increasing the transconductance and the gate area WL of the MOS transistor. The frequency for which the white noise is equal to the $1/f$ noise (the corner frequency) is given by:

$$f_k = \frac{2K_f}{W L \left(R_S + R_{12} + \frac{2\gamma}{g_m} \right)} \quad (5.60)$$

HARMONIC DISTORTION

Single tone input signal

Although components such as amplifiers and transistors are often considered as linear elements, they have nonlinear transfer characteristics. Fig. 5-18 shows the typical transfer characteristic of an amplifier. It is made up of a linear portion and two saturation zones. We apply a sinusoidal input signal:

$$x(t) = X_1 \cos(\omega_0 t) \quad \text{or} \quad x(\phi) = X_1 \cos(\phi) \quad (5.61)$$

with $\phi \equiv \omega_0 t$. As long as the signal amplitude is less than X_{max} , the output signal is likewise sinusoidal with the same frequency. When $X_1 > X_{max}$, the output signal will be subject to distortion. It then contains frequency components which are multiples of ω_0 or *harmonics*. The harmonic components will depend on the input amplitude, the maximum amplitude X_{max} , and the nonlinear characteristics.

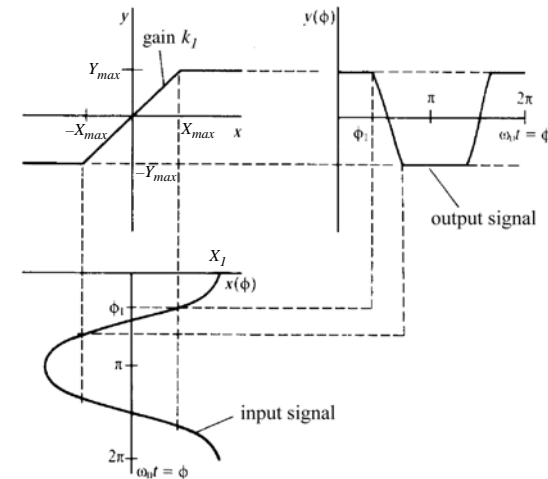


Fig 5-18: Transfer characteristic of an amplifier.

FOURIER SERIES OF THE OUTPUT SIGNAL

The output signal $y(t)$, remaining periodic, can be broken down into a Fourier series:

$$y(\phi) = \frac{a_0}{2} + \sum_{n=1}^{+\infty} a_n \cos(n\phi) + b_n \sin(n\phi) = \frac{a_0}{2} + \sum_{n=1}^{+\infty} r_n \cos(n\phi - \alpha_n) \quad (5.62)$$

The coefficients a_n , b_n , r_n and α_n are given by:

$$a_n \equiv \frac{1}{\pi} \int_{-\pi}^{\pi} y(\phi) \cos(n\phi) d\phi \quad \text{and:} \quad b_n \equiv \frac{1}{\pi} \int_{-\pi}^{\pi} y(\phi) \sin(n\phi) d\phi \quad (5.63)$$

$$r_n = a_n^2 + b_n^2 \quad \text{and:} \quad \alpha_n = \text{atan}(b_n/a_n)$$

In the case of the saturation characteristic of Fig. 5-18, we remark that the average value of the output signal is zero and thus $a_0 = 0$. In addition, the output signal $y(\phi)$ shown in Fig. 5-18 being an even function of ϕ , the coefficients b_n are all zero. Since the transfer characteristic is odd, the output only contains odd harmonics. It can be shown that the coefficient corresponding to the fundamental is given by:

$$a_1 = k_1 \cdot X_1 \cdot f(\xi) \quad \text{with:} \quad \xi \equiv X_1 / X_{\max} \quad (5.64)$$

where:

$$f(\xi) = \begin{cases} \frac{2}{\pi} \left[\text{asin}(1/\xi) + \frac{\sqrt{1-(1/\xi)^2}}{\xi} \right] & \xi > 1 \\ 1 & \xi \leq 1 \end{cases} \quad (5.65)$$

When $X_1 \leq X_{\max}$, the system is linear, and therefore there are no harmonics. In this case the output signal is simply given by $y(\phi) = k_1 \cdot x(\phi) = k_1 \cdot X_1 \cos(\phi)$ and so $a_1 = k_1 \cdot X_1$ which corresponds to $f(\xi) = 1$.

The amplitude of the harmonics greater than 1 is given by:

$$a_n = \frac{2k_1 X_1}{n\pi} \left[\frac{\sin((n+1)\phi)}{n+1} - \frac{\sin((n-1)\phi)}{n-1} \right] \quad \text{for: } n = 3, 5, 7, \dots \quad (5.66)$$

COMPRESSION

The function $f(\xi)$ given by (5.65) and permitting the calculation of the amplitude of the fundamental is shown in Fig. 5-19 as a function of ξ . This figure shows that the amplitude of the output signal fundamental decreases as a function of the input signal amplitude. This phenomenon is called compression.

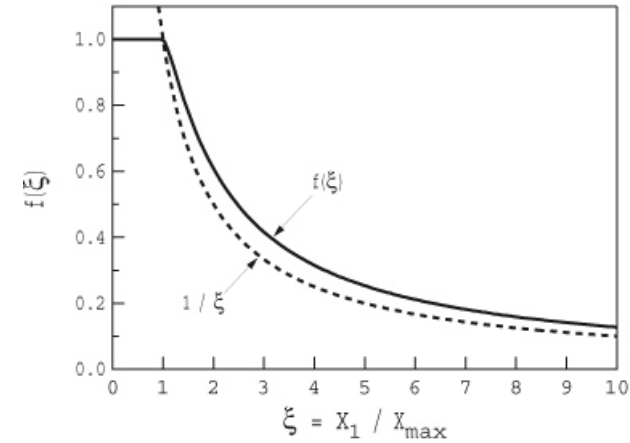


Fig 5-19: Function $f(\xi)$ given by (5.65) as a function of ξ .

The compression rate (CR) is defined as the ratio between the amplitude of the fundamental output signal of the nonlinear system and the amplitude of the fundamental output signal of an ideal linear system:

$$CR \equiv \frac{\text{fundamental amplitude}}{\text{linear system fundamental amplitude}} \cdot 100\% \quad (5.67)$$

For the characteristic in Fig. 5-18, the compression rate is:

$$CR = \frac{a_1}{k_1 X_1} = \frac{k_1 X_1 \cdot f(\xi)}{k_1 X_1} = f(\xi) \quad (5.68)$$

It is generally expressed in dB. It is common to refer to the amplitude corresponding to a compression rate of -1 dB.

APPROXIMATION OF HARMONIC AMPLITUDE

We can estimate the amplitude of the harmonics at the output of a nonlinear memoryless system excited by a sinusoidal signal, by expanding the nonlinear characteristic with a Taylor series:

$$y = k_0 + k_1x + k_2x^2 + k_3x^3 + \dots \quad (5.69)$$

By introducing the sinusoidal signal (5.61) and developing, we obtain:

$$y = Y_0 + Y_1 \cos(\phi) + Y_2 \cos(2\phi) + Y_3 \cos(3\phi) + \dots \quad (5.70)$$

with:

$$Y_0 = k_0 + \frac{1}{2}k_2X^2 + \dots \quad Y_1 = k_1X + \frac{3}{4}k_3X^3 + \dots \quad (5.71)$$

$$Y_2 = \frac{1}{2}k_2X^2 + \dots \quad Y_3 = \frac{1}{4}k_3X^3 + \dots$$

For a perfectly linear system without offset ($k_i = 0 \quad \forall i \neq 1$) the output signal is sinusoidal and its amplitude Y_1 simply reduces to k_1X . The factor k_1 then corresponds to the gain of the linear system. For a nonlinear system, the output signal is no longer sinusoidal (but is still periodic with the same period as the input signal). The amplitude of the fundamental Y_1 is modified by the cubic term $(3/4)k_3X^3$ and can thus be either larger or smaller than that obtained when considering the system to be linear. For a nonlinear system dominated by the cubic term, we then refer to an expansion characteristic when $k_3 > 0$ and a compression characteristic when $k_3 < 0$.

COMPRESSION POINT AT -1 dB

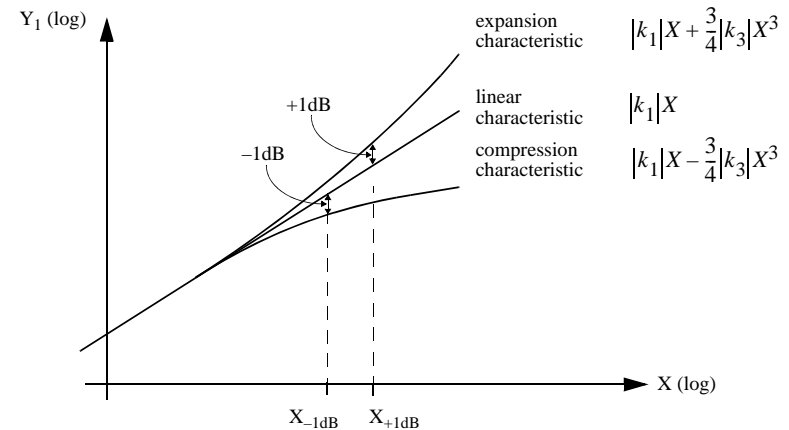


Fig 5-20: Expansion or compression point at ± 1 dB.

The compression point at -1 dB (or expansion point at +1 dB) corresponds to the amplitude X_{-1dB} (or X_{+1dB}) for which the fundamental is 1 dB from the value obtained when considering the system as perfectly linear (cf Fig. 5-20). These amplitudes are given respectively by:

$$X_{-1dB} = \sqrt{\frac{4}{3}(1 - 10^{-1/20})} \left| \frac{k_1}{k_3} \right| \quad X_{+1dB} = \sqrt{\frac{4}{3}(10^{1/20} - 1)} \left| \frac{k_1}{k_3} \right| \quad (5.72)$$

or expressed in dB:

$$20\log(X_{-1dB}) = 10\log\left(\left|\frac{k_1}{k_3}\right|\right) - 8.386 \quad [dB]$$

$$20\log(X_{+1dB}) = 10\log\left(\left|\frac{k_1}{k_3}\right|\right) - 7.886 \quad [dB] \quad (5.73)$$

HARMONIC DISTORTION INTERCEPT (HDI)

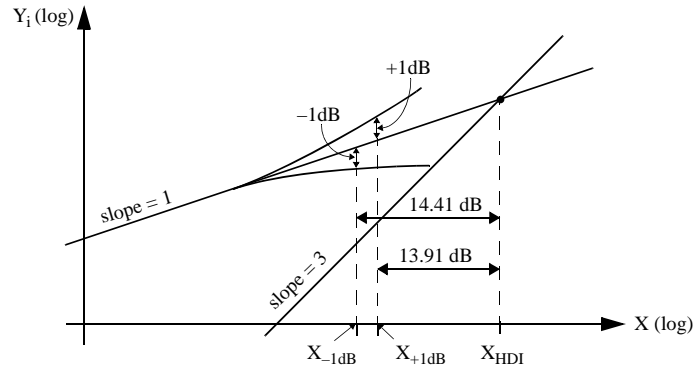


Fig 5-21: Harmonic distortion intercept.

Fig. 5-21 shows the harmonic components Y_1 and Y_3 as a function of the input signal amplitude X in a log-log graph for the case in which the nonlinearity is dominated by the cubic term. The compression of the fundamental is thus mainly due to the cubic term $\frac{3}{4}|k_3|X^3$ and the compression of the third harmonic is negligible. Notice that the amplitude of the 3rd harmonic increases three times as quickly as that of the fundamental (in a log-log diagram). The amplitude X_{HDI} (HDI=Harmonic Distortion Intercept) corresponding to the intersection point between the fundamental when considering the system to be linear, and the 3rd harmonic (without compression) is given by:

$$k_1 X_{HDI} = \frac{1}{4} k_3 X_{HDI}^3 \rightarrow X_{HDI} = 2 \cdot \sqrt{|k_1/k_3|} \quad (5.74)$$

or as: $20\log(X_{HDI}) = 10\log(|k_1/k_3|) + 6 \text{ dB} \quad (5.75)$

The compression point at -1 dB is located 14.41 dB below the intersection point:

$$\Delta X \equiv 20\log(X_{HDI}/X_{-1dB}) = -10\log\left(\frac{1}{3}(1 - 10^{-1/20})\right) = 14.41 \text{ dB} \quad (5.76)$$

EXAMPLE 1: EXPONENTIAL CHARACTERISTIC (1/2)

For the exponential characteristic of a bipolar transistor, the collector current for a base-emitter control voltage $v_{be}(t) \equiv V_{BEq} + \Delta V_{BE} \cdot \cos(\omega_0 t)$ is given by:

$$i_c(t) = I_s \cdot \exp\left[\frac{V_{BEq} + \Delta V_{BE} \cdot \cos(\omega_0 t)}{U_T}\right] = I_q \cdot \exp[X \cdot \cos(\omega_0 t)] \quad (5.77)$$

where $I_q \equiv I_s \cdot \exp[V_{BEq}/U_T]$ is the bias current defined for $\Delta V_{BE} = 0$ and $X \equiv \Delta V_{BE}/U_T$. We can thus normalize the current $i_c(t)$ to I_q :

$$y(t) \equiv \frac{I_c(t)}{I_q} = \exp[X \cdot \cos(\omega_0 t)] \quad (5.78)$$

It can be shown that the Fourier series development of the function (5.78) is given by:

$$y(t) = \exp[X \cdot \cos(\omega_0 t)] = I_0(X) + 2 \cdot \sum_{n=1}^{+\infty} I_n(X) \cdot \cos(n\omega_0 t) \quad (5.79)$$

where $I_0(X)$ is the modified Bessel function of order 0 and $I_n(X)$ is the modified Bessel function of order n . For an exponential function, it is thus possible to calculate the harmonics Y_n exactly. But unfortunately, this is not always possible. So we can compare the harmonics calculated exactly by (5.79) to those obtained by expanding the normalized exponential characteristic $y(t)$ in a Taylor series:

$$y(t) \equiv \frac{I_c(t)}{I_q} = e^x \cong 1 + x + \frac{x^2}{2} + \frac{x^3}{6} \quad (5.80)$$

where $x(t) \equiv X \cdot \cos(\omega_0 t)$.

EXAMPLE 1: EXPONENTIAL CHARACTERISTIC (2/2)

From (5.80) we get the coefficients $k_1 = 1$ and $k_3 = 1/6$ and the expansion point at +1 dB:

$$20\log(X_{+1dB}) = -0.1 \text{ dB} \quad (5.81)$$

and the intersection point of the harmonics:

$$20\log(X_{HDI}) = 13.8 \text{ dB} \quad (5.82)$$

The expansion point at +1 dB and the intersection point of the harmonic components are represented in Fig. 5-22. Notice that the approximation of the compression by using the expansion (5.80) is very close to the exact characteristic. In addition, we see that the third harmonic is subject to expansion and moves away from the right.

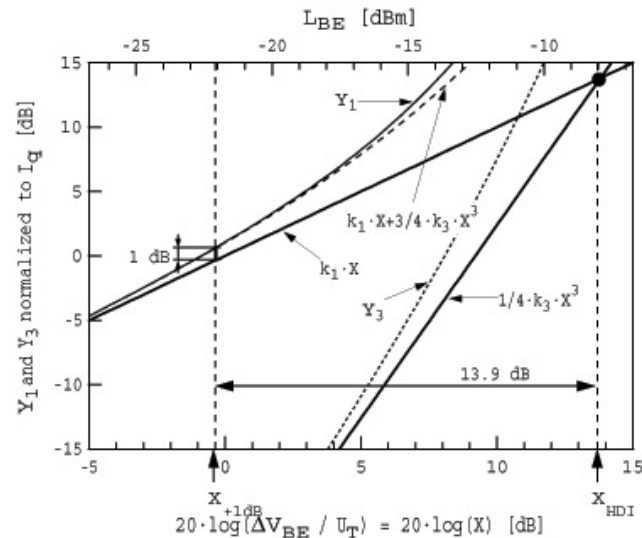


Fig 5-22: Expansion point at 1 dB and intersection of harmonic components for an exponential.

EXAMPLE 2: THE DIFFERENTIAL PAIR (1/2)

The differential current of a bipolar differential pair is simply given by:

$$y \equiv \frac{\Delta i}{I_q} = \tanh(x) \quad \text{with} \quad x \equiv \frac{V_{in}}{2U_T} \quad (5.83)$$

where V_{in} is the differential input voltage and I_q half of the tail current (or the bias current of each of the transistors when $V_{in} = 0$). Unlike the case of the exponential function, there is no analytic expression for the Fourier series expansion of (5.83) with $x(t) = X \cdot \cos(\omega_0 t)$. This characteristic can nevertheless be approximated with a Taylor series expansion:

$$y \equiv \tanh(x) \cong x - \frac{x^3}{3} \quad (5.84)$$

Notice that there is no even term. From (5.84) we get $k_1 = 1$ and $k_3 = -1/3$. This approximation is represented in Fig. 5-23 with the function $\tanh(x)$ as well as another approximation:

$$y \equiv \tanh(x) \cong x - 0.254 \cdot x^3 \quad (5.85)$$

We remark that the approximation (5.85) is better (error less than 2% for $|x| \leq 1$) than that given by the Taylor expansion (5.84) (error less than 2% for $|x| \leq 0.59$).

The amplitude of the fundamental calculated using approximations (5.84) and (5.85), along with the amplitude of the linear system, are shown in Fig. 5-24. The compression point calculated from (5.73) is given by -3.6 dB for (5.84) and -2.44 dB for (5.85). The first and third harmonics intersect at the point 10.8 dB using the approximation (5.84).

EXAMPLE 2: THE DIFFERENTIAL PAIR (2/2)

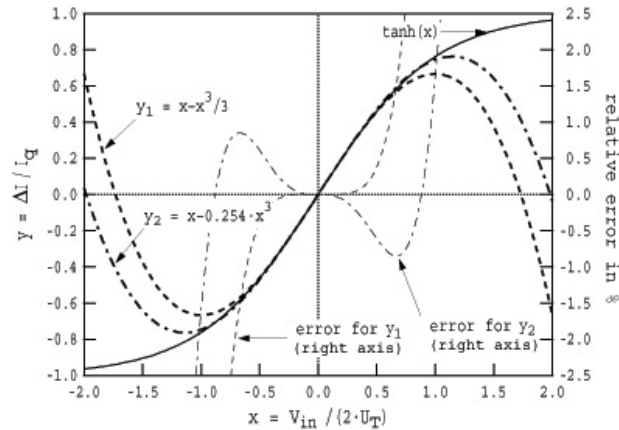


Fig 5-23: *Tanh(x) and 3rd degree approximation.*

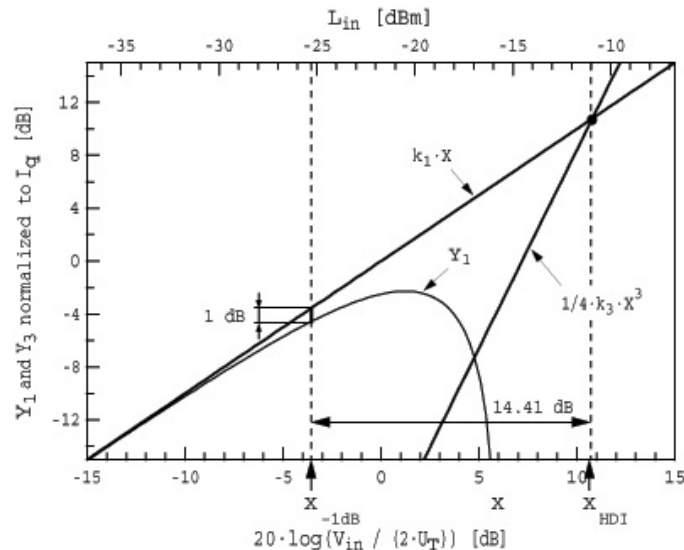


Fig 5-24: *Compression point at -1 dB and intersection point of harmonics 1 and 3 for a tanh characteristic.*

HARMONIC DISTORTION RATE

One measure of the distortion of a signal is given by the ratio between the harmonic amplitude n (r_n) and the amplitude of the fundamental r_1 , measured as a percentage:

$$\text{Distorsion rate for the harmonic } n \equiv \frac{r_n}{r_1} \cdot 100\% \quad (5.86)$$

The *total harmonic distortion* rate (THD) is the ratio between the RMS value of the harmonics $n \neq 1$ and the RMS value of the distorted signal at the output for a sinusoidal input signal:

$$\text{THD} \equiv \frac{\sqrt{\sum_{n=2}^{+\infty} a_n^2 + b_n^2}}{\sqrt{\sum_{n=1}^{+\infty} a_n^2 + b_n^2}} = \frac{\sqrt{\sum_{n=2}^{+\infty} r_n^2}}{\sqrt{\sum_{n=1}^{+\infty} r_n^2}} \cong \frac{\sqrt{r_2^2 + r_3^2}}{\sqrt{r_1^2 + r_2^2 + r_3^2}} \quad (5.87)$$

The THD can often be approximated by considering only the first harmonics, because the amplitude of the harmonics generally decreases very quickly.

INTERMODULATION

Sinusoidal “duo tone” input signal

Consider a nonlinear system with a static polynomial characteristic:

$$y = k_0 + k_1x + k_2x^2 + k_3x^3 + k_4x^4 + \dots \quad (5.88)$$

Let us consider the case of a signal composed of two sinusoidal waves:

$$x(t) = X_1 \cos(\omega_1 t) + X_2 \cos(\omega_2 t) = X_1 \cos(\phi_1) + X_2 \cos(\phi_2) \quad (5.89)$$

where $\phi_i \equiv \omega_i t$ ($i = 1, 2$). The output signal is obtained by substituting (5.89) into (5.88). Let's look at the result term by term. The linear term is given by:

$$k_1x = k_1X_1 \cos(\phi_1) + k_1X_2 \cos(\phi_2) \quad (5.90)$$

The amplitudes of the sinusoidal waves are simply multiplied by the gain k_1 . The quadratic term is given by:

$$\begin{aligned} k_2x^2 &= k_2[X_1 \cos(\phi_1) + X_2 \cos(\phi_2)]^2 \\ &= k_2[X_1^2 \cos^2(\phi_1) + 2X_1X_2 \cos(\phi_1) \cos(\phi_2) + X_2^2 \cos^2(\phi_2)] \\ &= \left. \frac{k_2X_1^2}{2} + \frac{k_2X_2^2}{2} \right\} = \text{constant term} \end{aligned} \quad (5.91)$$

$$\begin{aligned} &+ \left. \frac{k_2X_1^2}{2} \cos(2\phi_1) + \frac{k_2X_2^2}{2} \cos(2\phi_2) \right\} = \text{second harmonics} \\ &+ k_2X_1X_2 [\cos(\phi_1 + \phi_2) + \cos(\phi_1 - \phi_2)] \} = \begin{array}{l} \text{products of second order} \\ \text{intermodulation} \end{array} \end{aligned}$$

In addition to the constant term (at zero frequency) and second harmonics, the signal contains two equal amplitude components for which the frequencies are the sum and the difference of the input signal frequencies. These components are called second order intermodulation products (IM2). Thus, the nonlinearity corresponding to the quadratic term generates second order intermodulation products whose amplitudes depend linearly on X_1 and X_2 .

3rd ORDER INTERMODULATION PRODUCTS

The cubic term is given by:

$$\begin{aligned} k_3x^3 &= k_3[X_1 \cos(\phi_1) + X_2 \cos(\phi_2)]^3 \\ &= k_3[X_1^3 \cos^3(\phi_1) + 3X_1^2X_2 \cos^2(\phi_1) \cos(\phi_2) \\ &\quad + 3X_1X_2^2 \cos(\phi_1) \cos^2(\phi_2) + X_2^3 \cos^3(\phi_2)] \end{aligned} \quad (5.92)$$

After expansion, we get:

$$\begin{aligned} k_3x^3 &= \frac{3k_3}{2} \left(X_1X_2^2 + \frac{X_1^3}{2} \right) \cos(\phi_1) + \frac{3k_3}{2} \left(X_1^2X_2 + \frac{X_2^3}{2} \right) \cos(\phi_2) \} = \text{fundamentals} \\ &+ \left. \frac{k_3X_1^3}{4} \cos(3\phi_1) + \frac{k_3X_2^3}{4} \cos(3\phi_2) \right\} = \text{3rd harmonics} \\ &+ \left. \frac{3k_3X_1^2X_2}{4} [\cos(2\phi_1 + \phi_2) + \cos(2\phi_1 - \phi_2)] \right\} = \text{3rd order IM products} \\ &+ \left. \frac{3k_3X_1X_2^2}{4} [\cos(2\phi_2 + \phi_1) + \cos(2\phi_2 - \phi_1)] \right\} \end{aligned} \quad (5.93)$$

Eqn. 5.93 shows that the 3rd order nonlinearity produces fundamental components along with 3rd order harmonics. In addition, we find 3rd order IM products at the frequencies $2f_1 + f_2$, $2f_2 + f_1$, $2f_1 - f_2$ and $2f_2 - f_1$. When the frequencies f_1 and f_2 are close, the components at frequencies $2f_1 - f_2$ and $2f_2 - f_1$ become particularly bothersome, because they fall into the useful transmission band and are thus difficult to eliminate by selective filtering.

The same approach can be used for nonlinearities of order higher than 3. In general, an n th order nonlinearity produces harmonics that are multiples of the frequencies f_1 and f_2 up to n . If n is even (odd), they are all even (odd) multiples of f_1 and f_2 . If n is even, there is no fundamental, but there is a constant term.

INTERMODULATION PRODUCTS

In general, the intermodulation products generated by a nonlinearity of order n are given by:

$$\pm k \cdot f_1 \mp l \cdot f_2 \quad \text{where:} \quad k + l = m \quad \text{with:} \quad m = 2, 3, \dots, n \quad (5.94)$$

where the upper frequencies are obtained by taking the two plus signs and the lower frequencies are obtained by taking opposite signs such that the resulting frequencies remain positive. The two minus signs are thus never used. Taking $\Delta f \equiv |f_2 - f_1|$, certain odd-order IM products are given by:

n	$l \cdot f_2 - k \cdot f_1$	$k \cdot f_1 - l \cdot f_2$	$l \cdot f_2 + k \cdot f_1$	$k \cdot f_1 + l \cdot f_2$
3	$2f_2 - f_1$ $= f_2 + \Delta f$	$2f_1 - f_2$ $= f_1 - \Delta f$	$2f_2 + f_1$ $= 3f_2 - \Delta f$	$2f_1 + f_2$ $= 3f_1 + \Delta f$
5	$3f_2 - 2f_1$ $= f_2 + 2\Delta f$	$3f_1 - 2f_2$ $= f_1 - 2\Delta f$	$3f_2 + 2f_1$ $= 5f_2 - 2\Delta f$	$3f_1 + 2f_2$ $= 5f_1 + 2\Delta f$
7	$4f_2 - 3f_1$ $= f_2 + 3\Delta f$	$4f_1 - 3f_2$ $= f_1 - 3\Delta f$	$4f_2 + 3f_1$ $= 7f_2 - 3\Delta f$	$4f_1 + 3f_2$ $= 7f_1 + 3\Delta f$

The IM product components closest to the fundamental frequencies f_1 and f_2 are presented in Fig. 5-25.

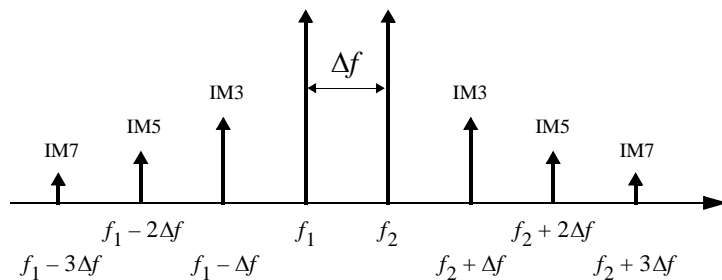


Fig 5-25: Odd IM products around f_1 and f_2

DESENSITIZATION AND BLOCKING (1/2)

A desired input signal $X_1 \cos(\phi_1)$ added to an interfering signal $X_2 \cos(\phi_2)$ is applied to a nonlinear system with the characteristic shown in Fig. 5-26 and described by:

$$y = \begin{cases} k_1 \cdot x + k_3 \cdot x^3 = 12x - x^3 & |x| \leq 2 \\ \pm 16 & |x| > 2 \end{cases} \quad (5.95)$$

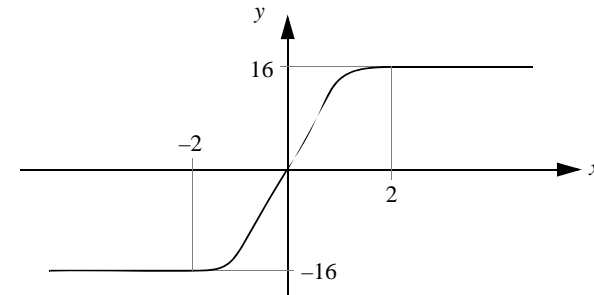


Fig 5-26: Odd nonlinear characteristic.

The output signal y_1 at the frequency f_1 for an input signal amplitude less than 2 (no saturation), is given by:

$$y_1 = 12X_1 \left(1 - \frac{X_1^2}{16} - \frac{X_2^2}{8} \right) \cos(\phi_1) \cong 12X_1 \left(1 - \frac{X_1^2}{16} \right) \cos(\phi_1) \quad \text{for } X_2 \ll X_1 \quad (5.96)$$

The compression rate for the case in which the amplitude of the interfering signal is much weaker than the amplitude of the desired signal is given by:

$$CR_{dB} = 20 \log \left(1 - \frac{X_1^2}{16} \right) \quad (5.97)$$

The amplitude corresponding to a compression rate of -1 dB is thus 1.32 V, which is in agreement with the hypothesis that $X_1 < 2V$. For small amplitudes X_1 , the system functions as a linear amplifier.

DESENSITIZATION AND BLOCKING (2/2)

Let us consider the case in which the amplitude of the useful signal is small (for example $X_1 < 0.4V$) and the interfering signal becomes dominant, so:

$$y_1 = 12X_1 \left(1 - \frac{X_2^2}{8}\right) \cos(\phi_1) \quad X_1, X_2 \leq 2 \quad (5.98)$$

We notice that the effect of the interfering signal is to reduce the amplitude of the useful signal at the output. This phenomenon, called desensitization, is similar to compression, but is caused by a strong interfering signal at a different frequency. We define a **desensitization ratio** by:

$$DS \equiv \frac{|\text{desired output signal in the presence of interfering signal}|}{|\text{desired output signal without interfering signal}|} \quad (5.99)$$

In our case we have:

$$DS_{dB} = 20 \log \left(1 - \frac{X_2^2}{8}\right) \quad X_2 \leq 2 \quad (5.100)$$

For $X_1 < 0.4V$ and $X_2 = 1.6V$, we have $DS_{dB} = -3.35dB$. We thus speak of a desensitization of about 3 dB that represents a reduction of the useful signal amplitude by a factor $\sqrt{2}$ and thus a reduction of the power by a factor of two.

In an extreme case, a large enough interfering signal can even cancel out the amplitude of the desired signal. This phenomenon is called **blocking**. In our case, the amplitude X_2 provoking the cancellation of the useful signal is given by $1 - X_2^2/8 = 0$, corresponding to $X_2 = 2.83V$. This amplitude is larger than 2 V and therefore does not satisfy the hypotheses. Nevertheless, we can imagine a system with a useful signal that is cancelled out entirely by an interfering signal at another frequency.

THIRD-ORDER INTERCEPT POINT (IP3) (1/2)

Consider the case in which the amplitude of the interfering signal is equal to the amplitude of the desired signal ($X_1 = X_2 = V_{in}$). The average power of the input signal P_{in} and its corresponding level L_{in} are:

$$L_{in} \equiv 10 \log \left(\frac{P_{in}}{1mW} \right) = 10 \log \left(\frac{V_{in}^2}{2R_{in} \cdot 1mW} \right) \quad [dBm] \quad (5.101)$$

The factor 2 in (5.101) comes from the fact that V_{in} is a peak value and not an RMS value. The level of the linear term of the signal at the system output is given by:

$$L_{out1} = 10 \log \left(\frac{P_{out1}}{1mW} \right) = 10 \log \left(\frac{GP_{in}}{1mW} \right) = L_{in} + G_{dB} \quad (5.102)$$

where G is the gain in power $G \equiv P_{out1}/P_{in}$, which can be expressed as a function of the voltage gain k_1 and the ratio between the input resistance R_{in} and the load resistance R_L :

$$G = \frac{V_{out}^2}{2R_L} \cdot \frac{2R_{in}}{V_{in}^2} = \frac{(k_1 \cdot V_{in})^2}{V_{in}^2} \cdot \frac{R_{in}}{R_L} = k_1^2 \cdot \frac{R_{in}}{R_L} \quad (5.103)$$

The amplitude of the 3rd order IM product at $2f_1 - f_2$ is equal to $\frac{3}{4}k_3V_{in}^3$. The average power corresponding to the load terminal R_L is thus:

$$P_{out3} = \frac{\left(\frac{3}{4}k_3V_{in}^3\right)^2}{2R_L} \quad (5.104)$$

corresponding to a level L_{out3} :

$$\begin{aligned} L_{out3} &= 10 \log \left(\frac{\left(\frac{3}{4}k_3V_{in}^3\right)^2}{2R_L \cdot 1mW} \right) = 10 \log \left(\frac{9}{4}k_3^2 \frac{R_{in}^3}{R_L} (1mW)^2 \left(\frac{V_{in}^2}{2R_{in} \cdot 1mW} \right)^3 \right) \\ &= 3L_{in} + 20 \log(k_3) + 10 \log \left(\frac{R_{in}^3}{R_L} \right) - 56.5 = 3L_{in} + K \end{aligned} \quad (5.105)$$

where:
$$K \equiv 20 \log(k_3) + 10 \log \left(\frac{R_{in}^3}{R_L} \right) - 56.5 \quad (5.106)$$

THIRD-ORDER INTERCEPT POINT (IP3) (2/2)

The levels L_{out1} corresponding to the fundamental and L_{out3} corresponding to the 3rd order IM product at $2f_1 - f_2$, are shown as a function of the input level L_{in} in Fig. 5-27. The intersection point of the lines L_{out1} and L_{out3} is called the third-order intercept point (PI3). This point can be specified either by its projection on the x-axis IIP , or by its projection on the y-axis of L_{out1} (OIP). Unfortunately, this point cannot be measured directly because it corresponds to an extrapolation. The phenomena of compression, desensitization, and higher-order IM products deteriorate the linearity of the system for high power signals.

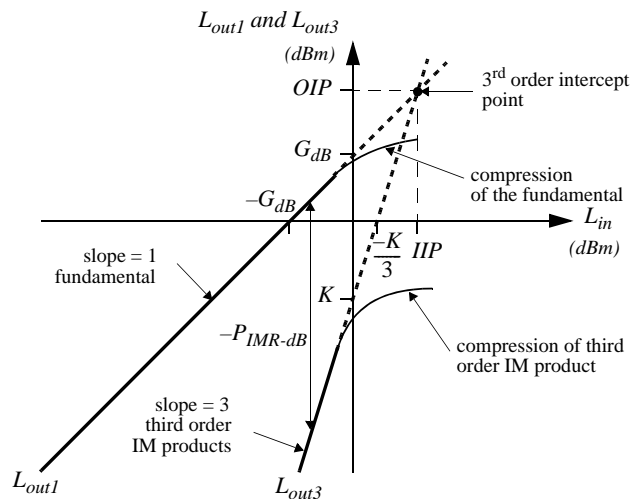


Fig 5-27: 3rd order intercept point.

The value of IIP can be expressed as a function of k_1 and k_3 by using equations (5.102), (5.103) and (5.105) in the following manner:

$$IIP = 10\log(k_1) - 10\log(k_3) - 10\log(R_{in}) + 28.24 \quad [dBm] \quad (5.107)$$

RELATIONSHIP BETWEEN THE COMPRESSION POINTS AND INTERCEPT POINTS IN “SINGLE TONE” AND “DUO TONE”

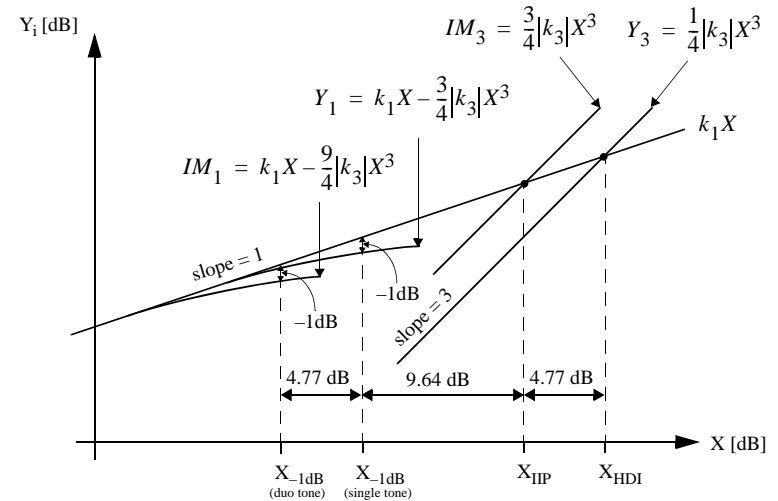


Fig 5-28: Relationship between the compression points at -1 dB and the intercept points measured in “single tone” and “duo tone.”

The relationship between the compression points at -1 dB and the intercept points measured in “single tone” and “duo tone” are illustrated in Fig. 5-28. Notice that the compression and intercept points measured in “single tone” are 4.77 dB higher than the compression and intercept points measured in “duo tone”. We can thus deduce the intercept point IIP from a “single tone” measurement, which is much easier to do than a “duo tone” measurement. This is not entirely correct in the case of a narrow-band system, because the harmonics of a sinusoidal signal generally fall outside of the useful band and are thus strongly attenuated while the 3rd order intermodulation products fall in the baseband and are not attenuated.

COMPARISON FOR A DIFFERENTIAL PAIR

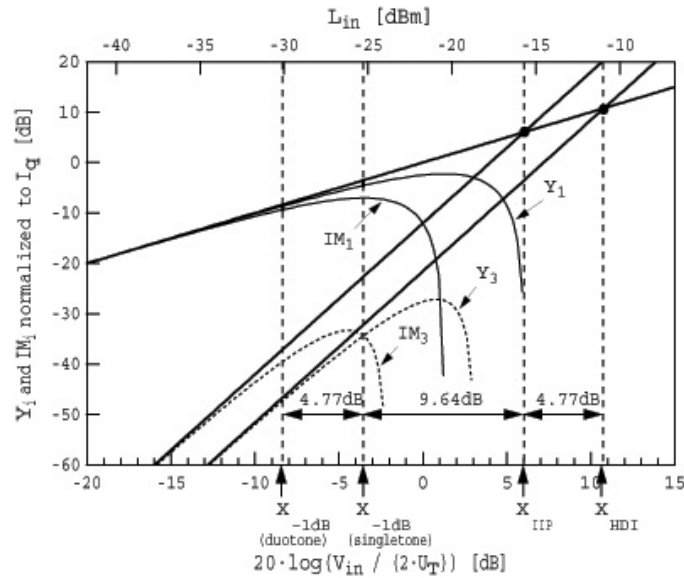


Fig 5-29: Comparison of compression and intercept points for “single tone” and “duo tone” signals for a differential pair.

A comparison between the compression and intercept points for “single tone” and “duo tone” signals in the case of a differential pair is presented in Fig. 5-29. Once again we find a difference of 4.77 dB.

INTERMODULATION DISTORTION RATIO

The Intermodulation Distortion Ratio (IMR) is the ratio between the amplitude of one of the 3rd order IM products and the amplitude of the linear term:

$$IMR \equiv \frac{\frac{3}{4}k_3 X_1^2 X_2}{k_1 X_1} = \frac{3k_3}{4k_1} X_1 X_2 \quad (5.108)$$

The ratio between the power of the 3rd order IM products at the output and the power of the linear term for the amplitudes $X_1 = X_2 = V_{in}$ is given by:

$$P_{IMR} \equiv \frac{P_{out3}}{P_{out1}} = \frac{\left(\frac{3}{4}k_3 V_{in}^3\right)^2}{2R_L} \cdot \frac{2R_L}{(k_1 V_{in})^2} = \left(\frac{3k_3}{4k_1} V_{in}^2\right)^2 = \left(\frac{3k_3}{4k_1} 2R_{in}\right)^2 \cdot P_{in}^2 \quad (5.109)$$

By definition, this ratio is equal to one when the input signal level is equal to IIP corresponding to a power P_{IIP} , from which we get:

$$P_{IMR} = \left(\frac{P_{in}}{P_{IIP}}\right)^2 \quad (5.110)$$

In decibels we have:

$$P_{IMR-dB} = 2 \cdot (L_{in} - IIP) \quad (5.111)$$

We can thus express IIP as a function of P_{IMR-dB} and L_{in} :

$$IIP = L_{in} - \frac{P_{IMR-dB}}{2} \quad (5.112)$$

The projection of the intersection point at the output is then simply given by:

$$OIP = L_{in} + G_{dB} - \frac{P_{IMR-dB}}{2} \quad (5.113)$$

MINIMUM DETECTABLE SIGNAL AND NOISE FLOOR

We have seen that the average noise factor \bar{F} represents the quotient of the signal-to-noise ratios at the input SNR_i and the output SNR_o of the two-port network. The minimum detectable signal (MDS) corresponds to the value of the signal which must be applied at the input in order to have a given signal-to-noise ratio at the output. From (5.26), we find:

$$MDS \equiv L_{min} = \bar{NF} + 10\log(kTB) + (SNR_o)_{dB} + 30 \quad [dBm] \quad (5.114)$$

For $T = 290\text{ K}$ and $SNR_o = 1$ we have:

$$MDS = \bar{NF} + 10\log(B_{kHz}) - 144 \quad [dBm] \quad (5.115)$$

where B_{kHz} is the bandwidth expressed in kHz. The output signal level corresponding to an MDS level at the input is called the Noise Floor. When the input signal exceeds the MDS , the output signal level increases linearly beyond the noise floor. The level of the IM product increases three times faster, but is initially lost under the noise floor.

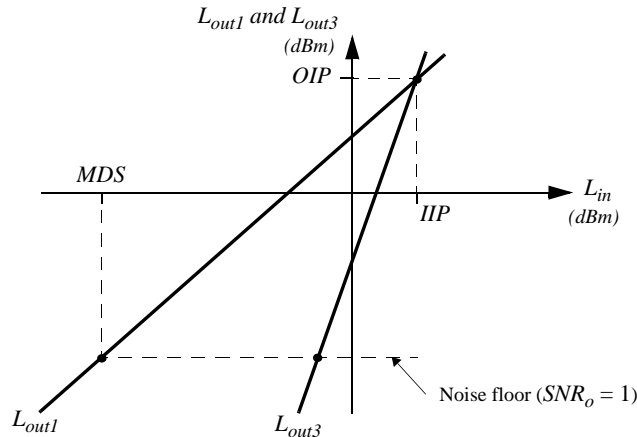


Fig 5-30: Relationship between the MDS and the noise floor.

DYNAMIC RANGE (1/2)

The dynamic range of a system is defined by the ratio between the maximum and minimum signals that the system can process. The minimum signal is limited by the noise while the maximum signal is limited by distortion. For a narrow-band system such as a receiver, the maximum signal is basically limited by the 3rd order IM products. The definition of the minimum signal level generally corresponds to the MDS . The maximum signal can be defined in multiple ways. One possible definition corresponds to the input signal level L_{IM} for which the level of the IM product is equal to the MDS (cf Fig. 5-31).

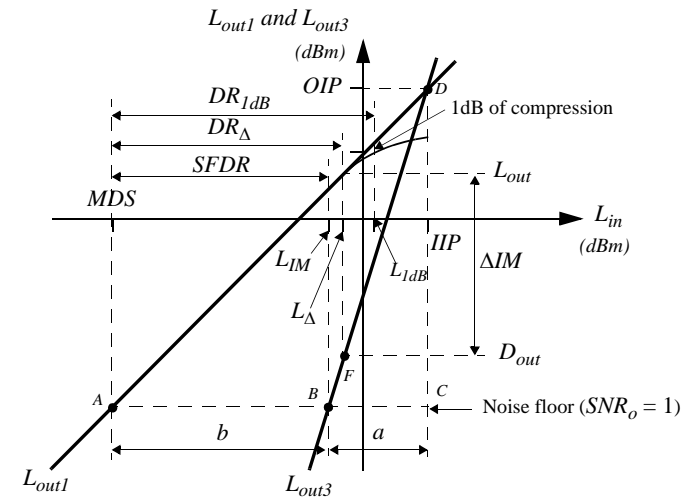


Fig 5-31: Relationship between the MDS and the dynamic range. The Spurious Free Dynamic Range ($SFDR$) of the system is then defined as the difference between L_{IM} and MDS :

$$SFDR \equiv L_{IM} - MDS \quad [dB] \quad (5.116)$$

DYNAMIC RANGE (2/2)

The maximum signal can be alternatively defined as the signal that produces a 1 dB compression of the fundamental. If L_{1dB} is the corresponding input level (cf Fig. 5-31), the dynamic range is equal to the difference between L_{1dB} and MDS :

$$DR_{1dB} \equiv L_{1dB} - MDS \quad [dB] \quad (5.117)$$

The dynamic range can also be defined as a function of the signal level L_{Δ} for which the third-order IM product L_{out3} is at a value $\Delta IM \equiv L_{out1} - L_{out3}$ (typically 60 dB) below the level L_{out1} corresponding to L_{Δ} :

$$DR_{\Delta} \equiv L_{\Delta} - MDS \quad (5.118)$$

One can define several relationships from the geometry shown in Fig. 5-31. Let b be the distance between the lines L_{out1} and L_{out3} and a be the distance between the line L_{out3} and the point IIP . Since the lines L_{out1} and L_{out3} have, respectively, slopes of 1 and 3, then $b = 2a$. Drawing a horizontal line that passes through the point F , we find that $b = \Delta IM$ and therefore $a = (\Delta IM)/2 = IIP - L_{\Delta}$, from which we find the relationship for IIP :

$$IIP = \Delta IM/2 + L_{\Delta} \quad (5.119)$$

In addition, we see that $a + b = 3a = (3b)/2$, which lets us write: $IIP - MDS = (3SFDR)/2$ and so:

$$SFDR = \frac{2}{3}(IIP - MDS) \quad (5.120)$$

In a similar way, we see that $IIP - L_{IM} = SFDR/2$, from which we find the maximum input signal level for which the level of the IM product is equal to the MDS :

$$L_{IM} = (2IIP + MDS)/3 \quad (5.121)$$

An input signal level higher than that given by (5.121) gives an IM product that increases three times faster than the desired signal, and causes an unacceptable distortion.

2nd ORDER INTERCEPT POINT (1/2)

The second-order IM products are given by $\pm f_2 \mp f_1$. For the case in which $f_2 \gg f_1$, the frequency $\Delta f \equiv f_2 - f_1 \approx f_2$ can be near f_2 and thus interfere with the system. In the same way as for the 3rd order IM products, we define an intercept point of the second-order IM products (cf Fig. 5-32).

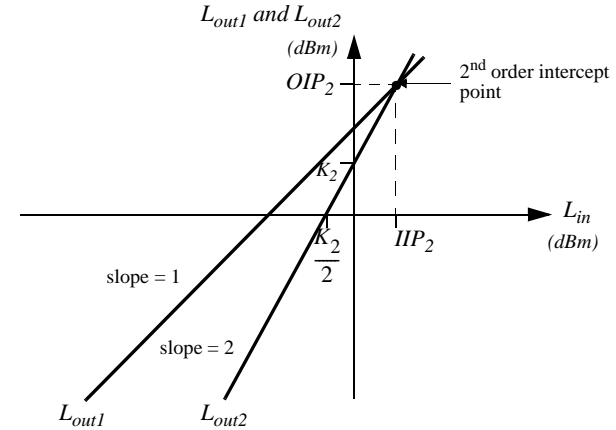


Fig 5-32: 2nd order intercept point.

The amplitudes of the second order IM products are both equal to $k_2 V_{in}^2$. The average power corresponding to the terminals of the load R_L is:

$$P_{out2} = \frac{(k_2 V_{in}^2)^2}{2R_L} \quad (5.122)$$

corresponding to a level L_{out2} :

$$\begin{aligned} L_{out2} &= 10 \log \left(\frac{(k_2 V_{in}^2)^2}{2R_L \cdot 1mW} \right) = 10 \log \left(\left(\frac{V_{in}^2}{2R_{in} \cdot 1mW} \right)^2 \frac{2R_{in}^2 k_2^2 1mW}{R_L} \right) \\ &= 2L_{in} + 20 \log(k_2) + 10 \log \left(\frac{R_{in}^2}{R_L} \right) - 27 = 2L_{in} + K_2 \end{aligned} \quad (5.123)$$

where:
$$K_2 \equiv 20 \log(k_2) + 10 \log(R_{in}^2/R_L) - 27 \quad [dB] \quad (5.124)$$

2nd ORDER INTERCEPT POINT (2/2)

The projection of the second-order intercept point is given by:

$$IIP_2 = 10\log\left(\frac{k_1^2}{k_2^2 R_{in}}\right) + 27 = 10\log\left(\frac{501k_1^2}{k_2^2 R_{in}}\right) \quad (5.125)$$

The difference between the projections of the 3rd and 2nd order intercept points is given by:

$$IIP_2 - IIP = 10\log\left(\frac{501k_1^2}{k_2^2 R_{in}}\right) - 10\log\left(\frac{66.67k_1}{k_3 R_{in}}\right) = 10\log\left(\frac{k_1 k_3}{1.33k_2^2}\right) \quad (5.126)$$

EXAMPLE (1/2)

Consider an electronic system with a bandwidth of 10kHz, and input and load resistances of 50Ω. The input is matched to two signal generators through the help of an adder for which the attenuation is 6dB. The frequency of the two sine waves applied to the input are $f_1 = 3800$ kHz and $f_2 = 3802$ kHz. When the adder is calibrated, the level of each of the signals before the adder is equal to 4 dBm. For this same input signal, the spectrum analyzer measures a level of each of these two signals at the output equal to 5 dBm and indicates that the 3rd order IM components are located 16 dB lower. We assume that the other IM components are negligible and that there is no compression. The measured noise level when there is no input signal is equal to -36 dBm. We are asked to calculate:

- 1) The corresponding input level L_{in} ;
- 2) The gain in power G_{dB} ;
- 3) The 3rd order intercept point IIP ;
- 4) The minimum detectable signal MDS ;
- 5) The dynamic range $SFDR$ of the system;
- 6) The noise figure NF ;
- 7) The maximum RMS voltage at the system input before the 3rd order IM products become perceptible.

EXAMPLE (2/2)

1) The input level is simply given by the difference between the level measured before the adder (+4 dBm) minus the attenuation of the adder (6 dB), so:

$$L_{in} = 4 - 6 = -2 \text{ dBm} \quad (5.127)$$

2) The gain in power is given by:

$$G = L_{out} - L_{\Delta} = 5 - (-2) = 7 \text{ dB} \quad (5.128)$$

3) From (5.119), with $L_{\Delta} = L_{in}$ and $\Delta IM = 16 \text{ dB}$, we get:

$$IIP = \frac{\Delta IM}{2} + L_{\Delta} = \frac{16}{2} + (-2) = 6 \text{ dBm} \quad (5.129)$$

4) In the graph in Fig. 5-31, the distance CD is equal to $36 + 7 + 6 = 49 \text{ dB}$, which also corresponds to the distance AC . So:

$$MDS = IIP - 49 = 6 - 49 = -43 \text{ dBm} \quad (5.130)$$

which corresponds to an RMS voltage at the input of 1.58 mV.

5) From (5.120) we get:

$$SFDR = \frac{2}{3}(IIP - MDS) = \frac{2}{3}(6 - (-43)) = 32.67 \text{ dB} \quad (5.131)$$

6) From (5.115) we get:

$$\overline{NF} = MDS - 10 \log(B_{kHz}) + 144 = -43 - 10 + 144 = 91 \text{ dB} \quad (5.132)$$

7) From (5.121) we get:

$$L_{IM} = \frac{2IIP + MDS}{3} = \frac{2 \cdot 6 - 43}{3} = -10.33 \text{ dBm} \quad (5.133)$$

which corresponds to an RMS voltage at the input of 68.1 mV.

IM DISTORSION AT THE OUTPUT

The 3rd order intercept point (PI3) in relation to the input is given by (5.119), and repeated here:

$$IIP = \Delta IM / 2 + L_{\Delta} \quad [\text{dBm}] \quad (5.134)$$

The PI3 in relation to the output is obtained simply from (5.134) by adding the gain (in dB):

$$OIP = IIP + G = \Delta IM / 2 + L_{\Delta} + G \quad [\text{dBm}] \quad (5.135)$$

Let L_{out} be the output level corresponding to L_{Δ} and D_{out} the distortion level at the output corresponding to an input level L_{Δ} . ΔIM is by definition equal to the difference between the output signal level (in dBm) and the corresponding level of the 3rd order IM component (cf Fig. 5-31):

$$L_{out} - D_{out} = \Delta IM \quad [\text{dBm}] \quad (5.136)$$

In addition: $L_{out} = L_{\Delta} + G \rightarrow L_{\Delta} = L_{out} - G \quad [\text{dBm}] \quad (5.137)$

By plugging the equations (5.136) and (5.137) into (5.135), we get:

$$OIP = \frac{3}{2}L_{out} - \frac{1}{2}D_{out} \quad [\text{dBm}] \quad (5.138)$$

If we express OIP not in dBm but directly in Watts we get:

$$OIP = \sqrt{P_{out}^3 / D_{out}} \quad [W] \quad (5.139)$$

The PI3 (in Watts) can thus be calculated from the measurement of the signal power P_{out} and from the IM distortion at the output D_{out} . Knowing OIP (in Watts), we can also express the distortion at the output corresponding to a certain power P_{out} :

$$D_{out} = \frac{P_{out}^3}{OIP^2} \quad [W] \quad (5.140)$$

IM DISTORSION AND THE CORRELATION COEFFICIENT

Fig. 5-33 shows a nonlinear amplifier, subject to a two-tone signal such as that described by (5.89), and producing IM products at its output. The power of the useful signal (in the passband of the system) is P_{in} and the power of the possible IM products falling in the passband and already existing at the input is D_{in} .

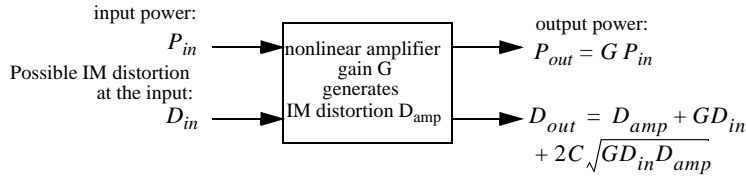


Fig 5-33: Input and output power of an amplifier subject to a two-tone test.

The IM distortion at the amplifier output is equal to the distortion produced by the amplifier D_{amp} , plus the distortion already present at the input multiplied by the gain G and an additive term $2C\sqrt{GD_{in}D_{amp}}$ taking into account the correlation existing between the distortion already existing at the input and the distortion generated by the amplifier itself. For the case in which the correlation coefficient C is zero, we have:

$$D_{out} = D_{amp} + GD_{in} \quad [W] \quad (5.141)$$

The two distortion terms add up in power (like independent noise sources). If they are perfectly correlated ($C = 1$), we get:

$$D_{out} = D_{amp} + GD_{in} + 2\sqrt{GD_{in}D_{amp}} = (\sqrt{D_{amp}} + \sqrt{GD_{in}})^2 \quad [W] \quad (5.142)$$

The two distortion components thus add up in voltage (or in current).

3rd ORDER INTERCEPT POINT FOR AN AMPLIFIER CASCADE (1/2)

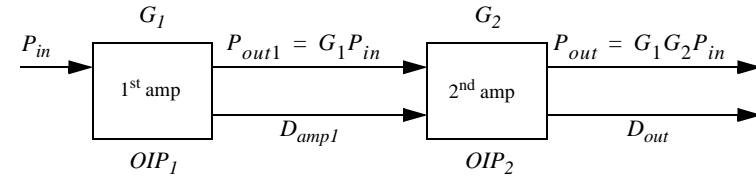


Fig 5-34: Two cascaded amplifiers subject to a two-tone input signal.

Consider the cascade connection of two amplifiers characterized by their gains in power G_i and their 3rd order intercept points OIP_i ($i = 1, 2$). If $C = 1$ we get:

$$D_{out} = (\sqrt{G_2 D_{amp1}} + \sqrt{D_{amp2}})^2 \quad [W] \quad (5.143)$$

From (5.139), the PI3 corresponding to the cascade connection of two amplifiers is:

$$OIP|_{C=1} = \frac{(G_1 G_2 P_{in})^{3/2}}{\sqrt{G_2 D_{amp1}} + \sqrt{D_{amp2}}} \quad [W] \quad (5.144)$$

But from (5.140), we get:

$$D_{amp1} = \frac{(G_1 P_{in})^3}{(OIP_1)^2} \quad \text{and:} \quad D_{amp2} = \frac{(G_1 G_2 P_{in})^3}{(OIP_2)^2} \quad [W] \quad (5.145)$$

and so:

$$OIP|_{C=1} = \left[\frac{1}{G_2 OIP_1} + \frac{1}{OIP_2} \right]^{-1} = \frac{G_2 OIP_1 OIP_2}{G_2 OIP_1 + OIP_2} \quad [W] \quad (5.146)$$

where $G_2 OIP_1$ corresponds to the PI3 of the first amplifier, in relation to the output of the second amplifier. The 3rd order intercept points combine like parallel resistances (for the case in which $C = 1$).

3rd ORDER INTERCEPT POINT FOR AN AMPLIFIER CASCADE (2/2)

If $C = 0$, Eqn. 5.141 gives:

$$D_{out} = D_{amp2} + G_2 D_{amp1} \quad [W] \quad (5.147)$$

and then after (5.139):

$$OIP|_{C=0} = \frac{(G_1 G_2 P_{in})^{3/2}}{\sqrt{G_2 D_{amp1} + D_{amp2}}} \quad [W] \quad (5.148)$$

Plugging in D_{amp1} and D_{amp2} with the help of (5.145), we get:

$$\begin{aligned} OIP|_{C=0} &= \left[\frac{1}{(G_2 OIP_1)^2} + \frac{1}{(OIP_2)^2} \right]^{-1/2} \\ &= \frac{G_2 OIP_1 OIP_2}{\sqrt{(G_2 OIP_1)^2 + (OIP_2)^2}} \quad [W] \end{aligned} \quad (5.149)$$

or brought back to the input:

$$IIP|_{C=0} = \left[\left(\frac{1}{IIP_1} \right)^2 + \left(\frac{G_1}{IIP_2} \right)^2 \right]^{-1/2} \quad (5.150)$$

The denominator of (5.149) being smaller than that of (5.146), the PI3 for $C = 0$ is greater than that obtained for $C = 1$. The real intercept point is usually between two extremes:

$$\frac{G_2 OIP_1 OIP_2}{G_2 OIP_1 + OIP_2} \leq OIP \leq \frac{G_2 OIP_1 OIP_2}{\sqrt{(G_2 OIP_1)^2 + (OIP_2)^2}} \quad (5.151)$$

nth ORDER INTERCEPT POINT FOR AN AMPLIFIER CASCADE

We can generalize (5.150) for the calculation of an nth order intercept point for a chain of amplifiers:

$$\frac{1}{IIP}|_{C=0} = \left[\left(\frac{1}{IIP_1} \right)^m + \left(\frac{G_1}{IIP_2} \right)^m + \left(\frac{G_1 G_2}{IIP_3} \right)^m + \dots + \left(\frac{G_1 G_2 \dots G_{r-1}}{IIP_r} \right)^m \right]^{1/m} \quad (5.152)$$

where $m \equiv n - 1$ and IIP (expressed in W) corresponds to the nth order intercept point brought back to the cascade input.